FROM BEHAVIOR TO GENES, AND BACK AGAIN

by

Sean E. Low

A dissertation submitted in partial fulfillment
of the requirements for the degree of
Doctor of Philosophy
(Neuroscience)
in the University of Michigan
2008

Doctoral Committee:

Professor Richard I. Hume, Co-Chair
Professor John Y. Kuwada, Co-Chair
Professor Michael D. Uhler
Assistant Professor Geoffrey G. Murphy
Assistant Professor Haoxing Xu
Assistant Professor Shawn Xu

ACKNOWLEDGEMENTS

The following work incorporated in this dissertation in preparation for publication are as follows:

Chapter I

Low SE, Blysma K, Saint-Amant L, Hirata H, Sprague SM, Zhou W, Cui WW, Hume RI, Kuwada JY. TRPM7 is required by vertebrate mechanosensitive cells for sensitivity to light, non-painful touch (in preparation).

Chapter II

*Low SE, *Zhou W, Saint-Amant L, Hirata H, Sprague SM, Cui WW, Hume RI, Kuwada JY. $NA_V1.6$ is required to transform a transient sensory input into a prolonged motor output (in preparation).

Chapter III

Low SE, Kuwada JY, Hume RI. The cloning and characterization of two new functional P2X receptor alleles from zebrafish (in preparation).

(*) Indicates that the authors contributed equally to the manuscript in preparation.

The following work not incorporated in this dissertation in publication are as follows:

Cui WW, Low SE, Hirata H, Saint-Amant L, Geisler R, Hume RI, Kuwada JY (2005) The zebrafish shocked gene encodes a glycine transporter and is essential for the function of early neural circuits in the CNS. J Neurosci 25:6610-6620.

Redmond TM, Ren X, Kubish G, Atkins S, Low S, Uhler MD (2004) Microarray transfection analysis of transcriptional regulation by cAMP-dependent protein kinase. Mol Cell Proteomics 3:770-779.

TABLE OF CONTENTS

LIST OF FIGURES

CHAPTER I

INTRODUCTION

Abstract

The aim of this thesis was to use forward and reverse genetics to explore the contribution of unknown and known genes to the touch-evoked escape behaviors belonging to zebrafish (*Danio rerio*).

A forward genetic screen identified two mutants that displayed abnormal touch-evoked escape behaviors. The first mutant *touchdown* (*tdo*) lacked sensitivity to light touch, but responded to noxious stimuli. *tdo* mutants were shown to result from mutations in the gene encoding for TRPM7, an ion channel with an attached kinase. A combination of electrophysiological and molecular techniques revealed that ion channel function was sufficient to restore sensitivity to light touch within excitable mechanosensitive neurons. Therefore TRPM7 is a candidate for a vertebrate mechanoreceptor responsible for sensitivity to light touch.

The second mutant identified from our forward genetic screen *non-active* (*nav*) initiated escape contractions, but failed to swim in response to touch. *nav* mutants were shown to result from mutations in the gene encoding $Na_V1.6$ that abolished channel activity. Electrophysiological recordings revealed that $Na_V1.6$ is required to turn on a locomotor network capable of generating rudimentary swimming. Furthermore the requirement of $Na_V1.6$ to turn this network might be its contribution of a persistent sodium current which is known to facilitate repetitive firing in other neurons.

Finally the cloning and characterization of the ATP-gated P2X receptor subunits P2X1 through P2X5.2 from zebrafish demonstrated that two subunits (P2X1 and P2X5.1) form functional homomeric receptors in contrast to previous reports. The use of reverse genetics (antisense knockdown) allowed the rejection of the hypothesis that signaling through P2X receptors is essential for myogenesis.

Model organisms

One powerful approach to determine the contribution of a gene to behavior would be to make a mouse knockout. For this reason and others, the NIH currently has a large initiative to produce targeted knock outs of every gene in the mouse. However this approach will take many years and cost millions of dollars. Furthermore this approach requires the correct identification of the gene prior to the onset of the experiment and therefore is not as readily adaptable to the identification of novel genes, and novel roles for known genes. This is a pursuit better suited for forward genetics which relies on random mutations followed by a screen for phenotypes of interest. This is the power of *Drosophila* and *C. elegans*. They breed easily in the lab, can be maintained in large numbers, are readily amendable to mutagenesis screens, and their nervous systems are relatively simple. In the case of *C. elegans* the complete map of connections between neurons are known from serial electron microscope reconstructions and the complete lineage that gives rise to all the cells in the nematode is known. However *Drosophila* and *C. elegans* are both invertebrates, and while many things are conserved between vertebrates and invertebrates, many things are different. For example *C. elegans* use sodium channels belonging to the Epithelial Sodium Channel (ENaC) family in non-ciliated mechanosensory neurons responsible for sensitivity to light touch (Goodman, 2006). However it is clear that this is not the case in mammals (Drew et al., 2004).

The notion that the closer you get to humans the more likely mechanisms are to be similar, coupled with the fact that scientists are never satisfied with the tools at hand, fueled the search for an organism that blended the feasibility of working with *Drosophila* and *C. elegans* with that of a vertebrate. Zebrafish, common in many home aquaria, is a vertebrate organism that shares many of the experimental advantages of *Drosophila* and *C elegans*. They breed extremely well in captivity; a single pair can mate three to four

times a week producing hundreds of embryos each time. Embryos develop *ex utero*, and can be maintained in a transparent state for several days facilitating the identification of various cell types (Westerfield, 1993). Development proceeds at a rapid rate, with a nervous system capable of generating rudimentary sensory-evoked motor behaviors within the first day of life (Saint-Amant and Drapeau, 1998). Zebrafish embryos are also hearty organisms, tolerating the failure of multiple organs, including the complete loss of cardiovascular function during the first few days of development. In addition techniques for recording from embryonic muscle (Buss and Drapeau, 2000) and neurons (Drapeau et al., 1999) have recently been optimized. Furthermore zebrafish is amendable to both forward (Haffter et al., 1996) and reverse genetics (Nasevicius and Ekker, 2000) facilitating the isolation of both novel genes, and novel roles for known genes.

However zebrafish are not without their own short comings. A major concern with molecular genetics in zebrafish is the partial genome duplication which resulted in the presence of parologs for some, but not all genes. This sometimes confounds the ability to make definitive conclusions. For instance both mutants examined in this thesis (*touchdown* and *non-active*) exhibit some recovery. While this on one hand may be a testament to the plasticity of these circuits, it on the other hand may represent the contribution of a parolog. This conundrum should be of less concern in the future with the conclusion of the zebrafish genome sequencing project.

It is worth noting that the partial genome duplication can actually be useful. Sometimes the duplication of gene can provide insight how new roles for old proteins evolve as the duplication event frees one gene to evolve new functional capabilities, without the concern that mutations could be lethal. Furthermore the roles of normally one protein can divided between two proteins, which can shed light on the contribution of domains to functional roles.

When compared to other genetic organisms zebrafish is also lacking in two critical areas. First, the lack of efficient homologous recombination prevents gene targeted knockouts beyond the three to four day limit currently obtainable through antisense morpholino knockdown. Instead one must rely on forward genetic screens, or insertional mutagenesis ventures currently underway (www.Znomics.com), and luck. Second, once a mutation is identified then the task of isolating the loci and understanding

the contribution of the gene begins. In cases where a gene is expressed in multiple areas this can be problematic. Advantageous would be a set of promoters complementary to the ones found in *Drosophila* and *C. elegans* to drive the expression of transgenes in a subset of cells. To my knowledge my use of the zCREST2-hsp70 promoter in this thesis is the first successful attempt to do so within zebrafish. While the majority of zebrafish's short comings will ultimately be addressed in the near future, one attribute that will linger is the generation time for zebrafish. Currently with continuous feeding the shortest time to sexual maturity that can be obtained is six weeks, with more consistent times ranging from eight to twelve weeks. This is similar to mouse, and is five times longer than for *C. elegans.*

The golden age of zebrafish begins

Although fish had been a staple in labs for some time, used not only as a developmental organism but also as subjects in learning and memory tasks (Agranoff and Klinger, 1964), it wasn't until George Stresinger showed in 1981 with the *golden* mutant that clones could be produced in zebrafish (*Danio rerio*) that fish were perceived as a potential genetic organism (Streisinger et al., 1981). Then in the 1990's two groups spearhead by Christiane Nusslein-Volhard (a Nobel laureate for her work on *Drosophila*) and Wolfgang Driever ushered in the golden age of zebrafish genetics with large scale mutagenesis screens (*Development*, 1996:123). Their efforts lead to the isolation of 4264 mutants, of which 894 were further characterized and assigned to 372 genes (Haffter et al., 1996). One aspect of their screen was touch-evoked motor behaviors which identified 166 mutations in 48 genes (Granato et al., 1996).

Touch-evoked motor behaviors develop early and require the function of sensory neurons, interneurons, motor neurons and muscle. Therefore tactile stimulation simultaneously screens for defects at each level, with the caveat that mutations at different levels may resemble each other. However *in vivo* electrophysiological recordings from these cells (Drapeau et al., 1999; Buss and Drapeau, 2000) can often isolate the level of defect, allowing mutants to be grouped into those affecting muscle or nervous system, facilitating the isolation of candidate genes consistent with a phenotype obtained through genetic mapping (Postlethwait et al., 1994). I will begin by describing

the cells required for touch-evoked motor behaviors, then the development of motor behaviors in zebrafish, and end by describing in more detail the three ion channels I studied within the context of touch-evoked escape behaviors in zebrafish.

The touch-evoked escape circuit

The two areas responsible for controlling early, touch-evoked behaviors in zebrafish, spinal cord and hindbrain, are very similar in structure and function to other vertebrates (Kimmel et al., 1995). The hindbrain is segmented into eight rhombomeres, with easily identifiable reticulospinal neurons (Metcalfe et al., 1986) that are accessible to manipulation (Kimmel et al., 1990). The spinal cord contains around thirty segments, each with a similar complement of neurons (Bernhardt et al., 1990; Kuwada et al., 1990); the muscles the spinal cord innervate are also similar in organization to other vertebrates muscle (van Raamsdonk et al., 1978).

Beginning with a touch to the head or tail in a presumed order of activation, the cells involved in touch-evoked behaviors include: 1) the mechanosensitive neurons of the trigeminal ganglia and Rohon-Beard neurons (RBs) located in the spinal cord, 2) the giant reticulospinal Mauthner (M) cells and approximately 89 other pairs of reticulospinal neurons in the hindbrain (Gahtan et al., 2002), 3) the three primary spinal motor neurons (RoP, MiP, and CaP) and a host of secondary spinal motor neurons (Myers et al., 1986; Westerfield et al., 1986), and 4) both fast and slow twitch axial skeletal muscle (Buss and Drapeau, 2000) (Figure 1.1A). Although there are additional cells involved, such as those active during swimming, they will not be discussed here but are covered later.

RBs are a type of mechanosensitive neuron common to lower vertebrates, whose function in zebrafish are gradually replaced beginning on the third day of development by sensory neurons located in the dorsal root ganglia (Williams et al., 2000). At around 17 hpf RBs begin to project neurites which innervate the skin and pioneer the Dorsal Longitudinal Fasciculus on its way to the hindbrain where it terminates near the lateral dendrite of M cells (Bernhardt et al., 1990). RBs, for which there are typically 4-6 per segment, most likely represent a heterogeneous population of neurons in zebrafish (Kucenas et al., 2003) whose *in vivo* properties have only recently been examined (Ribera and Nusslein-Volhard, 1998; Pineda et al., 2005; Pineda et al., 2006). However zebrafish

RBs are analogous to the well characterized RBs from *Xenopus* tadpoles and therefore much may be directly applicable to zebrafish RBs (Roberts, 2000). Noteworthy is that in response to touch *Xenopus* RBs fire multiple action potentials (Roberts and Hayes, 1977). Furthermore the stimulation of a single RB (via depolarizing current injection to the cell body) is sufficient to trigger ventral root nerve bursting (Clarke et al., 1984). Currently much less is known regarding the excitable properties of mechanosensitive neurons of the trigeminal ganglia, but anatomical studies have shown that they are the first neurons to contact M cells (Kimmel et al., 1990).

The giant fiber M cells, born at 7 hpf (Mendelson, 1986b) begin to project axons into the spinal cord around 22 hpf (Mendelson, 1986a). Once in the spinal cord they appear to make *en passant* synapses with primary motor neurons (Westerfield et al., 1986). *In vivo* live imaging using dye labeled cells revealed that M cells and motor neurons actively extend filopodia toward each other (Jontes et al., 2000), suggestive of a synaptic connection. The size, accessibility, and early birth date have long made M cells a favorite target of study within fish (Korn and Faber, 2005). Activity in M cells has been shown to follow an aversive stimulus (Eaton et al., 1988), precede the onset of an escape response (Eaton and Emberley, 1991), and be sufficient for the initiation of an escape response (Nissanov et al., 1990). These features lead to the idea that M cells in fish are "command neurons", similar to neurons found in other organisms.

M cells are not alone in their activation in response to touch. In 2002 Gahtan and colleagues labeled zebrafish reticulospinal neurons with a fluorescent calcium indicator and imaged cellular activity in response to touch (Gahtan et al., 2002). They observed activity in 82 % of the approximately 110 bilateral pairs of reticulospinal neurons found in zebrafish. The recruitment of additional/different cells, including the serial homologs of M cells called MiD2cm and MiD3cm, has been proposed to account for the differential touch-evoked escape contractions exhibited by fish in response to head versus tail touch (see below) (O'Malley et al., 1996; Liu and Fetcho, 1999).

Next in the order of activation are the primary and secondary motor neurons. Primary motor neurons begin differentiation around 15 hpf, with three in each hemisegment (Myers et al., 1986; Westerfield et al., 1986). The primary motor neurons are designated by their rostro-caudal orientation with RoP (rostral primary motor neuron),

MiP (middle primary motor neuron), and CaP (caudal primary motor neuron). The identity of a primary motor neuron can also be determined following electrophysiological recordings by their axonal trajectories revealed through the inclusion of fluorescent dyes within the recording pipette (Drapeau et al., 1999) with RoP, MiP and CaP innervate lateral, dorsal, and ventral musculature, respectively. Secondary motor neurons develop later, are smaller, branch less extensively within the musculature, and innervate fewer fibers than primary motor neurons (Myers et al., 1986).

The last cell type activated during touch-evoked behaviors is the axial muscles. The first indication of myogenesis can be detected at 10.5 hpf, only thirty minutes after the onset of somitogenesis (Weinberg et al., 1996). Around this time the adaxial cells adjacent to the notochord morph from a cuboidal state to a more elongated state, reminiscent of more mature fibers, and then migrate radially to form the superficial mononuclear layer of slow twitch skeletal muscle (Devoto et al., 1996). Thereafter a second wave of pioneering adaxial cells elongate and migrate laterally at the level of the horizontal myoseptum to join the radially migrating layer of superficial slow twitch muscle. The remaining myogenic precursors then differentiate and fuse to form multinucleated fast twitch muscle that are medial to the slow twitch muscles (van Raamsdonk et al., 1978; Devoto et al., 1996). Electrophysiological recordings indicate that both slow twitch and fast twitch fibers are active during fictive swimming (Buss and Drapeau, 2000).

Motor behaviors

Within the first 27 hours of development, typically a full day before emerging from their chorion, zebrafish embryos exhibit three highly stereotyped motor behaviors. In order of developmental onset these are 1) spontaneous coiling, 2) touch-evoked escape contractions and 3) touch-evoked swimming (Figure 1.1B). The first, spontaneous coiling begins around 17 hpf peaks in frequency (1 Hz) at 19 hpf, and decreases over the next seven hours of development to under 0.1 Hz (Saint-Amant and Drapeau, 1998). Spontaneous coiling is characterized by alternating contractions of the trunk and tail towards the head. Spontaneous coiling is intrinsic to the spinal cord as coiling persists in an alternating fashion following spinalization (Saint-Amant and Drapeau, 1998).

Furthermore spontaneous coiling is neurogenic in nature as they are blocked by cholinergic antagonists (Saint-Amant and Drapeau, 1998). The finding that spontaneous coiling is neurogenic in nature indicates that motor neurons have successfully innervated muscle consistent with the exit of motor axons from the spinal cord (Eisen et al., 1986), and suggests that contralateral inhibition between neurons required to prevent bilateral contractions have been established.

The next motor behavior to develop, touch-evoked escape contractions, is first observed at 21 hpf (Saint-Amant and Drapeau, 1998). Touch-evoked escape contractions are characterized by 2-3 alternating contractions of the trunk and tail towards the head. Initially touch-evoked escape contractions were found to differ from spontaneous coiling in that they required supraspinal input (Saint-Amant and Drapeau, 1998), however this finding has been recently challenged (Downes and Granato, 2006). Although it is unclear whether touch-evoked escape contractions require supraspinal input, what is clear is that the emergence of touch-evoked escape contractions signals the integration of the sensory system with the motor system.

Unlike spontaneous coiling, touch-evoked escape contractions persist into adulthood. In adults they are characterized by "J-bends" and "C-bends" depending upon the source of tactile stimuli. In response to tail touch contralateral musculature contracts resulting in a slight bending of the tail away from the source of the stimulus (J-bend), which is then followed by swimming. In contrast, touching of the head evokes a more robust contraction of contralateral musculature resulting in displacement of the head away from the source of the stimulus (C-bend), which is then followed by swimming. How these differential behaviors are mediated was partially revealed with elegant experiments using calcium indicators which demonstrated that head versus tail tap results in the differential recruitment of reticulospinal neurons (O'Malley et al., 1996; Liu and Fetcho, 1999).

The last of the embryonic motor behaviors to develop is touch-evoked swimming. Touch-evoked swimming is first observed at 27 hpf, when after performing escape contractions embryos begin to generate tail beating sufficient to propel itself forward for ~1 s (Saint-Amant and Drapeau, 1998). Thereafter the swimming becomes stronger and longer in duration such that upon hatching (~ 52-55 hpf) larvae are capable of sustained

bouts of "burst swimming" lasting several seconds to a minute (Buss and Drapeau, 2001). Video analysis has revealed that newly hatched larvae can swim at frequencies between 35 and 70 Hz, consistent with touch-evoked spiking observed in motor neurons (Buss and Drapeau, 2001) and muscle (Buss and Drapeau, 2002). The use of NMDA to drive activity within the locomotor network (McDearmid and Drapeau, 2006), coupled with lesion experiments (Saint-Amant and Drapeau, 1998) has indicated that supraspinal input is required to both evoke touch-evoked swimming, and to generate patterned swimming prior the 72 hpf (Chong and Drapeau, 2007).

While anatomical and electrophysiological studies have revealed much of the neural circuitry underlying escape behaviors, much less is known about the contribution of specific genes to the formation and function of these neural circuits. In an attempt to gain insight into the roles of specific genes I undertook a reverse and forward genetic approach to explore the potential contribution of a known family of ligand-gated ion channels, and characterized two mutations that affected motor behaviors in zebrafish.

Ion channels

There are literally hundreds of genes which encode ion channels. They are found in the genomes of all groups of living organisms; single celled microbes, plants and animals (Hille, 2001). I will now give a brief description of the three ion channels I studied in the context of the touch-evoked escape circuit belonging to zebrafish. They are in order by chapter, the mechanosensitive TRPM7 channel, the voltage-gated sodium channel $Na_V1.6$, and the ATP-gated P2X receptors.

TRP Channels

The identification of the founding member for this family of ion channels came from work done in *Drosophila* which identified a novel ion channel as the causative gene in a mutant that exhibited a Transient Receptor Potential in its photoreceptors in response to sustained light (Montell and Rubin, 1989). Since then the identification of additional TRP receptors within the genomes of yeast to humans has resulted in a large "superfamily" with 33 members in mammals, and approximately 60 predicted in the zebrafish genome (Montell, 2005). This superfamily of TRP channels can be subdivided

into seven subfamilies based on sequence similarity (TRPM, TRPC, TRPP, TRPA, TRPV, TRPML and TRPN) (Montell et al., 2002). Structurally, TRP channels resemble voltage-gated potassium channels, with each subunit possessing six transmembrane domains (TM), and four subunits assembling to form a functional channel (Figure 1.1A). However unlike voltage-gated potassium channels, TRP channels are permeable to multiple cations including sodium and calcium as well as potassium. In addition TRP channels are activated by a range of stimuli including light, temperature, pheromones and mechanical stimuli. Given this wide range of activating stimuli, it's not surprising that TRP channels have been linked to several sensory systems including vision, chemosensation, thermosensation, nociception, and mechanosensation (Clapham, 2003). The role of a TRP channel in a sensory system can be direct or indirect as a downstream player in an intracellular signaling cascade (as was the case for founding member of this family TRP-1)(Montell and Rubin, 1989).

Examples of members with direct roles are the temperature sensitive TRPs. Currently there are four TRP channels know to be responsive to warm temperatures. In order of temperature sensitivity they are: TRPV4 (~29^{o}C), TRPV3 (~32^{o}C), TRPV1 (>42^{o}C) and TRPV2 (>50^{o}C) (Clapham, 2003). Two temperature sensitive TRPs, TRPA1 (Story et al., 2003) and TRPM8 (McKemy et al., 2002), respond to a decrease in temperature with activity beginning at less than 18^{o}C (noxious cold) and less than 25^{o}C (modest cooling) respectively. Interestingly these two receptors also account for sensitivity to mustard oil which is the pungent compound in wasabi (TRPA1) (Bautista et al., 2006), and the cooling sensation of menthol (TRPM8) (Bautista et al., 2007). TRPA1 and TRPM8 are not alone in their sensitivity to temperature. These TRP channels represent an area of sensory science referred to as "chemesthesis", or the ability of molecules to activate receptors associated with other sensations such as temperature, touch and pain.

In addition to a role as thermosensors three TRP channels have also been implicated in mechanosensation, in particular hearing and touch. The first, *osm-9*, was identified in a *C. elegans* screen for mutants deficient in osmotic avoidance and nose touch (Colbert and Bargmann, 1995). Cloning of the mammalian *osm-9* ortholog identified a channel belonging to the TRPV subfamily (TRPV4) which was responsive to

hypotonic stimuli, a stimulus thought to induce physical stress similar to that induced by touch (Liedtke et al., 2000). Expression analysis revealed mammalian *trpv4*/TRPV4 expression within known mechanosensitive cells (Liedtke et al., 2000; Suzuki et al., 2003b) and demonstrated that mammalian TRPV4 could rescue touch insensitivity in *osm-9* mutants (Liedtke et al., 2003). This finding argued for a conservation of function for TRPV4 in mechanosensation across species, and highlights the use of genetically tractable organisms to isolate candidates involved in mechanosensation. A *trpv4* knockout mouse showed that TRPV4 contributes to pressure sensitivity, but is not necessary for normal sensitivity to light touch (Suzuki et al., 2003a).

The second TRP channel linked to mechanosensation, *nompC*, was identified in a *Drosophila* mutagenesis screen for its apparent clumsiness. Further characterization of *nompC* mutants lacked a significant proportion of the mechanically activated current in the mechanosensitive cells that innervated the sensory bristles (Walker et al., 2000). BAC rescue and subsequent cloning revealed that *nompC* mutants arose from mutations in the gene encoding TRPN1. Evidence for TRPN1 serving a similar role in vertebrate mechanosensation gained momentum when a zebrafish ortholog was identified and shown to be necessary for mechanically induced microphonic potentials of hair cells, and the uptake of dyes known to permeate the mechanotransduction channel (Sidi et al., 2003). However, mechanosensation of higher vertebrates is not mediated by TRPN1 since it is missing from the genomes of higher vertebrates, including rodents and humans (Clapham, 2003).

The third TRP channel, TRPA1 was also implicated in mechanosensation based on work in model organisms. In *Drosophila*, a mutant that displayed abnormal responsiveness to noxious stimuli named *painless* (Tracey et al., 2003) was subsequently shown to result from a disruption in the gene encoding TRPA1 (Al-Anzi et al., 2006). TRPA1 was localized in the dendrites of multidendritic sensory neurons, an expression pattern consistent with a role in mechanosensation. More recently the ortholog of TRPA1 in *C. elegans* (TRPA-1) was shown to be necessary for normal responsiveness to repeated mechanical stimuli *in vivo*, and exhibited sensitivity to mechanical stimuli when studied heterologously (Kindt et al., 2007). Furthermore TRPA1 was previously identified as a potential mechanotransduction channel in vertebrate hair cells (Corey et

al., 2004). However *trpa1* knockout mice exhibited normal auditory function and responsiveness to light touch showing that it was not required for these functions in mammals (Bautista et al., 2006; Kwan et al., 2006). Thus the mediator for light/non-painful touch in vertebrates has to date eluded us.

Recently zebrafish joined the ranks of model organisms amendable to both genetic manipulation and *in vivo* electrophysiology. In our screen for zebrafish motor mutants we uncovered a new allele of the touch unresponsiveness/ hypopigmented mutant *touchdown* (*tdo*^{mi174}). Alleles of *touchdown* are known to harbor mutations in the gene encoding TRPM7 (Elizondo et al., 2005). In chapter II of this thesis I characterized in detail the phenotype of the *tdo*^{mi174} mutants and explore the possibility that TRPM7 might be directly responsible for mechanosensation in zebrafish sensory neurons.

Voltage-gated Sodium Channels

Voltage-gated sodium channels are best known for contributing to the rising phase of action potentials in muscle and neurons. Action potentials allow sensory information to travel down axons, across synapses, and trigger excitation-contraction coupling in muscle. Considering the importance of action potentials, it is not surprising that many animals have evolved toxins to disrupt actions potentials as a means of discouraging predation, or of stunning prey. The most well known of such toxins is Tetradotoxin (TTX), a sodium channel blocker produced by a bacterium in a symbiotic relationship with puffer fish. These fish are prized in Japanese cuisine, and if properly prepared produce an odd tingling sensation when consumed because a tiny amount of TTX containing tissue is not removed (a feeling I have had the opportunity to directly verify). Saxitoxin and scorpion toxin are also prized commodities within the scientific community as they have facilitated the characterization and purification of the sodium channels responsible for action potentials.

Well before the biochemical purification of sodium channels through the use of toxins (Beneski and Catterall, 1980) scientists had been studying the characteristics of sodium channels in their native cells. The first recordings date back to 1930's and culminated in the pioneering work by Hodgkin and Huxley (Hodgkin and Huxley, 1952). Their work demonstrated the three main characteristics of sodium channels: (1)

selectivity for sodium ions over other ions, (2) voltage dependence of activation, and (3) fast inactivation. For their efforts Hodgkin and Huxley were awarded the 1963 Nobel Prize in Physiology and Medicine. While their efforts were clearly monumental, in order to more closely study the properties of voltage-gated ion channels scientists prefer to study them in non-excitable cells, devoid of any other confounding voltage-gated currents. Therefore substantial progress in understanding them at the molecular level had to wait until the 1980s, when cloning of cDNAs became possible and the race was one to clone the first sodium channel.

This was accomplished in 1984, when a full-length cDNA encoding the α subunit was obtained that predicted an 1820 amino acid protein which formed four repeated "domains" in a pseudosymmetric manner in the cell membrane (Noda et al., 1984). Subsequent efforts revealed a sodium channel family made up of nine voltage-gated members ($Na_V1.1$ – $Na_V1.9$), and a tenth voltage-insensitive member included based on sequence similarity (Na_X) (Catterall et al., 2005a; Catterall et al., 2005b). Although a crystal structure for a sodium channel has not been obtained, considerable indirect evidence indicates that they form a structure that resembles the solved crystal structure of potassium channels (Doyle et al., 1998; Jiang et al., 2003b), with one major exception. Whereas potassium channels assemble as a tetramer of four subunits, with each subunit comprised of six transmembrane spanning segments (S1-S6), the four subunits of a sodium channel are tethered together, giving rise to Domains I-IV (Figure 1.1B).

Models derived from potassium channels suggests that the pore of the sodium ion channel is formed in two halves, one extracellular and one intracellular (Doyle et al., 1998; Jiang et al., 2003b). The extracellular portion is comprised of the intervening amino acids between S5 and S6 of each domain. This region is thought to dip in and out of the membrane forming "reentrant loops". The intracellular half of the pore is comprised of the four S6 segments, one from each domain, which appear to bend in towards the center of the complex. These two halves come together to form a structure reminiscent of two cones whose apexes have been glued together, with the extracellular portion forming the selectivity filter.

How a sodium channel transforms a shift in the membrane potential into the opening of a pore is not completely understood, but is known to involve the movement of

the four S4 segments from each domain, collectively referred to as the voltage sensor. The voltage sensor typically contains a positively charged amino acid at every third position (Noda et al., 1984). All current models suggest that in response to membrane depolarization the voltage sensor moves in the membrane resulting in a physical movement within the sodium channel but the nature of the movement is still under active investigation (Jiang et al., 2003a). This physical movement is translated into the opening of the channel, allowing sodium ions to run down their electrochemical gradient. This model is based on the fundamental physics of electricity and was first supported by the finding that a "gating current" can observed prior to channel opening (Armstrong and Bezanilla, 1973). The attribution of gating to S4 is based on the observation that alterations of positive charges within S4 alters this gating current (Yang and Horn, 1995). Isolation of the gating current has not only facilitated a model of how shifts in membrane potential might be translated into the opening of an ion channel, but has also lead to a better understanding of different mutations in sodium channels disrupt channel function. Mutants that might have otherwise been grouped together simply as "non-functional", can be subdivided into mutations that affect gating verses conduction, as this distinction is often blurred by the fact that electrophysiologists typically measure conductance as a product of gating (Colquhoun, 1998). Gating currents are the consequence of any movement of charge in the membrane, and in Chapter II we interpret some of our findings concerning the role of TRPM7 as a possible gating current signal.

Although the structure of the whole sodium channel has not be been solved, the intervening portion between Domains III and IV, which forms the fast inactivation gate has been determined by nuclear magnetic resonance (NMR) imaging (Rohl et al., 1999). It was found to form an alpha-helix, with a stretch of three amino acids forming an IFM motif (Isoleucine-Phenylalanine-Metionine) positioned such that could swing up and into the intracellular portion of the pore in agreement with the "Ball and Chain" model proposed many years earlier (Armstrong and Bezanilla, 1977). In fact a mutation that alters the charge association in this region (IFM to ICM) that slows fast inactivation, can be reversed through the application of a methanthiosulfonate-benzyl reagent (MTSBN) which restores the charge association (Chahine et al., 1997). While subsequent studies into sodium channel function has supported the original model proposed by Hodgkin and

Huxley one aspect, rapid and complete inactivation in response to depolarization has been challenged with the identification of characterization of a "persistent sodium current" (Crill, 1996).

The persistent sodium current "$I_{Na}p$" first identified in neurons of guinea pigs (Hotson et al., 1979) represents a non-inactivating component of sodium channel activity. $I_{Na}p$ is characterized by an ability to activate at membrane potentials insufficient to trigger action potentials, and to persist in response to prolonged membrane depolarization. $I_{Na}p$ was sensitive to external TTX and to internal QX-314, and was absent following substitution of external Na^+ for Choline (Connors and Prince, 1982), suggesting that $I_{Na}p$ was conferred by traditional sodium channels. Confirmation that $I_{Na}p$ was carried by a voltage-gated sodium channel came with the molecular identification of the "*motor endplate disease*" mouse which harbored a mutation in the gene encoding $Na_V1.6$ (*scn8a*) (Raman et al., 1997). Neurons from *med* mice were found to exhibit a reduced $I_{Na}p$ compared to wild type neurons, and a decreased ability to sustain prolonged bouts of action potentials. In addition viable *scn8a* mutations in mice result in a range of motor disorders including paralysis, ataxia, atrophy and dystonia (Meisler et al., 2004).

Effects on channel activity are not limited to portions of the principle α subunit. Accompanying the purification of the α subunit from nervous tissue were auxiliary subunits termed "ß" (Beneski and Catterall, 1980). A cDNA encoding the ß subunit was obtained in 1992 (Isom et al., 1992) and subsequent searches have identified a family comprised of four members, each encoded by their own gene (Isom et al., 1995; Shah et al., 2000; Yu et al., 2003). Co-expression of ß subunits revealed that in addition to altering channel kinetics of the principle α subunits, ß subunits also facilitate membrane insertion of the α-ß complex. Furthermore ß subunits have recently been shown to play a structural role a the Nodes of Ranvier (Chen et al., 2004) and in the outgrowth of cerebellar granule cells grown in vitro (Davis et al., 2004).

In zebrafish surprisingly little is known about the α and ß subunits of the sodium channel complex. Currently only four α subunits have been identified ($Na_V1.1$, $Na_V1.4$, $Na_V1.5$ and $Na_V1.6$)(Tsai et al., 2001; Novak et al., 2006a). Of these only the contribution of $Na_V1.1$ and $Na_V1.6$ have been studied *in vivo* (Pineda et al., 2005; Pineda

et al., 2006; Chen et al., 2008) while only $Na_V1.5$ and $Na_V1.6$ have been examined *in vitro* (Chopra et al., 2007; Fein et al., 2007). Although the complete family of ß subunits is believed to have been identified and is represented by a single ortholog for ß1-3, and two ß4 related genes (Chopra et al., 2007; Fein et al., 2007) only the effects of ß1 on $Na_V1.5$ and $Na_V1.6$ have been assayed (Chopra et al., 2007; Fein et al., 2007).

From our forward genetic screen for zebrafish motor mutants we uncovered two alleles of a mutation we've named *non-active* (*nav*). *nav* mutants were identified by an inability to swim in response to touch. Mapping and cloning revealed that both alleles of *nav* harbor mutations in the gene encoding $Na_V1.6$ that abolish channel activity. Electrophysiological characterization of the escape circuit revealed that sensory information was able to activate interneurons that are normally sufficient to trigger swimming, but fail to do so in *nav* mutants. Considering that a persistent sodium current had been linked to sustained fictive locomotion in rodents (Tazerart et al., 2007; Zhong et al., 2007) we examined whether zebrafish $Na_V1.6$ exhibited a persistent sodium current, and whether its absence could account for the *nav* phenotype in Chapter III.

P2X Receptors

ATP is the energy currency of cells. It powers everything, either directly or indirectly, from the ion pumps that set up the electrochemical gradient across cell membranes to the actin-myosin motors that generate muscle contraction. Therefore the suggestion that ATP was a neurotransmitter in certain parts of the body was not initially well received by some scientists (Burnstock, 1972). However subsequent research has clearly identified two types of receptors activated by ATP (Burnstock, 2007). First the P2Y receptors, which are a family of G-protein coupled receptors which will be addressed later in the general discussion. Second, the P2X family of ligand-gated ion channels which are the focus of this section and are the topic of Chapter IV.

The effect of ATP on tissue, and in particular on skeletal muscle, has been known for some time. In 1944 Buchthal and Folkow injected the artery in frogs which supplied the muscle innervated by the sciatic nerve with ATP and noted that it induced tetanus-like contractions (Buchthal and Folkow, 1944). Later in rats ATP was found to be released upon nerve stimulation from the cholinergic phrenic nerve which innervates the

diaphragm (Silinsky and Hubbard, 1973), consistent with the Burnstock purinergic hypothesis proposed two years earlier. Then in 1983 evidence that ATP could act in a transmitter like fashion came when Kolb and colleagues applied ATP to cultured avian myoblasts and myotubes under voltage clamp (Kolb and Wakelam, 1983). Our understanding of the role of ATP in avian skeletal muscle was substantially updated by work Marcia Honig and Steve Thomas did while in the Hume lab (Hume and Honig, 1986; Hume and Thomas, 1988; Thomas and Hume, 1990b). However the molecular identity of an ion channel gated by ATP in muscle would have to wait until 1994 when the isolation of the first P2X receptor (Valera et al., 1994). Since then the P2X family has grown to include typically seven subunits, each encoded by a different gene (North, 2002), with distant relatives found in the genomes of algae (Fountain et al., 2008) and *Dictyostelium* (Fountain et al., 2007).

Each P2X receptor subunit is comprised of two transmembrane domains with a large extracellular domain of around 300 amino acids with the amino and carboxyl termini that are located intracellularly (Figure 1.2C). A P2X receptor is thought to be comprised of three subunits (Nicke et al., 1998; Stoop et al., 1999) that can assemble either as homomers and heteromers (Torres et al., 1999). Although it appears that ATP binds between subunits (Wilkinson et al., 2006; Marquez-Klaka et al., 2007), the absence of a crystal structure precludes confirmation, However sensitivity to ATP is known to require two positively charged lysine residues immediately adjacent to the extracellular sides of TM1 and TM2 (Ennion et al., 2000; Jiang et al., 2000). Finally, P2X receptors are generally cation channels, with only one member (P2X5) exhibiting permeability to chloride (Bo et al., 2003).

Although the molecular identity of P2X receptors has been known for over a decade, only a handful of *in vivo* functions have been clearly attributed to them through studies of knock out mice. Namely in the neurogenic control of smooth muscle (Mulryan et al., 2000), gustation (Finger et al., 2005) nociception (Cockayne et al., 2000; Souslova et al., 2000) and LTP (Sim et al., 2006). Because of their absence from the genomes of *C. elegans* and *Drosophila* they have not been subjected to the pressure of forward genetics screens, which has helped identify the roles of many other proteins. Furthermore, because the assembly of P2X receptors is relative promiscuous (Torres et

al., 1999) its possible that the omission of one subunit may not generate a phenotype sufficiently well enough to be detected. This is in fact the case for P2X receptors wherein the use of P2X2/3 double knockouts revealed a role in nociception that was far more subtle in either single knock out. However the use of double knockouts also increases the probability of death *in utero* or perinatally due to an unrelated function not of interest to an investigator.

Given that some of the earliest effects of ATP on native tissue were described in skeletal muscle it's ironic that a clear role for P2X receptors within skeletal muscle has remained elusive. However some hypotheses do exist, namely that P2X signaling contributes to myogenesis both following injury and during development. *In vitro* P2X receptor signaling has been shown to be required for the differentiation of C2C12 cells (Araya et al., 2004), an immortalized cell line capable of differentiating into muscle. In addition P2X receptor signaling has been shown to be essential for the differentiation of satellite cells (Ryten et al., 2002). Satellite cells are a population of pluriopotent progenitor cells that lie between the basal lamina and the sarcolemma. In response to injury satellite cells are triggered to exit from their quiescent state and re-enter the cell cycle to proliferate, followed by differentiation to form new muscle. Consistent with a role in regeneration *in vivo* the up-regulation of several P2X receptors has been observed in regenerating skeletal muscle of the mouse model for muscular dystrophy "*mdx*" (Ryten et al., 2004). A role for P2X receptor signaling in myogenesis during development stems from the finding that P2X receptors are expressed during myogenesis in multiple organisms (Meyer et al., 1999; Ruppelt et al., 2001; Ryten et al., 2001; Diaz-Hernandez et al., 2002; Soto et al., 2003), and the idea that development may mirror regeneration.

Our lab has been interested in the function of P2X receptors *in vivo*, and in particular the function of P2X receptors in skeletal muscle (Hume and Honig, 1986; Hume and Thomas, 1988; Thomas and Hume, 1990a, b; Thomas et al., 1991; Thomas and Hume, 1993; Wells et al., 1995). To explore P2X receptor function *in vivo* we turned to zebrafish as a model organism and took a reverse genetic approach in chapter IV. We first cloned the P2X family from zebrafish, and then employed the use of antisense morpholinos to systematically knockdown the expression of P2X receptors. We uncovered several polymorphisms that partially account for the previously reported

inactivity of some P2X receptors from zebrafish. In addition we demonstrate that P2X5.1 in zebrafish is required for skeletal muscle's responsiveness to ATP, but is not required for myogenesis during development. Thus the search for a role for P2X receptors is skeletal muscle continues.

Figures

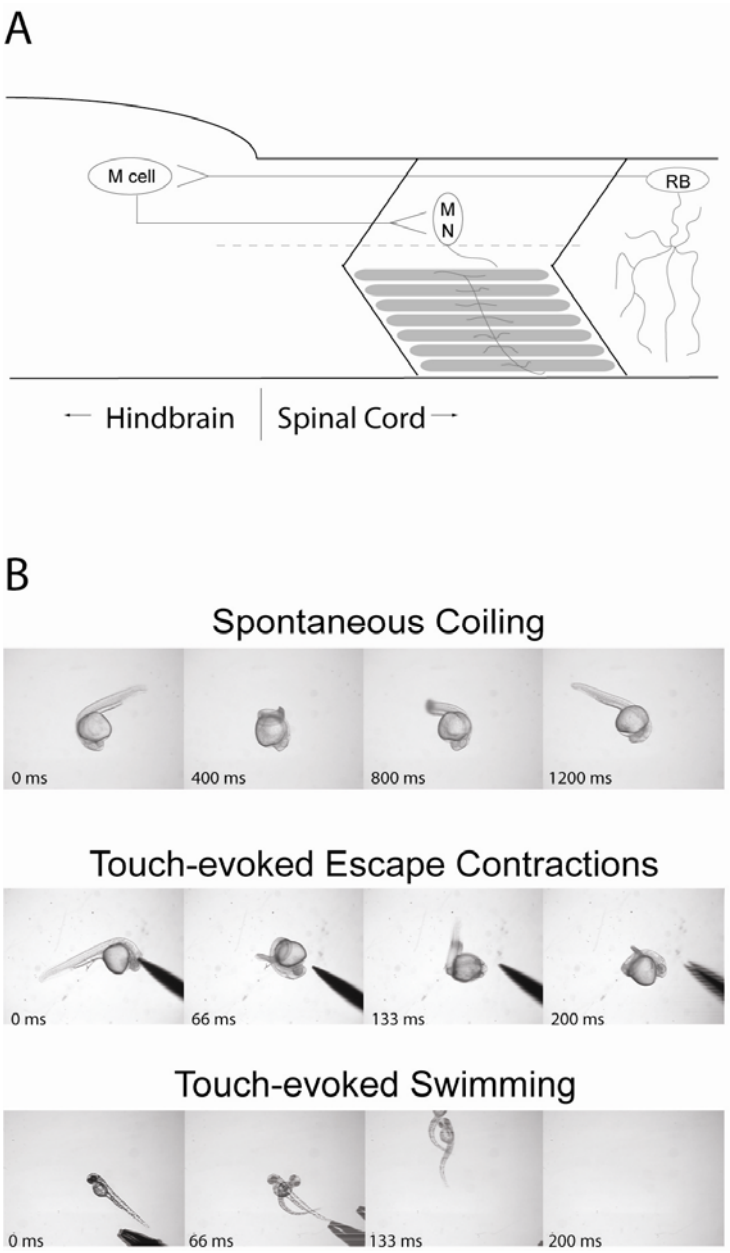

Figure 1.1: The touch-evoked escape circuit belonging to zebrafish. **(A)** A schematic depicting sensory input originating from the activation of the mechanosensitive Rohon-Beard (RB) neurons which project into the hindbrain and lead to the activation of M cells. M cells in turn make monosynaptic connections with motor neurons (MN) innervating axial skeletal muscle. Not shown is sensory input originating from sensory trigeminal, or additional primary motor neurons. **(B)** Motor behaviors exhibited by zebrafish within the first 48 hpf.

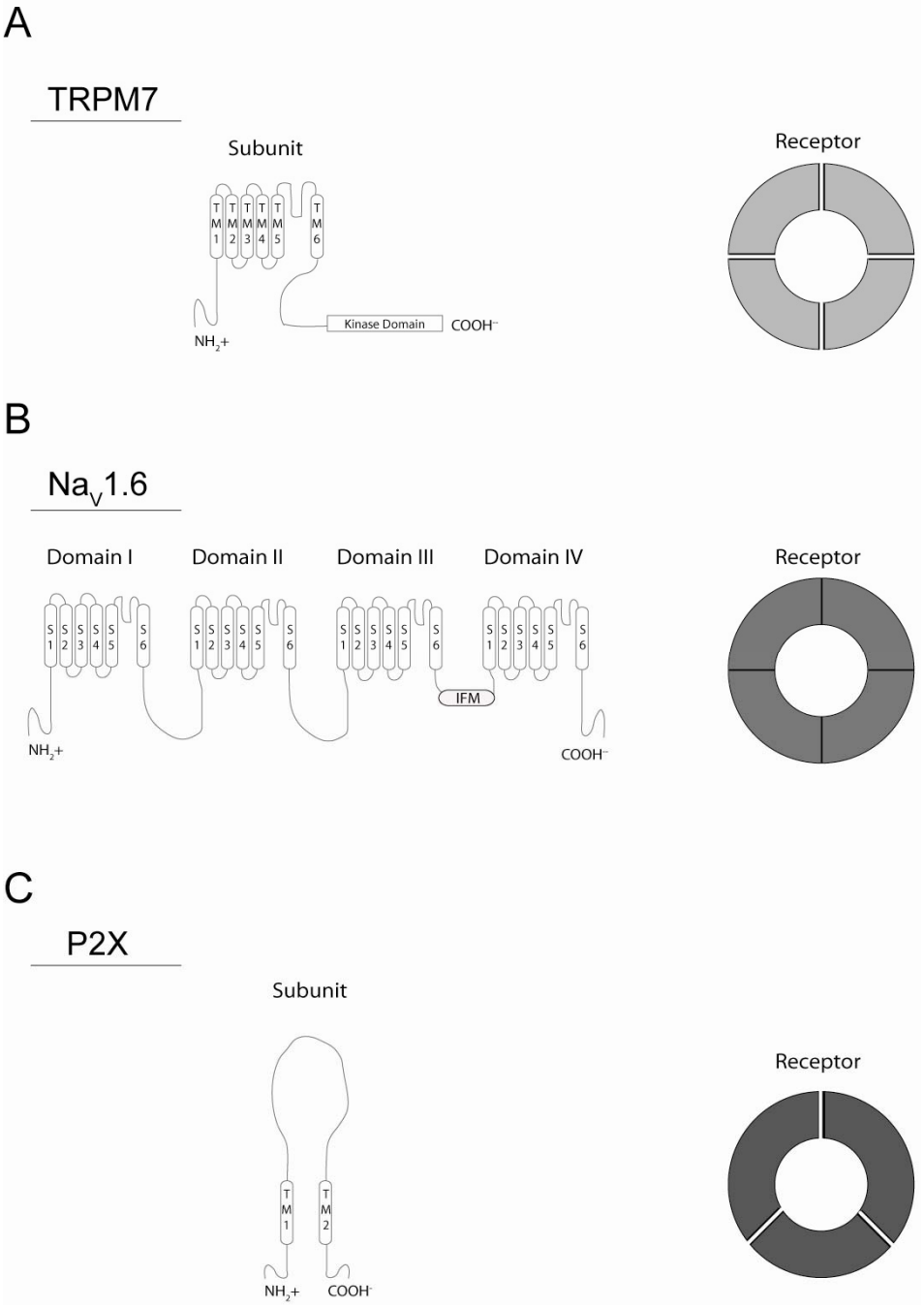

Figure 1.2: Topology and assemble of TRPM7, a voltage-gated sodium channel and P2X receptor. **(A)** TRPM7 is thought to assemble as a tetramer similar to voltage-gated potassium channels. Each subunit is predicted to be comprised of six transmembrane domains (TM1-6), with the pore region formed between TM5 and TM6. The atypical alpha kinase is located on the C-terminal. **(B)** Voltage-gated sodium channels are one continuous protein, with four pseudosymmetric domains each comprised of six membrane spanning segments (S1-S6). The pore is formed between S5 and S6. **(C)** The ligand gated P2X receptor is thought to assemble as a trimer, with each subunit possessing two transmembrane domains with a large extracellular domain.

CHAPTER II

TRPM7 IS REQUIRED BY VERTEBRATE MECHANOSENSITIVE CELLS FOR SENSITIVITY TO LIGHT, NON-PAINFUL TOUCH

Summary

The touch unresponsive zebrafish mutant *touchdown* arises from mutations in the gene encoding TRPM7. We show that *touchdown* mutants fail to respond to light touch, but respond to various forms of noxious stimuli with partial escape behaviors. TRPM7 was found to be expressed by mechanosensitive neurons, wherein the expression of wild type TRPM7 was sufficient to restore escape behaviors in response to light touch and noxious stimuli. The ability of TRPM7 to rescue sensitivity to light touch required a functional channel, but was independent of TRPM7's kinase activity and permeability to divalent cations. Heterologous expression of TRPM7 conferred mechanical sensitivity to an otherwise mechanically insensitive cell. From these findings we propose that TRPM7 is a component of the system producing sensitivity to light touch.

Introduction

TRPM7 belongs to a large family of ion channels whose members have been implicated in many different physiological processes including thermosensation, chemosensation, and visual transduction (Clapham, 2003). There is also mounting evidence that members of the TRP family may play a role in mechanosensation (Colbert and Bargmann, 1995; Haffter et al., 1996; Liedtke et al., 2000; Walker et al., 2000; Liedtke et al., 2003; Sidi et al., 2003; Tracey et al., 2003; Corey et al., 2004; Al-Anzi et al., 2006; Kindt et al., 2007). However, identifying the molecular elements required for mechanotransduction in vertebrates has proved to be a frustrating task, with substantial counterevidence arising every time a strong candidate for the mechanosensor protein has appeared (Suzuki et al., 2003a; Bautista et al., 2006; Kwan et al., 2006). The studies reported here began with a detailed analysis of the phenotype of a zebrafish mutant which fails to respond to light touch. Our results establish that TRPM7 is required for sensory neurons to communicate touch information to second order interneurons, and suggest the possibility that TRPM7 might play a direct role in the transduction of light touch into electrical signals in zebrafish sensory neurons.

Materials and Methods

Animal Care and Use

Zebrafish were bred and raised according to approved guidelines set forth by the University Committee on Use and Care of Animals, University of Michigan. Developmental staging of embryos was performed either by counting somites prior to 24 hours post-fertilization (hpf), or by assessing the migration of the lateral line primordia as described previously (Kimmel et al., 1995). *Touchdown* alleles tdo^{b508} and tdo^{tz310c} were kindly provided by Dr. Paul Henion (The Ohio State University, Columbus, OH) and The Zebrafish International Resource Center, (P40 RR12546 from NIH-NCRR), respectively. *Touchdown* allele tdo^{mi174} was identified in a screen conducted at the University of Michigan, Ann Arbor following standard procedures (Haffter and Nusslein-Volhard, 1996). All experiments other than complementation analysis were performed using *touchdown* allele tdo^{mi174}.

Behavioral experiments and complementation analysis

Embryos obtained by crossing heterozygous parents were raised in a 28.5 ^{0}C water bath. Prior to the beginning of an experiment, embryos were dechorionated with pronase, staged as described above and placed into the chambers of 24-well plates (one embryo per well). Touch-evoked behaviors were elicited by touching the head, yolk sac, trunk or tail region up to 3 times with the tips of a pair of No. 5 forceps. Noxious stimuli was delivered either by pinching the tail up to 3 times with the tips of a pair of No. 5 forceps, or by transferring an embryo into a chamber of a 24-well plate preloaded with mustard oil (allyl-isothiocyanate) or glacial acetic acid to a final concentration of 0.1 % (v/v). Touch-evoked behaviors were recorded (30 Hz) using a Panasonic CCD camera (wv-BP330) mounted to a Leica stereomicroscope at ~32 X magnification. Images were captured and analyzed off-line using Scion Image (www.scioncorp.com).

For complementation analysis heterozygous carriers for *touchdown* alleles tdo^{mi174}, tdo^{mi174}, and tdo^{mi174} were pair wised crossed and scored for hypopigmentation and touch responsiveness at 55 hpf.

Cloning of *trpm7*

5’ and 3’ RACE ready cDNA (GeneRacer kit, Invitrogen, Carlsbad, CA) was synthesized from total RNA extracted from the WIK background at 48 hpf using TRIzol® Reagent (Invitrogen, Carlsbad, CA). Cloning of *trpm7* was performed by PCR amplification (Pfu Turbo Polymerase, Stratagene, La Jolla, CA) using RACE kit primers and the following primers raised against the published TRPM7 sequence (AY860421):
forward, 5'- GTGAAGTCGATCTCTAACCTGGT -3';
reverse, 5'- TAGGATGAAGTGATAGCGCTGATA -3’.
The PCR product was A-tailed using Taq DNA Polymerase (Promega, Madison, WI) and subcloned into pGEM-Teasy (Promega, Madison, WI). Five individual clones were sequenced and compared.

An endogenous Xho I site was removed from the *trpm7* coding sequence by base pair substitution at position 3258 to facilitate future directional subcloning using a QuikChange Site-Directed Mutagenesis kit (Stratagene, La Jolla, CA). The primers used were as follows: forward, 5’- GTGTGCGAACTCAAGTGAGGAA -3’;
reverse, 5’- TTCCTCACTTGAGTTCGCACAC -3’. The underlined base pair indicates the position of substitution. Assembly of the full length *trpm7* cDNA was achieved via splice by overlap extension using the *trpm7* specific primers listed above for the RACE reaction, in conjunction with the following primers: forward, 5'-GGTACCATGTCCCAGAAGTCCTGG-3'; reverse, 5'-CTCGAGTCACAGCATTAAGCGCAT-3'. The underlined sequence denotes the inclusion of Kpn I and Xho I sites for directional subcloning into pcDNA3.0 (Invitrogen, Carlsbad, CA).

To clone *trpm7* from *tdo*^{tz310c}, *tdo*^{b508} and *tdo*^{mi174}, total RNA from homozygous mutants was extracted as above followed by reverse transcription using an oligo(dT) primer and SuperScript III™ according to manufactures guidelines (Invitrogen, Carlsbad, CA). Full length mutant *trpm7* was assembled by splice by overlap extension as above. Five individual clones were sequenced and compared.

Site-directed mutagenesis

Wild type *trpm7* in pcDNA3.0 or in zCREST2-hsp70:TRPM7-EGFP was used as template. Mutations were generated using the QuikChange site-directed mutagenesis kit (Stratagene, La Jolla, CA). All mutations were confirmed by DNA sequencing (University of Michigan DNA Sequencing Core), and are referred to as $TRPM7_{D1686A}$ to represent the substitution of Aspartate 1686 with an Alanine.

Electrophysiological characterization of TRPM7 expressed by *Xenopus* oocytes

Capped RNA encoding wild-type zebrafish TRPM7, $TRPM7_{R891stop}$, $TRPM7_{L858P}$, $TRPM7_{\Delta 1410\text{-}1432stop}$, and $TRPM7_{E1026K}$, $TRPM7_{E1026Q}$, $TRPM7_{D1686A}$ were synthesized from the T7 site of pcDNA3.0 using the mMESSAGE mMACHINE® T7 kit (Ambion, Austin, TX). RNA (25 ng) dissolved in 50 nl of DEPC-ddH_20 was injected into stage V-VI defolliculated *Xenopus laevis* oocytes using a Nanoinject II system (Drummond Scientific Company, Broomall, PA). Oocytes were maintained in Barth's solution at 17 °C for ~72 hrs before electrophysiological characterization. Two-electrode voltage-clamp recordings were made with a TurboTec 3 amplifier (NPI Electronics, Tamm, Germany) at room temperature (22°C). The external recording solution was as follows (in mM): 90 NaCl, 1 KCl, 1 $MgCl_2$, 2 $CaCl_2$ and 10 HEPES, pH 7.6. Electrodes pulled from Borosilicate glass were broken manually to yield resistances ~0.5 MΩ and contained 3M KCl. Data acquisition was controlled by pClamp 8 software using a Digidata 1322A interface (Axon Instruments, Union City, CA). The initial data analysis was done in pClamp, and current-voltage relationships were fit using functions included in Sigma Plot 9.0 (SPSS, Chicago, IL).

Whole-mount *in situ* hybridization

In situ hybridization was performed as by methods similar to those previously described (Westerfield, 1993). Template was prepared by cutting 1.2 µg of plasmid DNA by restriction enzyme digest and Phenol/Chloroform precipitated by the following method. Following a 1-2 hr digest 2 mg of Protinase K plus SDS to a final concentration of 0.5% was added and incubated at 50 ^{0}C for 30 minutes. Thereafter 200µl ddH_20, 8µl 5M NaCl, 1µl glycogen was added and mixture vortexed. Then 100µls Phenol and 100µl

Chloroform were added and mixture vortexed. The mixture was then centrifuged at 14,000 rpm for 5 minutes at room temperature. The top phase was transferred to a fresh eppendorf tube and 200µl of Chloroform was added. The mixture was vortexed and centrifuged as before with the top phase again transferred to a fresh eppendorf tube, followed by the addition of ice cold 100% ethanol (600 µl). The mixture was placed at -80 ^{0}C for 30 minutes and then centrifuge at 4 ^{0}C for 20 minutes at 14,000 rpm. Supernatant was removed and precipitated template was resuspended in DEPC-H_2O. Riboprobes were synthesized and sheared to ~600 base pairs by alkaline hydrolysis. Probe integrity was checked by gel electrophoresis. Embryos were reared in 1-phenyl-2-thiourea (PTU) beginning ~22 hpf to prevent pigmentation and fixed at 36 and 55 hpf with 4% paraformaldehyde in PBS for one hour at room temperature (22 ^{0}C). Embryos were then dehydrated with an increasing percentage of methanol in PBS and stored at -20 ^{0}C for at least 30 minutes. Thereafter embryos were rehydrated by decreasing the percentage of methanol in PBST (PBS containing 0.1% Tween) and incubated at 37 ^{0}C with Proteinase K for 12 minutes to increase the penetration of riboprobes. Antisense and sense control riboprobes (5 µg/ml) were hybridized for ~16 hours at 65 °C. Anti-DIG antibody conjugated to alkaline phosphatase (Roche Products, Welwyn Garden City, UK) was bound overnight at 4 ^{0}C followed by chromogenic detection using a NBT/BCIP stock solution (Roche Products, Welwyn Garden City, UK). The chromogenic reaction was quenched at various time points for both antisense and sense control conditions. Staining for *trpm7* was considered specific when corresponding staining was absent in sense control.

Recording methods

All reagents and drugs were purchased from Sigma-Aldrich, St. Louis, MO. All recordings were made between 55 and 60 hours post-fertilization. Electrophysiological recording were obtained from axial skeletal muscle and motor neurons as previously described (Drapeau et al., 1999). In brief larvae were anesthetized in 1X Evans recording solution (in mM): 134 NaCl, 2.9 KCl, 2.1 $CaCl_2$, 1.2 $MgCl_2$, 10 glucose, 10 HEPES, pH 7.8, containing 0.02% tricaine and pinned to a 35 mm dish coated with Sylgard® through the notochord using 25 µm tungsten wires. The skin overlying the trunk and tail was first

scored with a broken pipette and then removed with a fine pair of #5 forceps. The solution was exchanged with 1X Evans containing TTX (1 μM), or d-tubocurarine (3 μM for muscle, 15 μM for motor neuron and Mauthner cell recordings). Throughout the recording session the bath solution was continuously exchanged at ~1 ml/min. To make motor neuron recordings the bath solution was replaced with recording solution containing 1 mg/ml collagenase Type XI and incubated at room temperature (22 ^{0}C) until the axial skeletal muscle started to separate at the somitic boundaries. Thereafter the muscle was peeled away using suction applied to a broken pipette (~50 μm). The internal solution for muscle and motor neuron recordings contained (in mM): 116 K-gluconate, 16 KCl, 2 $MgCl_2$, 10 HEPES, 10 EGTA, at pH 7.2 with 0.1% SulforhodamineB for cell type identification. Electrodes pulled from Borosilicate glass had resistances of ~1 MΩ for Mauthner cell recordings when filled with external recording solution, and 6-10 MΩ for muscle or 10-14 MΩ for motor neuron recordings when filled with internal recording solution. Recordings were made with an Axopatch 200B amplifier (Axon Instruments, Union City, CA) low passed filtered at 1-5 kHz and sampled at 1-10 kHz. Data acquisition was controlled by pClamp 8.2 software using a Digidata 1322A interface. The initial data analysis was done with Clampfit 9.2, and figures were prepared using Sigma Plot 9.0.

Touch-evoked responses were elicited by pressure application of bath solution via a broken pipette (~20μm) to the head or tail region. The pressure (20 psi) and duration (50 ms) of a stimulus was controlled by a Picospritzer II (Parker Hannifin, Fairfield, NJ). NMDA-evoked fictive swimming was achieved by perfusing the bath with recording solution containing 100 μM NMDA.

Expression of exogenous proteins in Trigeminal and Rohon-Beard neurons

Plasmid based rescue was achieved by substitution of EGFP's initial methionine in pEGFP-1 (Clontech, Mountain View, CA) containing the hsp70 promoter and zebrafish *trpm7*'s stop codon with EcoR V sites. Zebrafish *trpm7* was then subcloned into pEGFP-1 between Kpn I and EcoR V. The zCREST2 enhancer was kindly provided by Dr. Okamoto (Riken Institute, Japan) and PCR amplified using the following primers: forward, 5'-AACTCGAGGTGCAGCTTTAGACATTTA-3'; and reverse, 5'-

AAAGCTTGAATTCCAGCACCATAATT-3'. The underlined sequence denotes the inclusion of Xho I and Hind III sites. PCR product was digested with Xho I and Hind III and directionally subcloned into the hsp70:TRPM7-EGFP to generate zCREST2-hsp70:TRPM7-EGFP.

50 pg of plasmid diluted in 5 nl of water containing 0.1% phenol red and 1X Deinhardts solution was injected into one cell stage embryos using a Nanoinject II system (Drummond Scientific Company, Broomall, PA). Rescued embryos were identified by their lack of pigmentation, responsiveness to touch at 54-55 hpf.

Results

TRPM7 is required for sensitivity to light touch

Early in development zebrafish display two touch-evoked escape behaviors: contractions and swimming (Saint-Amant and Drapeau, 1998). These escape behaviors first orientate the fish away from the source of the touch, and then propel the fish out of the perceived threatening environment. In a forward genetic screen for zebrafish mutants that displayed abnormal touch-evoked behaviors, we found a hypopigmented mutant (*mi174*) that was unresponsive to touch during the second day of development (Figure 2.1A). To determine whether *mi174* mutants were also insensitive to other forms of sensory stimuli we applied reagents and stimuli known to illicit noxious responses in other organisms including harsh touch (pinch), mustard oil, and weak acid. These stimuli applied to wild type larvae routinely evoked both escape contractions and swimming. In contrast, the application of these stimuli to *mi174* mutant larvae typically resulted in escape contractions, but episodes of swimming were rarely observed (Figure 2.1B). Therefore *mi174* mutants appear to be deficient in sensitivity to light touch, and also exhibited an inability to swim in response to noxious stimuli.

Given that hypopigmentation is an easily observable phenotype we reasoned that *mi174* might be allelic to a previously identified hypopigmented mutants. Complementation analysis revealed that *mi174* was an allele of the *touchdown* / *touchtone* series of mutations. As *touchdown* was the first allele to be reported (Haffter et al., 1996; Arduini and Henion, 2004), alleles of *touchdown* and *touchtone* will be herein referred to as *touchdown* (*tdo*).

Alleles of *tdo* are known to harbor mutations in the gene encoding TRPM7 (Elizondo et al., 2005), a member of the TRP channel superfamily which possess an C-terminal enzymatically active kinase. We cloned *trpm7* from the *tdo* alleles tdo^{mi174} and tdo^{tz310c}, which revealed a nonsense mutation in the intracellular loop between TM2 and TM3 ($TRPM7_{R891stop}$), and a missense mutation within TM2 ($TRPM7_{L858P}$), respectively (Figure 2.1C). To determine the consequence of these mutations, along with a third mutation found in the previously reported allele tdo^{b508} ($TRPM7_{\Delta 1410\text{-}1432stop}$) (Elizondo et al., 2005), we assessed TRPM7 channel activity in *Xenopus* oocytes. Oocytes injected

with RNA encoding wild type TRPM7 were found to exhibit an outwardly rectifying current when subjected to voltage ramps (Figure 2.1D-left), consistent with the previously reported activity of mammalian TRPM7 expressed in *Xenopus* oocytes (Chubanov et al., 2004). In contrast, oocytes injected with RNA encoding $TRPM7_{R891stop}$, $TRPM7_{L858P}$, or $TRPM7_{\Delta 1410\text{-}1432stop}$ failed to generate currents above uninjected oocytes indicating a loss of TRPM7 channel activity in these three alleles of *tdo*.

Accompanying the initial discovery of mammalian TRPM7 was a description of a splice variant which lacked the exons encoding the transmembrane domains of TRPM7 (Runnels et al., 2001). This splice variant, referred to as the "M7-kinase", would not be expected to be affected by the mutations found in *tdo*. Therefore we initiated a screen for a zebrafish *trpm7* splice variant consistent with an M7-kinase. The use of RACE and a search of the NCBI database for the presence of a zebrafish expressed sequenced tag (EST) predicting an M7-kinase failed to uncover a splice variant consistent with an M7-kinase. Furthermore the injection of an antisense oligonucleotide (morpholino) directed against regions predicted to block the expression of mRNA encoding both splice variants mimicked, but failed to exacerbate the *tdo* phenotype. Thus zebrafish do not appear to express an M7-kinase.

Finally membrane insertion of the closely related TRPM family member TRPM6 has been shown to be facilitated by co-expression with TRPM7 (Chubanov et al., 2004). The phenotype exhibited by *tdo* might be an indirect effect on TRPM6 expression and therefore we cloned and characterized TRPM6 from zebrafish. A 1875 protein with >70 % sequence similarity to mouse TRPM6 was identified that when expressed by oocytes produced currents similar to zebrafish TRPM7 (Figure 2.1D-right). To test the contribution of TRPM6 to the *tdo* phenotype we injected a morpholino against *trpm6* into wild type clutches. Injection of the *trpm6* morpholino failed to replicate the *tdo* phenotype in wild type larvae. Thus the absence of sensitivity to light touch in *tdo* does not result from the loss of TRPM6.

TRPM7 is required for the activation of the touch-evoked escape circuit

To better understand how the loss of TRPM7 results in the loss of touch-evoked escape behaviors, we undertook an *in vivo* electrophysiological characterization of the touch-evoked escape circuit in *tdo*. Allele tdo^{mi174} was chosen for this and subsequent experiments as it represented the most severely truncated allele of *tdo*.

In zebrafish, sensitivity to touch is mediated by two groups of mechanosensitive neurons: neurons within the trigeminal ganglia relay touch to the craniofacial region, and Rohon-Beard neurons (RBs) in the spinal cord that relay touch to the trunk and tail (Figure 2.2A). Both groups of mechanosensitive neurons project axons into the hindbrain, where they lead to the activation of ~90 bilateral pairs of reticulospinal neurons during an escape response (Gahtan et al., 2002). These reticulospinal neurons in turn drive activity in other neurons including motor neurons, leading to muscle contractions and escape behaviors.

TRPM7 has been localized to mouse cholinergic synaptic vesicles where it contributes to the release of transmitter (Krapivinsky et al., 2006). We therefore determined whether the *tdo* phenotype could be partially explained by a disruption in cholinergic transmission at the zebrafish neuromuscular junction by comparing miniature end-plate currents (mEPCs) between wild type sibling and tdo^{mi174} mutants. Comparison of mEPSCs revealed that although the frequency of mEPSCs was slightly higher in wild type siblings (0.33 ± 0.04 Hz vs. 0.24 ± 0.02 Hz), the amplitude distributions of these events were not substantially different (Figure 2.2B). Therefore that TRPM7 is not required for the release of acetylcholine from cholinergic vesicles at the neuromuscular junction in zebrafish and therefore does not account for the tdo^{mi174} phenotype.

The primary muscle type involved in locomotion in zebrafish is axial skeletal muscle of the trunk and tail. Axial skeletal muscle is comprised of slow and fast twitch fibers, both of which are active during swimming (Buss and Drapeau, 2002). Evoked synaptic drive to skeletal muscle was recorded in the presence of 3 μM curare, a concentration sufficient to attenuate membrane depolarization below the level of spiking. Under these conditions touch to wild type animals was found to evoke bouts of rhythmic membrane depolarizations in skeletal muscle consistent with previous reports of fictive swimming in zebrafish (Figure 2.2C; n = 5/5) (Buss and Drapeau, 2002). In contrast, a

similar stimulus failed to induce membrane depolarizations of *tdo*^{mi174} mutant skeletal muscle (n = 0/5).

An absence of synaptic drive to skeletal muscle in *tdo*^{mi174} mutants might reflect a problem with activity dependent release of neurotransmitter at the NMJ, or a defect within the nervous system of *tdo*^{mi174} mutants. Recordings were therefore made from wild type and *tdo*^{mi174} mutant primary motor neurons. Each hemisegment in zebrafish contains three primary motor neurons (RoP, MiP, CaP), which can be identified based on their size, position within the spinal cord, and innervation pattern of skeletal muscle (Westerfield et al., 1986; Drapeau et al., 1999). Recordings made from primary motor neurons revealed episodes of bursting following touch in wild type larvae (Figure 2.2D; n = 5/5). In contrast a similar stimulus failed to induce events in motor neurons of *tdo*^{mi174} mutant larvae (n = 0/5). This finding indicates that a defect within the central nervous system is present in *tdo*^{mi174} mutants.

Of the ~90 or so reticulospinal neurons known to be active during escape behaviors, the role of the Mauthner (M) cells in fish is best understood (Korn and Faber, 2005). M cells receive direct sensory input from mechanosensitive neurons, and in turn make monosynaptic connections with motor neurons. Activity in M cells follows an aversive stimuli, precedes the onset of escape behaviors, and is sufficient to trigger escape behaviors. These features have lead to the labeling of M cells as "command neurons", and as such M cells serve as an indicator of activity within the zebrafish escape circuit. Furthermore activity in M cells can be readily detected by using an extracellular recording electrode as a shift in the local field potential (LFP) when M cells fire action potentials. In wild type siblings, touch evoked an LFP in the majority of larvae (Figure 2.2E; n = 8/15). The absence of activity in some wild type larvae may reflect the immaturity of the circuit at this stage of development (55-60 hpf) (Eaton and Farley, 1975). In contrast, a similar stimulus failed to evoke an LFP in *tdo*^{mi174} mutants (n = 0/15). These findings indicate that TRPM7 is required to activate the touch-evoked escape circuit in zebrafish.

TRPM7 is required to the activate an intact locomotor network

Although touch failed to activate the touch-evoked escape circuit in *tdo*^{mi174} mutants we wondered whether the locomotor network that underlies swimming in zebrafish was intact in *tdo*^{mi174} mutants. The excitatory amino acid NMDA has been shown to induce patterned synaptic activity in motor neurons similar to that induced by touch (McDearmid and Drapeau, 2006). To assess activity within the locomotor network we recorded from axial skeletal muscle as zebrafish muscle is polyinnervated, and therefore recordings from muscle sample a large fraction of CNS output. Prior to the application of NMDA spontaneous bouts of fictive swimming were rarely observed (wild type siblings n = 1/5, *tdo*^{mi174} n = 0/5). In contrast the application of NMDA to the bath induced repetitive bouts of fictive swimming in both wild type (Figure 3.3A, top) and mutant larvae.

Upon closer examination (Figure 3.3A, bottom) episode periods, episode durations and the frequency of fictive swimming induced by NMDA were similar between wild type and mutant larvae (Figure 3B-C). In wild type, the average episode period was 3.82 ± 0.40 seconds, with average episode duration of 1.12 ± 0.15, and average fictive swimming frequency 22.95 ± 0.90 Hz. In *tdo*^{mi174} mutants the average episode period was 4.43 ± 0.83 s, with average episode duration of 1.01 ± 0.16 s, and average fictive swimming frequency of 24.46 ± 0.92 Hz. Therefore the locomotor network that underlies swimming is normal in *tdo*^{mi174} mutants which indicates, (1) evoked transmitter release at the neuromuscular junctions is normal in *tdo*^{mi174}mutants, and (2) that TRPM7 is required for touch to turn on activity in this network.

Restoration of TRPM7 channel activity within mechanosensitive neurons is sufficient to rescue sensitivity to touch

To gain insight into how the loss of TRPM7 leads to an inability of touch to trigger activity within an intact locomotor network, we assessed the expression of *trpm7* during the period of touch unresponsiveness. *In situ* hybridization revealed that *trpm7* is expressed at low levels by most cell types, and at higher levels by trigeminal neurons and RBs (Figure 2.4A). To determine whether expression of wild type TRPM7 by these mechanosensitive neurons is sufficient to restore touch-evoked behaviors, we fused

TRPM7 to EGFP and placed it under control of the zCREST2-hsp70 sensory neuron enhancer-promoter construct which has been demonstrated to drive the expression of transgenes in trigeminal neurons and RB neurons (Uemura et al., 2005). Clutches of embryos obtained from crosses of heterozygous parents injected with the "rescue" plasmid zCREST2-hsp70:TRPM7-EGFP exhibited the expected proportion of homozygous recessive hypopigmented larvae (28.1 ± 1.2 %; $n = 5$ trials, >20 embryos each), however the majority of hypopigmented larvae were touch responsive, exhibiting both escape contractions and swimming (Figure 2.4B). To determine whether expression by these mechanosensitive neurons also rescued swimming in response to noxious stimuli we isolated touch responsive mutants (rescued), and exposed them to mustard oil. We found that the majority of rescued mutants (93 ± 5%; $n = 3$ trials, >20 mutants for each trial) also displayed robust escape contractions followed by swimming in response to mustard. Thus TRPM7 is required by mechanosensitive neurons for eliciting escape behavior in response to light touch and noxious stimuli.

The initial report detailing the identification of TRPM7 concluded that kinase activity modulated channel activity (Runnels et al., 2001). However subsequent experiments have clearly demonstrated that the activity of TRPM7's kinase is not required for the activity of its ion channel (Nadler et al., 2001; Matsushita et al., 2005). While these series of experiments have addressed the role of the kinase *in vitro*, evidence for the contribution of TRPM7 channel and kinase activity *in vivo* is lacking. Therefore we used our rescue plasmid to examine the *in vivo* contribution of TRPM7's kinase and channel activity to zebrafish touch-evoked behaviors. We made several amino acid substitutions within TRPM7 known to either remove the phosphotransferase activity of TRPM7's kinase domain ($TRPM7_{D1686A}$) (Matsushita et al., 2005), reduce TRPM7's permeability to divalent cations including calcium ($TRPM7_{E1026Q}$) (Li et al., 2007), or abolish TRPM7 channel activity altogether ($TRPM7_{E1026K}$) (Li et al., 2007). TRPM7 channel activity was first assessed by recordings made from oocytes expressing these mutated versions of TRPM7. The removal of an essential aspartate residue in the "TDP" motif necessary for kinase activity in $TRPM7_{D1686A}$ exhibited normal channel activity. The pore mutant $TRPM7_{E1026Q}$ lacked outward rectification consistent with a severe reduction in $Ca2^{+}$ permeability rendering TRPM7 a monovalent cation channel. Finally

the pore mutant $TRPM7_{E1026K}$ failed to generate currents above background (Figure 2.4C). These findings are in agreement with the previous reported activity of analogous mutations in mammalian TRPM7 (Matsushita et al., 2005; Li et al., 2007).

Similar to wild type TRPM7, when expression of $TRPM7_{D1686A}$ and $TRPM7_{E1026Q}$ was driven in sensory neurons by injecting mutant forms of zCREST2-hsp70:TRPM7-EGFP into embryos, touch sensitivity was restored (Figure 2.4D). In contrast, mutants injected with $TRPM7_{E1026K}$ failed to display a significant sensitivity to touch when compared to mutants from uninjected clutches. From these findings we conclude that TRPM7's kinase activity, and permeability to divalent cations are dispensable for zebrafish touch-evoked behaviors, but that an intact ion channel is required.

TRPM7 is not required for the survival of mechanosensitive neurons

Several studies have suggested a role for TRPM7 in cell survival (Nadler et al., 2001; Aarts et al., 2003; Schmitz et al., 2003), including a cell-autonomous role in the melanin synthesizing cells (melanophores) of zebrafish (Cornell et al., 2004). To explore whether TRPM7 is required by mechanosensitive cells for survival, wild type and *tdo*^{mi174} mutant larvae we incubated in acridine orange, a vital dye that labels dying cells in zebrafish (Seiler and Nicolson, 1999). Acridine orange failed to label RBs of the dorsal spinal cord, or cells near the trigeminal ganglion in both wild type and *tdo*^{mi174} mutants.

Cell death was further assessed by crossing *tdo*^{mi174} into the stable transgenic ssx-mini-ICP:EGFP which expresses EGFP within RBs and trigeminal neurons (Higashijima et al., 2000) which revealed EGFP in both trigeminal neurons and RBs (Figure 2.5A). In addition the morphology of peripheral branches of trigeminal neurons and RB neurons within the skin did not differ between *tdo*^{mi174} mutants and wild type larvae. Therefore neither the loss of mechanosensory neurons, nor an abnormality in their morphology accounts for the loss of sensitivity to touch in *tdo*^{mi174} mutants.

Mechanosensory neurons retain the ability to generate action potential in the absence of TRPM7

RBs from wild type and mutant larvae were found to exhibit a similar resting membrane potential (wild type: -64.3 ± 1.2 mV vs. *tdo*^{mi174}: -63.3 ± 1.7 mV). Although it

was not possible to achieve a space clamp within the spinal cord of zebrafish, RBs studied under voltage-clamp in wild type and mutant larvae exhibited inward and outward currents consistent with the previous reports of sodium and potassium channel activity (Pineda et al., 2005) (Figure 2.6A). Arguably a more relevant measure of RB membrane properties is the ability of RBs to generate action potentials in response to membrane depolarization. We found that the threshold for triggering overshooting action potentials was similar in wild type and *tdo*^{mi174} mutant (wild type: -46.0 ± 2.8 mV vs. *tdo*^{mi174}: -45.7 ± 1.8 mV) (Figure 6B). Thus a loss TRPM7 does not affect the ability of RBs to generate action potentials, and therefore an inability of RBs to spike cannot account for the loss of sensitivity to touch in *tdo*^{mi174} mutants.

TRPM7 confers sensitivity to mechanical stimuli to HEK cells

Members of the TRP channel superfamily have been shown to exhibit sensitivity to mechanical force when expressed in heterologous systems (Kindt et al., 2007; Numata et al., 2007). To explore whether zebrafish TRPM7 exhibits sensitivity to mechanical stimuli we recorded from HEK cells expressing TRPM7-EGFP while applying a mechanical force. Traditionally this has been achieved through the application of suction to cells under the whole-cell patch clamp configuration, or to patches of membrane excised from cells expressing a putative mechanoreceptor with intent to mimic mechanical stress (Liedtke et al., 2003; Kindt et al., 2007). However this approach does not fully recapitulate the time course of mechanoreceptor activation that is thought to occur in less than 5 ms. We therefore elected to induce mechanical stress by delivering voltage commands to the piezoelectric manipulator controlling our recording pipette, resulting in discrete micrometer deflections of the cell membrane with an onset on the order of microseconds (Moffatt and Hume, 2007). We observed brief pulses of current at the onset and the offset of movements, which were absent in untransfected cells (Figure 2.7A). In addition the amplitude of the responses increased with stimulus intensity (Figure 2.7B). However, the current was inward when the movement began and outward when it ended, and were of similar amplitude and duration. These results suggest that zebrafish TRPM7 can confer a mechanically sensitive “gating-like” current to an otherwise mechanically insensitive cell.

Discussion

The touch unresponsive zebrafish mutant *touchdown* (*tdo*) arises from mutations in the gene encoding TRPM7. *In vivo* electrophysiological recordings from *tdo* mutants revealed that normal synaptic communication was present at the neuromuscular junction and in the locomotor network that underlies swimming. However the Mauthner cell, a key second order interneuron, failed to activate in response to touch. Thus in *tdo* mutants there is a breakdown in communication between sensory neurons and reticulospinal neurons. Consistent with a defect at this level, we detected elevated expression of *trpm7* by known mechanosensitive cells. These mechanosensitive cells were present and appeared morphologically normal. Furthermore RBs in mutant animals retained the ability to generate action potentials in response to depolarizing current injections. Most importantly, when wild type TRPM7 was selectively expressed in RB neurons, normal escape behavior in response to light touch and noxious stimuli were restored.

The ability to rescue escape behavior by reintroduction of TRPM7 into sensory neurons allowed us to test *in vivo* the importance of various parts of this large, complex molecule. We found in the context of the escape behaviors, the kinase activity appears to be unimportant, as a mutant known to eliminate catalytic activity was still able to efficiently rescue the phenotype. Similarly, the ability to allow calcium to flow through the channel was not required to rescue the phenotype. However, a mutant with an impaired pore failed to rescue, so the depolarization caused by activation of this channel likely is important.

We considered several possible roles for TRPM7 within sensory neurons. For instance this molecule might be present in the central terminals of the sensory neurons, and facilitate transmitter release, as it has been proposed to do in mammalian autonomic neurons (Krapivinsky et al., 2006). If TRPM7 played this role in other classes of sensory neurons as well, it might explain our observation that TRPM7 was also required to trigger swimming in response to noxious stimuli. Alternatively, TRPM7 might be directly involved in detecting the light touch, similar to the role proposed for TRPV4 in *C. elegans* (Colbert and Bargmann, 1995). In support of the idea that TRPM7 plays a direct role in mechanosensation in the peripheral terminals of sensory neurons, we

demonstrated that in HEK 293 cells transfected with TRPM7, but not untransfected controls, moving the recording pipette a few micrometers to induce gentle stress on the membrane was sufficient to produce a transient current. The transient currents induced by movement in TRPM7 transfected HEK cells are inconsistent with ion flow through the open TRP channel because, under voltage clamp at a negative holding potential, there is no plausible mechanism to produce an inward current when the pipette is moved away from the cell and an outward current when the pipette is restored to its original position. However these currents are consistent with the movement of charges within the membrane (i.e. a gating current). Thus a potential mechanism is that mechanical stress gives rise to a conformational change in the TRPM7 protein that moves charges within the membrane, and that under some circumstances (but not those present in HEK cells) this conformational change then leads to opening of the TRPM7 channel producing a depolarization.

Figures

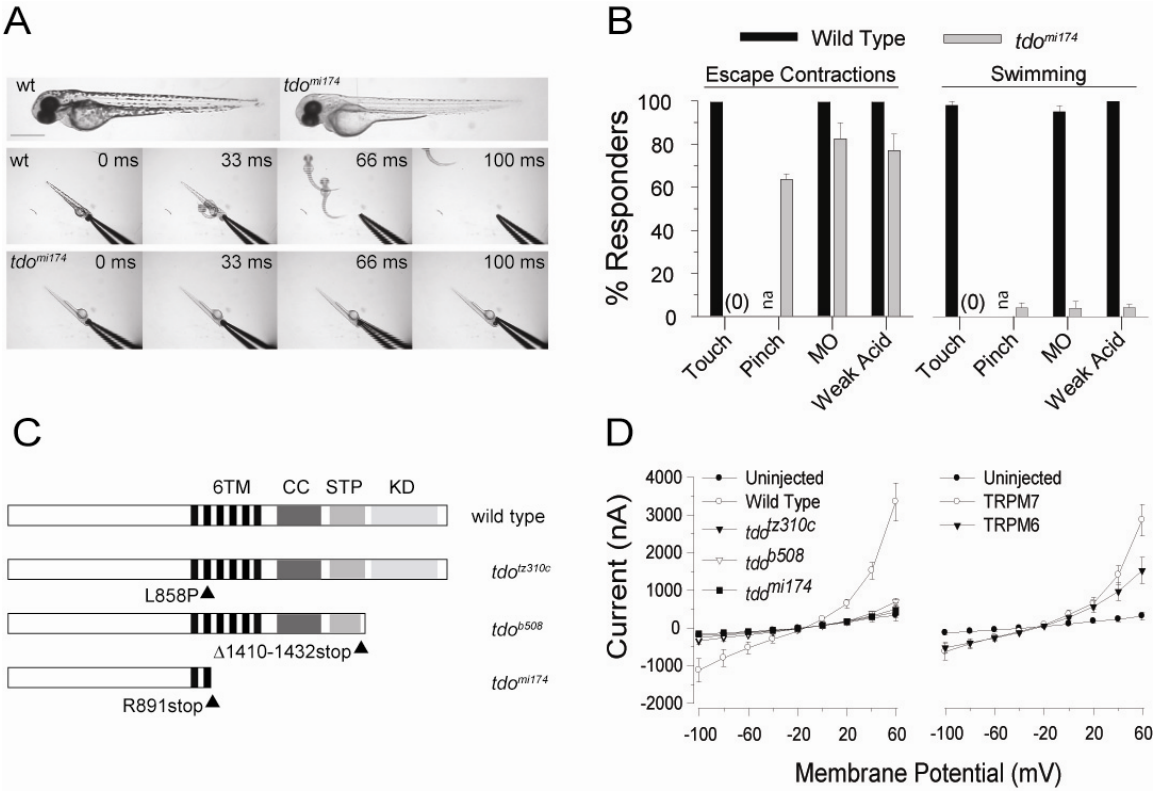

Figure 2.1: Characterization of the *tdo* phenotype. **(A)** Top: a comparison of the hypopigmented phenotype between wild type and *tdo*^{mi174} mutant larvae (scale bar: 0.5mm). Middle and Bottom: time lapse video analysis of touch-evoked behaviors. Middle: in response to light touch a single 54 hpf wild type larvae initiated an escape contraction followed by swimming which propelled the embryo out of the field of view. Bottom: a similar touch to head of a *tdo*^{mi174} mutant failed to result in either escape contractions or swimming. Identical results were obtained for *tdo*^{tz310c} and *tdo*^{b507} mutant larvae. **(B)** Ability of noxious stimuli to evoked escape behaviors. Values are the average ± SEM of three trials for each stimulus, n = 24 larvae per trial for wild type and mutant. **(C)** Graphical representation of the mutations associated with three alleles of *tdo* compared to wild type. (6TM) six transmembrane domains, (CC) coiled-coil domain, (STP) Serine-Threonine-Proline rich domain, (KD) kinase domain. *tdo*^{tz310c} results from a missense mutation which results in the substitution of leucine 858 for a proline within the second transmembrane domain. *tdo*^{b508} results from a point mutation causing improper processing of RNA transcripts producing altered amino acids from position 1410 to 1432, followed by a premature stop. *tdo*^{mi174} results from a nonsense mutation which truncates the protein prior to the channel and kinase domains. **(D)** Current-voltage relationships of TRPM6 and TRPM7 currents from *Xenopus* oocytes under two-electrode voltage clamp. Values represent the average ± SEM, n = 10 for each.

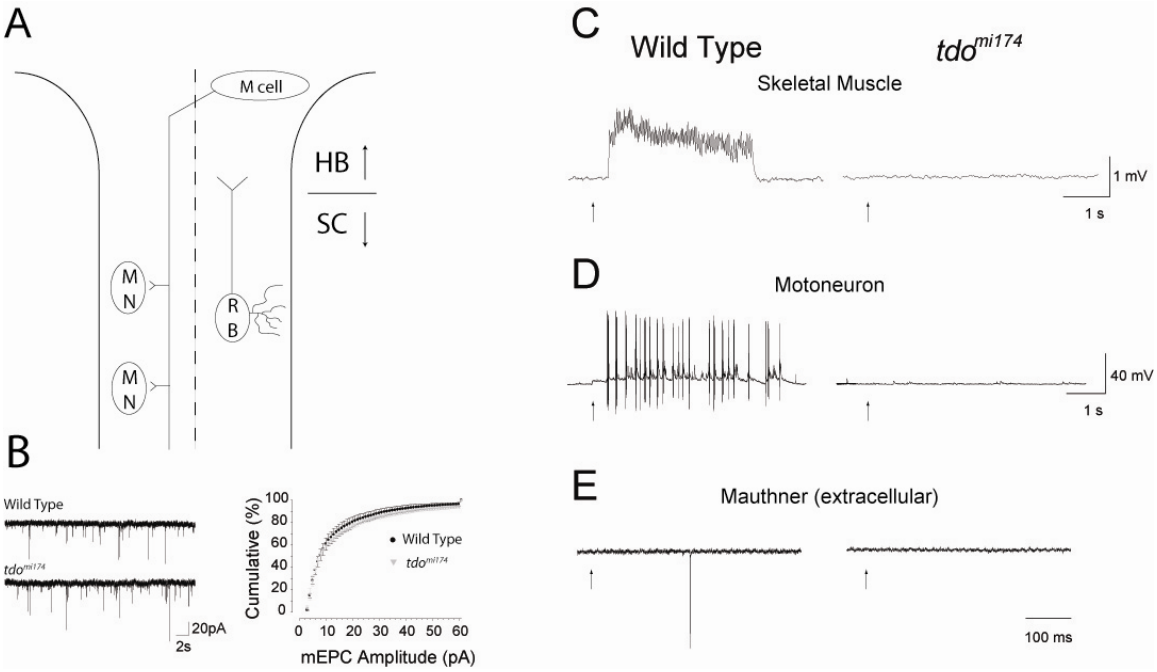

Figure 2.2: *In vivo* electrophysiological characterization of the zebrafish touch-evoked escape circuit. **(A)** A schematic of the touch-evoked escape circuit of zebrafish at the level of the Spinal Cord (SC) Hindbrain (HB) boundary. The dashed line indicates the dorsal midline. (RB) Rohon-Beard neuron, (M) Mauthner cell, (MN) motor neuron, not shown is axial skeletal muscle. **(B)** Cumulative histogram for mEPSC amplitude for wild type compared to *tdo*^{mi174} mutants (n = 5 for each). **(C)** Touch-evoked fictive swimming induced by pressure application to the tail of a wild type larvae. A similar stimulus fails to evoke fictive swimming in a *tdo*^{mi174} mutant larvae. Arrows in C-E indicate approximate time of stimulus. **(D)** Touch-evoked bursting in a motor neuron induced by pressure application to the tail of a wild type larvae. A similar stimulus fails to evoke bursting in a motor neuron of a *tdo*^{mi174} mutant larvae. **(E)** Two Mauthner cell extracellular field potential recordings wherein the (*) indicates the LFP.

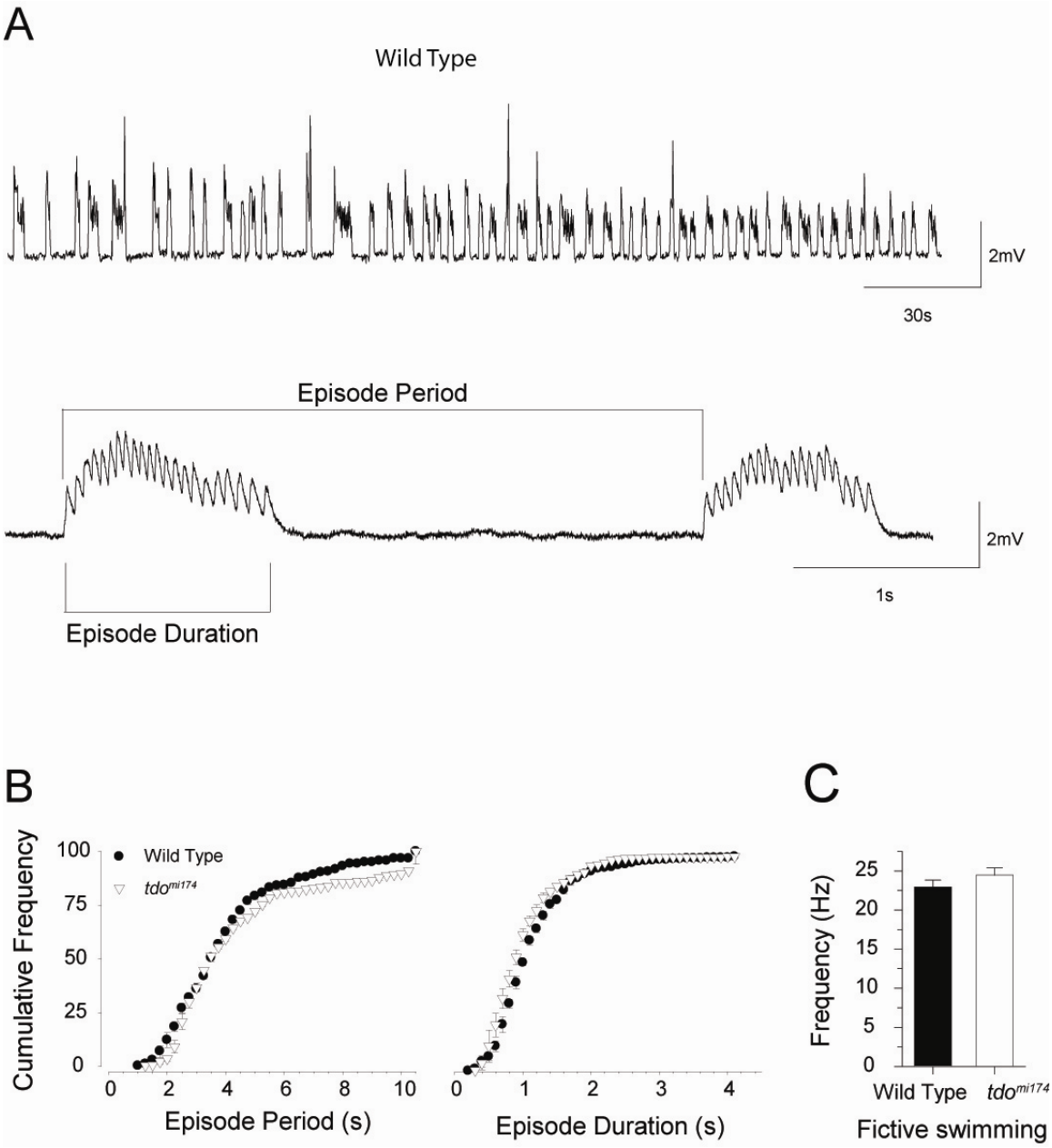

Figure 2.3: *In vivo* characterization of the *tdo* locomotor network**. (A)** Several minutes of NMDA-evoked fictive swimming. **(B)** Faster sweep of NMDA-evoked fictive swimming where Episode Period (EP) is time between the first event of a bout of fictive swimming to the first event of the following bout of fictive swimming, and Episode Duration (ED) is the time between the first event and last event within a bout of fictive swimming. **(C)** Episode period and Episode Duration cumulative histograms. **(D)** Fictive swimming frequency, defined as the number of events within an episode divided by the episode duration.

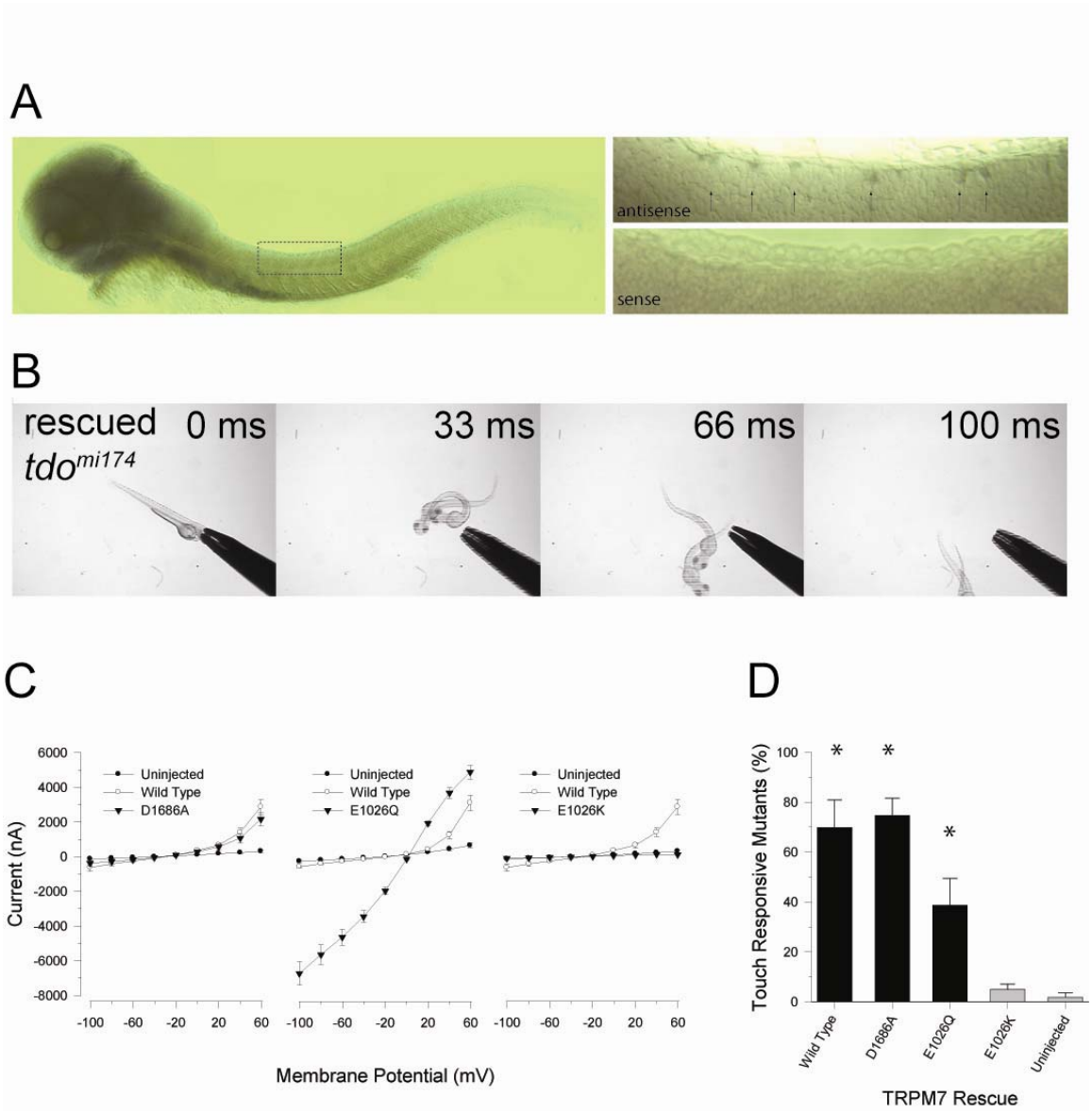

Figure 2.4: *trpm7*/TRPM7 expression analysis. **(A)** Whole-mount *in situ* hybridization of a 52 hpf larvae (top-left), with enlargement of boxed area (top-right), and a similar area in a sense control (bottom-right). Arrows indicate presumptive RB cells. **(B)** Rescue of touch-evoked behaviors in a 55 hpf mutant larvae. **(C)** Electrophysiological analysis of TRPM7 variants expressed by *Xenopus* oocytes and studied under two-electrode voltage-clamp. Values represent the average ± SEM, $n = 10$ for each. **(E)** Ability of TRPM7 variants to rescue touch-evoked behaviors. Values represent the average ± SEM for 3-5 trials, $n = 20$-30 mutants for each trial.

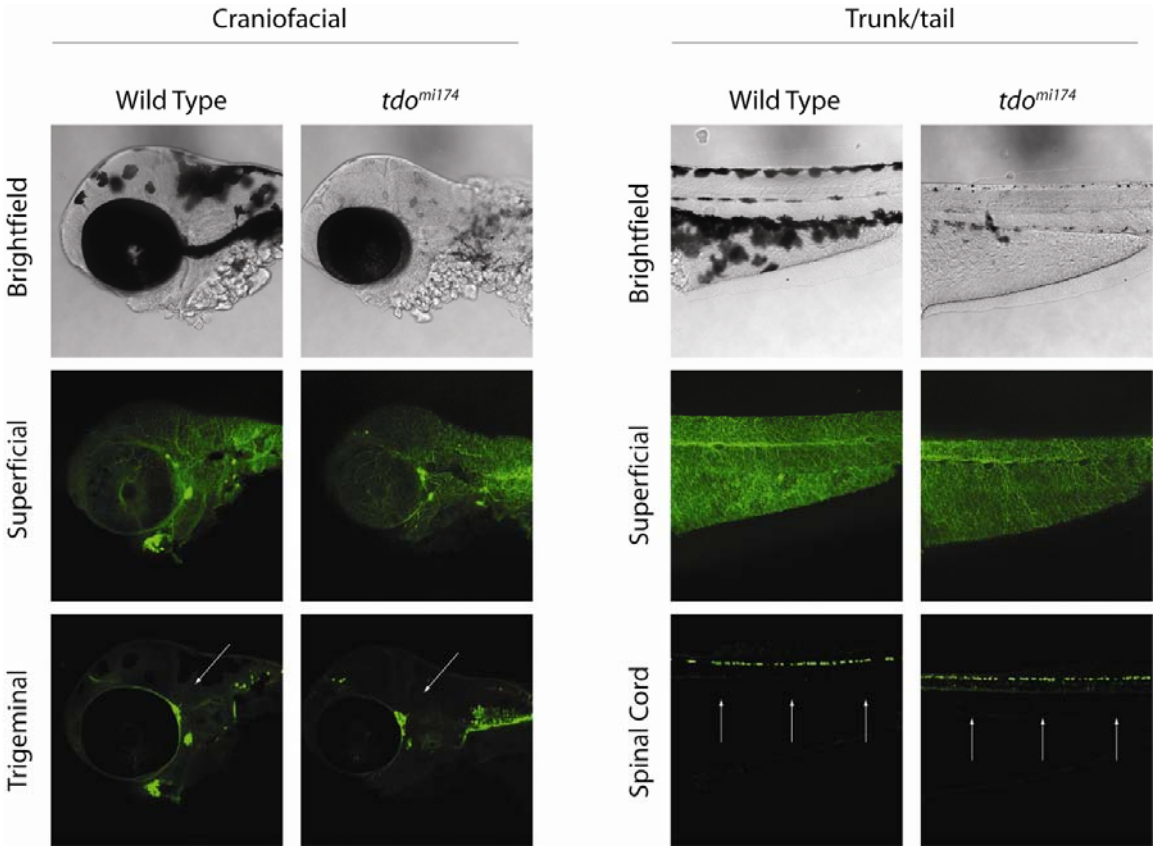

Figure 2.5: Anatomical organization and morphology of mechanosensitive cells. Whole-mount immunohistochemistry (anti-EGFP) of wild type and *tdo*^{mi174} mutant larvae in the ssx-mini-ICP:EGFP background (55 hpf). Arrows indicate trigeminal ganglia (left) and cells bodies of Rohon-Beard neurons (right).

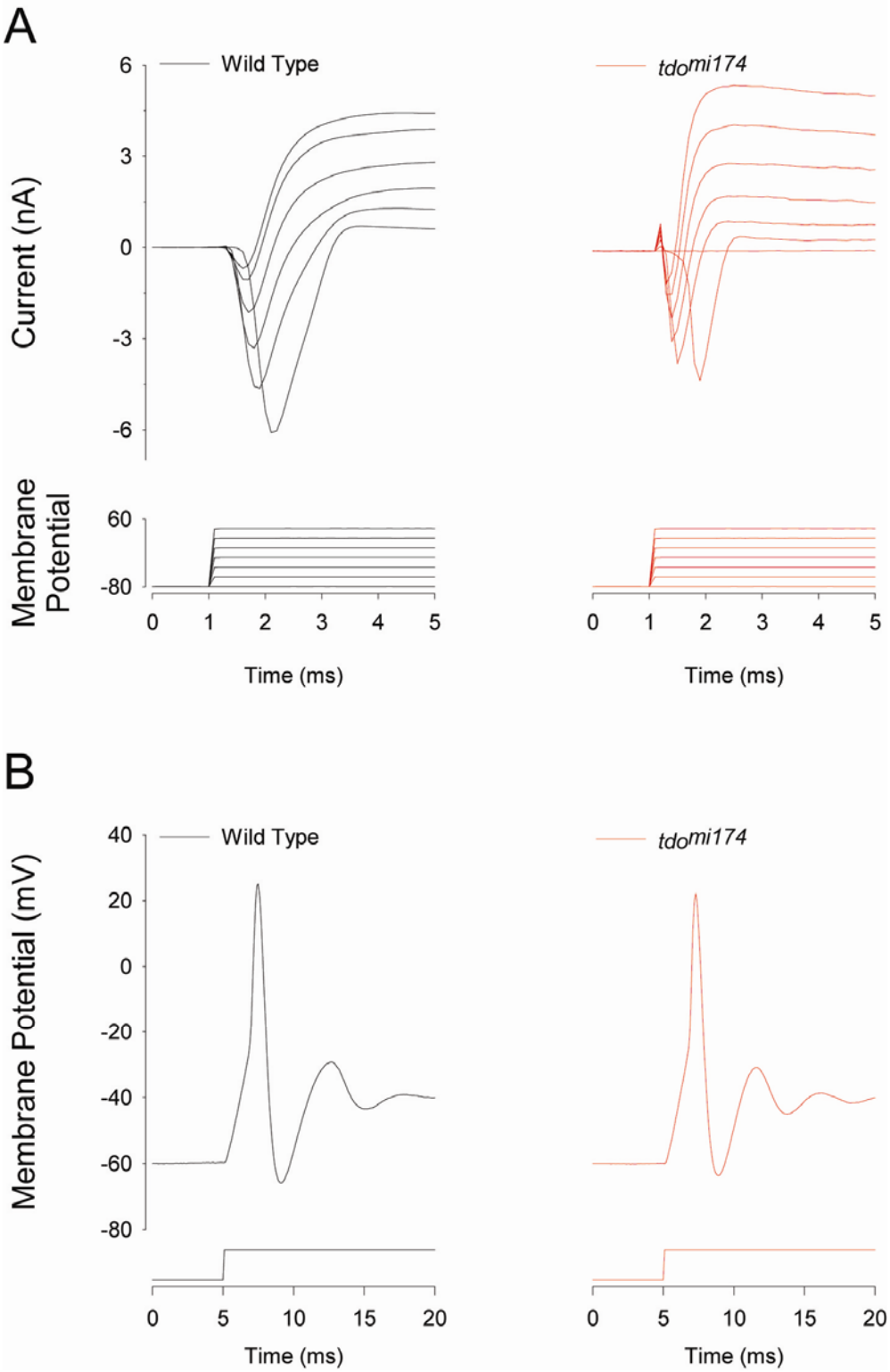

Figure 2.6: *In vivo* characterization of mechanosensitive cell membrane properties. **(A)** Representative traces obtained for whole-cell voltage clamp recordings of RBs from wild type (n = 5) and mutant (n = 3) in response to voltage steps from -80 mV to +60 mV. **(B)** Representative traces from same RBs in response to depolarizing current injections.

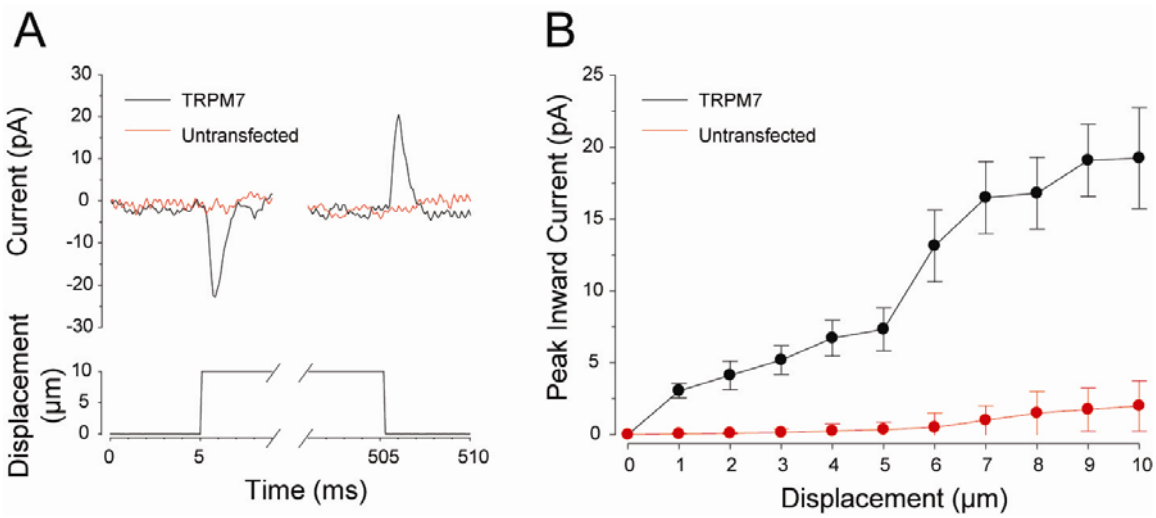

Figure 2.7: Mechanically evoked gating current of TRPM7 expressing HEK cells. **(A)** Currents in response to mechanical stimuli delivered to the membrane of a HEK cell expressing wild type TRPM7 verse untransfected HEK cell. **(B)** Amplitude of mechanically activated inward current relative to stimulus intensity (n = 3, each).

CHAPTER III

$NA_V1.6$ IS REQUIRED TO TRANSFORM A TRANSIENT SENSORY INPUT INTO A PROLONGED MOTOR OUTPUT

Summary

In a genetic screen for zebrafish motor mutants we identified two alleles of a mutation we have termed *non-active* (*nav*). Both alleles were found to display abnormal touch-evoked behaviors during the second day of development. *In vivo* electrophysiological analysis of the *nav* touch-evoked escape circuit revealed that tactile stimuli triggers activity in neurons normally sufficient to activate swimming, but fails to induce so in *nav* mutants despite the presence of a locomotor network capable of generating rudimentary fictive swimming.

Meiotic mapping identified the gene encoding $Na_V1.6$ (*scn8a*) on chromosome 23 as a potential candidate for *nav*. Subsequent cloning of *scn8a* from alleles of *nav* uncovered two different missense mutations in $Na_V1.6$ which abolished channel activity. Furthermore the injection of wild type *scn8a* RNA was found to rescue the *nav* mutant phenotype, confirming that *scn8a* is the causative gene in *nav*.

As a persistent sodium current has been implicated in facilitating fictive locomotion, we assessed whether zebrafish $Na_V1.6$ exhibits a persistent current, and whether the absence of a persistent current could account for the absence of touch-evoked swimming in *nav* mutants. We found that zebrafish $Na_V1.6$ exhibits a Riluzole sensitive persistent current when expressed by *Xenopus* oocytes, and that acute application of Riluzole phenocopies the *nav* behavioral responses to touch. We propose two models for the role of $Na_V1.6$ in the transformation of transient sensory input into prolonged bouts of motor activity.

Introduction

How genes, and the proteins they encode, contribute to behavior is a central question in neurobiology. Several different approaches to address this question have been employed including the physical mapping of naturally occurring mutations, targeted knockout of candidate genes, and the use of mutagenic agents to induce random mutations followed by screening for phenotypes of interest also known as forward genetics. These approaches have been fruitful in the identification of the sensory receptors required for the initial detection of a stimulus, and the downstream elements required to transmit this information to other parts of the body.

In some cases the activity of a single gene can be linked to a complex behavioral repertoire. These include, but are in no way limited to, *trpc2* in pheromone detection and mating behaviors of mice (Stowers et al., 2002; Kimchi et al., 2007), *ocr-2* and *osm-9* in social feeding behaviors of *C. elegans* (de Bono et al., 2002), and in the gene encoding the voltage-gated sodium channel $Na_V1.7$ (*scn9a*) in human nociception (Cox et al., 2006; Harty et al., 2006). While these and other studies have shed light into underpinnings of many behavioral repertoires, one behavior which has proven rather elusive to unravel has been the process by which a transient touch is transformed into a persistent motor response, as in the case of touch-evoked escape behaviors.

Touch-evoked escape behaviors, common to most animals, are typically characterized by running or flight in terrestrial organisms, and swimming in aquatic organisms. Although seemingly different motor behaviors, much of the neural circuitry is similar. Touch is first perceived by mechanosensitive neurons located throughout the body. These mechanosensitive neurons relay this information to other neurons within the hindbrain and spinal cord. These interneurons in turn drive activity within motor networks resulting in muscle contraction and motion. While much has been learned about the circuitry underlying this behavior in vertebrates through comparative anatomy and *in vivo* electrophysiology, relatively little is known about the contribution of specific genes. To this end we undertook a forward genetic screen in zebrafish with the aim of identifying mutants that displayed abnormal touch-evoked behaviors.

To date we have reported the isolation and characterization of six motor mutants that disrupt normal escape behaviors in response to touch (Hirata et al., 2004; Cui et al., 2005; Hirata et al., 2005; Zhou et al., 2006; Hirata et al., 2007; Saint-Amant et al., 2008). Here we report and characterize two non-complementing alleles of a seventh, which we've named *non-active* (*nav*). Both alleles of *nav* were identified by their diminished escape behaviors in response to touch. Positional mapping identified *scn8a* on chromosome 23 as a potential candidate for the *nav* mutant, and subsequent cloning uncovered two different missense mutations which result in non-functional $Na_V1.6$ channels when expressed by *Xenopus* oocytes. *In vivo* electrophysiological analysis of the circuits that underlie escape behaviors revealed that tactile stimuli is capable of evoking activity within neurons usually sufficient to trigger escape behaviors in zebrafish, and the presence of a locomotor network capable of generating rudimentary fictive swimming. Thus tactile stimulation is failing to be transformed into persistent motor behaviors due to a loss of $Na_V1.6$. Interestingly the contribution of $Na_V1.6$ in generating swimming may not be its peak current, but instead may be the contribution of its persistent current, which is known to be required for persistent firing in other neurons (Raman et al., 1997).

Materials and Methods

Animal care and use

Zebrafish were bred and maintained according to approved guidelines set forth by the University Committee on Use and Care of Animals, University of Michigan. The two alleles of *non-active* (*nav*) *nav*^{mi89} and *nav*^{mi130} were isolated in a mutagenesis screen conducted at the University of Michigan, Ann Arbor using established procedures (Haffter and Nusslein-Volhard, 1996). Prior to an experiment zebrafish were dechorionated with pronase and developmentally staged as described previously (Kimmel et al., 1995).

Behavioral analysis

Embryos obtained from crosses of *nav* heterozygous carriers were raised at 28.5 ^{0}C. Touch-evoked behaviors were elicited by touching the tail with a fine tungsten wire (125 μm), or with the tips of a pair of No. 5 forceps. Motor behaviors were recorded by video microscopy using a Panasonic CCD camera (wv-BP330) attached to a Leica dissection microscope between 16 and 32 X magnification. Images were captured at 30 Hz with a Scion LG-3 video card on a Macintosh G4 computer. The images and videos were analyzed offline with the Scion Image software and processed with NIH ImageJ. Riluzole was diluted to the indicated concentration from a stock solution of 100 mM.

Mapping and cloning of *scn8a*

A mapping family for each allele was established by crossing a *nav*^{mi89} and *nav*^{mi130} female carrier (Michigan local strain) with a wild type WIK male (Zebrafish Resource Center, Eugene, Oregon). One female and one male *nav* carrier were identified from each mapping family and used throughout the mapping process. Bulk segregate analysis (Postlethwait et al., 1994) was conducted according to the Zon lab protocol (http://zfrhmaps.tch.harvard.edu) using 20 wild type sibling and 20 mutant embryos. Thereafter 8 wild type siblings and 88 mutant embryos were subjected to intermediate resolution mapping using linked microsatellite (SSLP) markers identified

from bulk segregate analysis. For higher resolution mapping 900 mutants were tested for the linked microsatellite marker Z4421 (http://zfin.org).

The *scn8a* gene was physically mapped to the LN54 radiation hybrid panel by PCR (Hukriede et al., 1999). Primers were designed against the genomic contig Zv4_scaffold 1916 (http://www.ensembl.org/Danio_rerio/):
forward primer 5'-AAGCCGCCACCTAAGCCAGAC-3';
reverse primer 5'-TGTTGCCACCATGCCAGGAG-3'.

To clone *scn8a* we isolated total RNA from 27-30 hpf Michigan wild types or homozygous *nav* mutants using Trizol® reagent (Invitrogen, Carlsbad, California, USA). Total cDNA was synthesized using oligo-dT primers and Superscript II reverse transcriptase (Invitrogen, Carlsbad, California, USA) following the manufacturer's protocol (Superscript II manual, version 11-11-203). The coding sequence of *scn8a* was cloned by PCR from wild type and *nav* by using 6 pairs of PCR primers designed against the published zebrafish *scn8a* sequence (NM_131628). PCR products were gel-purified and sequenced, or cloned into the pGEM®-T easy vector (Promega Madison, Wisconsin, USA) prior to sequencing. Sequence analysis was performed using Lasergene software (DNAStar, Madison, Wisconsin, USA).

Expression of *scn8a* by *Xenopus* oocytes and mutant rescue

Wild type *scn8a* template in pBluescript SK+ was provided by Dr L.L. Isom (University of Michigan, Ann Arbor). Mutant *scn8a* templates were obtained by subcloning a fragment encoding the *nav* mutations in place of wild type sequence in the above construct. All constructs were verified by DNA sequencing prior to use. Capped RNA encoding wild type or mutant *scn8a* were synthesized using the mMESSAGE mMACHINE® T3 kit (Ambion, Austin, TX). Defolliculated Stage V-VI *Xenopus* oocytes were injected with 12.5 ng of wild type or mutant RNA diluted in 50 nl of DEPC-ddH_20 using a Nanoinject II system (Drummond Scientific Company, Broomall, PA). In some experiments oocytes were co-injected with 12.5 ng of RNA encoding the zebrafish ß1 subunit. Following injection oocytes were maintained in Barth's solution at 17°C for 48-72 hours before electrophysiological recordings. Two-electrode voltage clamp recordings were made with an NPI Electronics (Tamm, Germany) TurboTec 3

amplifier. The recording pipette solution contained 3 M KCl, and the oocyte external recording solution was as follows (in mM): 90 NaCl, 1 KCl, 1.7 MgCl2, and 10 HEPES, pH 7.6 (with NaOH). The oocyte external solution was controlled using a BPS-8 solution switcher (ALA Scientific Instruments, Westbury, NY). Experiments were performed at 22°C by holding oocytes at -50 mV, followed by voltage steps to the indicated membrane potentials. Data acquisition and the switching of solutions were controlled by Clampex8.2 (Molecular Devices, Sunnyvale, California, USA) software using a Digidata 1322A interface (Axon Instruments, Union City, CA). Data analysis was done using Clampfit 9 (Molecular Devices, Sunnyvale, California, USA), and figures were prepared using Sigma Plot 9.0. Tetrodotoxin (TTX) and Riluzole were diluted to the indicated concentrations from stock solutions of 1mM and 100mM, respectively. To quantify the amplitude of the persistent current we first fit an exponential function to the decay of the inward currents in response to a membrane depolarization from -100 mV to – 30 mV. We then defined the persistent current as the amplitude of current remaining five time constants after the peak current, divided by the amplitude of the peak current.

For mutant rescue RNA encoding wild type *scn8a* from above was diluted to a concentration of 100 ng/µl in DEPC-ddH_20 containing 0.1% phenol red. Approximately 1.5 ng of RNA (visual assessment) was injected into each embryo at the 1-4 cell stage using a Picospritzer II (Parker Hannifin, Fairfield, NJ).

Immunolabeling and whole-mount *in situ* hybridization

Secondary motor axons were labeled using the zn-5 (1:200) antibody (Developmental Studies Hybridoma Bank, Iowa City, IA) according to a previously published protocol (Li et al., 2004). Primary antibodies were visualized using or Alex-594 conjugated anti-mouse IgG (Molecular Probes, Eugene, OR). Fluorescent images were collected and processed with a Leica confocal microscope (www.leica.com).

In situ hybridization was carried out following standard protocols (Li et al., 2004). The anti-sense DIG-labeled probe for zebrafish *scn8a* was made from the 1.3kb cDNA fragment at its 3' end and hydrolyzed to approximately < 500 base pairs for

application to embryos. After quenching the color reaction embryos were mounted in 70% glycerol/PBS and imaged with DIC microscopy.

In vivo electrophysiology

All reagents and drugs were purchased from Sigma-Aldrich, St. Louis, MO. Embryos (48-52 hpf) were prepared for *in vivo* recordings from axial skeletal muscle and motor neurons as previously described (Drapeau et al., 1999; Buss and Drapeau, 2000). In brief embryos were anesthetized in 1X Evans recording solution (in mM): 134 NaCl, 2.9 KCl, 2.1 $CaCl_2$, 1.2 $MgCl_2$, 10 glucose, 10 HEPES, pH 7.8, containing 0.02% tricaine. Embryos were then pinned to a 35 mm dish coated with Sylgard® through the notochord using 25 μm tungsten wires. The skin overlying the trunk and tail was first scored with a broken pipette, and then removed with a pair of fine No.5 forceps. The bath solution was continuously exchanged at ~1 ml/min throughout the recording session with 1X Evans containing either 2-3 μM d-tubocurarine for muscle or 15 μM for motor neuron and Mauthner cell recordings. Mauthner recordings were performed using a broken patch pipette with resistances ~1 MΩ when filled with external recording solution. To expose the spinal cord for motor neuron recordings the bath solution was replaced with recording solution containing 1 mg/ml collagenase Type XI and incubated at room temperature (22 ^{0}C) until the axial skeletal muscle started to separate at the somitic boundaries. Thereafter the muscle was peeled away using suction applied to a broken pipette (~50 μm). The internal recording solution contained (in mM): 116 K-gluconate, 16 KCl, 2 $MgCl_2$, 10 HEPES, 10 EGTA, at pH 7.2 with 0.1% SulforhodamineB for cell type identification. Electrodes pulled from Borosilicate glass had resistances of 6-10 MΩ for muscle, 10-14 MΩ for motor neurons when filled with internal recording solution. Recordings were made with an Axopatch 200B amplifier (Axon Instruments, Union City, CA) low passed filtered at 5 kHz and sampled at 1-10 kHz. Data acquisition using a Digidata 1322A interface was controlled by pClamp 8.2 software. The initial data analysis was done with Clampfit 9.2, and figures were prepared using Sigma Plot 9.0.

Touch-evoked responses were evoked by pressure application of bath solution via a broken pipette (~20μm) to the tail region. The pressure and duration of a stimulus

was controlled by a Picospritzer II (Parker Hannifin, Fairfield, NJ). NMDA-evoked fictive swimming was achieved by perfusing the bath with recording solution containing 100 μM NMDA.

Results

non-active (*nav*) mutants exhibit abnormal touch-evoked behaviors

To gain insight into how genes, and the proteins they encoded, contribute to the formation and function of the neural circuits that underlie behaviors we initiated a forward genetic screen in zebrafish. We focused on mutants that displayed abnormalities in the three earliest motor behaviors exhibited by zebrafish. In order of onset these are spontaneous coiling, touch-evoked escape contractions, and touch-evoked swimming.

Spontaneous coiling, which is characterized by alternating contractions of the trunk and tail, begins around 17 hours post-fertilization (hpf), peaks at 19 hpf at a frequency around 1 Hz, and then decreases in frequency over the next 7 hours to under 0.1 Hz (Saint-Amant and Drapeau, 1998). The cells that mediate spontaneous coiling are intrinsic to the spinal cord as coiling persists following spinalization (Saint-Amant and Drapeau, 1998). The next motor behavior to develop is touch-evoked escape contractions with an onset around 21 hpf. Touch-evoked escape contractions consist of one to three alternating contractions of the trunk and tail towards the head in response to touch delivered along the length of an embryo. Touch-evoked escape contractions were initially found to require supraspinal input (Saint-Amant and Drapeau, 1998), however this belief has been recently challenged (Downes and Granato, 2006). Finally around 27 hpf, after first performing escape contractions, embryos begin to exhibit the first episodes of touch-evoked swimming. These two touch-evoked escape behaviors orientate the fish away from the source of the stimulus and then propel it out of the perceived threatening environment.

Two recessive motor mutants from our screen were found to be allelic, and were collectively named *non-active* (*nav*^{mi89} and *nav*^{mi130}). Both alleles exhibit similar spontaneous coiling frequencies during development when compared to wild type siblings (Figure 3.1), but display abnormal touch-evoked behaviors during the second and third day of development. Beginning around 24 hpf when wild type siblings normally respond to touch with one to three escape contractions, *nav* mutants either failed to respond to touch, or did so with fewer escape contractions which were weaker

(Figure 3.1C-D). Later around 48 hpf, when wild type embryos respond to touch with escape contractions followed by swimming, *nav* mutants displayed only escape contractions and no swimming (Figure 3.1E). Thus *nav* mutants are able to detect tactile stimuli, but fail to initiate episodes of swimming. Finally we found that the *nav* phenotype is transient as mutants swam in response to touch after 60 hpf (Figure 3.1F). However, the mutation is lethal as *nav* mutants do not survive beyond two weeks.

Touch triggers activity within the escape circuit of *nav*, but of shorter duration

To better understand the genesis of the *nav* phenotype we undertook an *in vivo* electrophysiological characterization of the circuit that underlies touch-evoked escape behaviors in zebrafish (Fig. 3.2A). In zebrafish sensitivity to touch is conferred by two groups of mechanosensitive neurons: neurons within the trigeminal ganglia respond to tactile stimuli to the head, whereas Rohon-Beard neurons (RBs) located in the dorsal spinal cord respond to tactile stimuli to the trunk and tail. Both groups of mechanosensitive neurons send projections into the hindbrain which lead to the activation of ~90 pairs of reticulospinal neurons during escape behaviors (Gahtan et al., 2002). Reticulospinal neurons make monosynaptic connections with several spinal cord neurons including primary motor neurons, which in turn drive activity within skeletal muscle resulting in motion.

The primary muscle type in zebrafish involved in motor behaviors is the axial skeletal muscle of the trunk and tail. Axial skeletal muscle is comprised of slow and fast twitch fibers, both of which are active during swimming (Buss and Drapeau, 2002). We found that touch evoked episodes of fictive swimming in slow twitch fibers of wild type siblings 48-52 hpf (Fig. 3.2B). The frequency of fictive swimming correlated with the frequency of tail beating observed during swimming (~25 Hz) at this stage. In contrast *nav* slow twitch fibers displayed membrane depolarizations that were large, short and arrhythmic in response to touch. The duration and arrhythmic pattern of the membrane depolarizations was consistent with the *nav* phenotype; escape contractions but no swimming.

The abnormal touch-evoked activity observed in *nav* muscle is consistent with a defect within the central nervous system (CNS) which results in abbreviated synaptic

drive to muscle. However, it is also consistent with defect in skeletal muscle which disrupts the muscle's responsiveness to sustained input from motor neurons. To determine whether the CNS was defective in *nav*, we assessed touch-evoked synaptic drive to motor neurons. Each hemisegment in zebrafish contains three primary motor neurons (RoP, MiP and CaP) that are identifiable based upon their morphology and position within the spinal cord (Westerfield et al., 1986). In addition the identity of neurons can be confirmed by their morphology following diffusion of FITC-dextran included in the intracellular recording solution (see methods). We found that touch evoked a prolonged burst of action potentials in primary motor neurons (Figure 3.2C) consistent with previous reports (Buss and Drapeau, 2001). However, in primary motor neurons of *nav* mutants, touch evoked only a short burst of action potentials. A finding consistent with the abbreviated pattern of fictive swimming observed in *nav* skeletal muscle. Although this finding does not preclude an additional defect within *nav* skeletal muscle, it does indicate a problem within the nervous system of *nav* mutants.

Of the ~90 reticulospinal neurons known to be activate during escape behaviors (Gahtan et al., 2002) the role of Mauthner (M) cells in fish are the best understood (reviewed by (Korn and Faber, 2005). M cells receive input from mechanosensitive neurons and in turn make monosynaptic connections with motor neurons. Activity in M cells follows sensory stimulation, precedes the onset of escape contractions, and is sufficient to trigger escape behaviors. We found that touch evoked activity within M cells of wild type and *nav* mutants, observable as a spike in the local field potential (Figure 3.2D). Thus sensory information is capable of triggering activity within the escape network which is normally sufficient to generate escape behaviors.

nav mutants display shortened periods of NMDA-evoked fictive swimming

Our recordings and behavioral observations indicated that *nav* mutants were able to detect tactile stimuli, but fail to transform it into a swimming response. To determine whether the locomotor network that underlies swimming is defective in *nav* mutants we bathed embryos in the excitatory amino acid NMDA. Bath application of NMDA has been shown to induce patterned synaptic drive to zebrafish motor neurons similar to that elicited by touch (McDearmid and Drapeau, 2006). We found that NMDA evoked

repetitive bouts of fictive swimming in both wild type and mutant embryos (Figure 3.3A-B).

However upon closer examination some aspects of NMDA-evoked fictive swimming were found to be different. Notably the duration of a typical episode and the frequency of fictive swimming were found to be shorter and lower in *nav* mutants when compared to wild type siblings, respectively (Figure 3.3C-D). These results suggest that the *nav* gene product is serving two roles. First, it is required in the locomotor network to generate *normal* patterns of fictive swimming in response to NMDA. Second it is required upstream of the locomotor network to trigger rudimentary swimming in response to touch.

The *nav* phenotype arises from missense mutations in the gene encoding $Na_V1.6$ (*scn8a*) which abolish channel activity

The responses to touch and NMDA indicated a defect within the nervous system of *nav* mutants. Therefore we sought gene candidates that when altered would produce a phenotype consistent with *nav*. Through meiotic mapping we identified the microsatellite marker, z4421, which failed to recombine with either allele (0/1140). In the zebrafish genome z4421 is located on chromosome 23, near the *scn8a* gene that encodes the voltage-gated sodium channel $Na_V1.6$. As mutations of *scn8a* in mice are known to display a range of movement defects (Meisler et al., 2002) zebrafish *scn8a* was identified as a candidate for *nav*. The cloning of *scn8a* from nav^{mi89} and nav^{mi130} uncovered two different nucleotide substitutions that predict two different missense mutations in $Na_V1.6$ (M1461K and L277Q, respectively; Figure 3.4A). These missense mutations occur at highly conserved locations in $Na_V1.6$, and in the voltage-gated sodium channel family as a whole.

To examine the functional consequences of these mutations RNA encoding either wild type or mutant *scn8a* was expressed by *Xenopus* oocytes and studied under two-electrode voltage clamp. Wild type *scn8a* produced voltage-gated sodium currents (Figure 3.4B) similar to previous reports of zebrafish $Na_V1.6$ expressed by *Xenopus* oocytes (Fein et al., 2007). In contrast, both mutant *scn8a* RNAs failed to produce currents above control oocytes. We also co-injected mutant *scn8a* RNAs with RNA

encoding the zebrafish ß1 subunit which is known to facilitate membrane insertion of $Na_V1.6$, and also more accurately reflects conditions *in vivo*. This approach also failed to generate voltage-dependent currents.

To further confirm that *scn8a* was the causative gene in *nav* we attempted to rescue the *nav* phenotype by injecting RNA encoding wild type *scn8a* into clutches of embryos obtained from heterozygous *nav* parents. We found that only 15.6% (28/180) of the injected embryos, compared to 24.1% (52/216) of the uninjected embryos failed to respond to touch, or did so with weak escape contractions at 27 hpf. The finding that the proportion of embryos was lower than the predicted Mendelian ratios of 25% is consistent with rescue of some *nav* mutants. To further confirm a rescue of the *nav* phenotype by wild type *scn8a* RNA, we assayed the responsiveness of the injected embryos at 48 hpf, a time point when the effect of the injected RNA may have worn off leading to a reversion to the *nav* phenotype (Zhou et al., 2006). At 48 hpf 26.7% (48/180) of the injected embryos were found to display the *nav* phenotype, failing to swim in response to touch. This indicates that 20 of the 180 embryos ($\chi 2 < 0.005$, $n = 180$) that exhibited normal touch-evoked escape contractions at 27 hpf were actually mutants, but displayed a wild type phenotype as a result of the injected wild type *scn8a* RNA. Although mutant rescue was only partially successful, this result coupled with the findings that both missense mutations result in nonfunctional channels indicates that *scn8a* is the causative gene in *nav*.

Scn8a is widely expressed in the zebrafish nervous system

Voltage-gated sodium channels represent a well characterized family of ion channels (Catterall et al., 2005a; Catterall et al., 2005b). The family is comprised of ten members ($Na_V1.1$-9, and Na_X), of which the first nine are known to be sensitive to membrane depolarization. Sodium channels, or "α" subunits, are typically complexed with one or more subtypes of the auxiliary ß subunit in a 2 ß:1 α ratio. There are typically four auxiliary ß subunits, (ß1-4) each encoded by a different gene (Isom, 2001). ß subunits alter the kinetics of the α subunit, promote insertion of the α-ß complex into the cell membrane, and serve as cell adhesion molecules whose absence disrupts nodal structure (Chen et al., 2004). Mutations in sodium channels have been

linked to a host of motor disorders including dystonia, ataxia, and progressive paralysis (Meisler et al., 2002).

Considering this we first examined the expression pattern of *scn8a* at 24 and 48 hpf to better understand how the loss of $Na_V1.6$ could lead to a loss of swimming in *nav*. Whole-mount *in situ* hybridization uncovered *scn8a* expression in early differentiated neurons in the spinal cord and brain at 24 hpf, consistent with previous reports (Pineda et al., 2005; Novak et al., 2006a; Pineda et al., 2006; Chopra et al., 2007; Chen et al., 2008). The size and positions of some of the *scn8a*-positive neurons identified them as posterior lateral line ganglion cells, and Rohon-Beard neurons (RBs) (Figure 3.5A). At 48 hpf *scn8a* expression was found to be more widespread in the central and peripheral nervous systems including trigeminal ganglion cells (Figure 3.5B).

nav mutants exhibit normal patterning of motor axons

The contribution of zebrafish $Na_V1.6$ to early development has previously been investigated with the use of antisense oligonucleotides which block the expression of $Na_V1.6$. These studies have indicated the following: $Na_V1.6$ contributes the majority of sodium current in mechanosensitive RBs (Pineda et al., 2005), $Na_V1.6$ is not essential for the frequency of spontaneous contractions but does influence to the extent to which embryos contract (Chen et al., 2008), and $Na_V1.6$ contributes in a non cell-autonomous manner to the patterning of secondary motor axons (Pineda et al., 2006). Considering that abnormal patterning of secondary motor axons could account for the abnormal NMDA-evoked fictive swimming in *nav*, we assessed secondary motor axons at 48 hpf, a time point when the locomotor phenotype was most robust. When compared to wild type siblings the pattern of secondary motor axon projections in *nav* mutants was found to be similar (Figure 3.6A-B). Thus the loss of $Na_V1.6$ in *nav* appears not to disturb the outgrowth of motor axons during this time in development.

The _nav_ phenotype can be attributed to a loss of persistent sodium current

Voltage-gated sodium channels are best known for directly contributing to the rising phase of action potentials in both neurons and muscle. However a few family

members, including $Na_V1.6$ exhibit a persistent current which facilitates repetitive firing in neurons (Raman et al., 1997). In addition two recent reports have demonstrated an essential role for a persistent sodium current in sustained activity within the neurons that underlie fictive locomotion in neonatal rodents (Tazerart et al., 2007; Zhong et al., 2007). Considering that the *nav* phenotype could be attributed to a premature termination of activity within the touch-evoked escape circuit, we explored whether zebrafish $Na_V1.6$ exhibits a persistent current. To this end RNA encoding $Na_V1.6$ was expressed by *Xenopus* oocytes and studied under two-electrode voltage clamp. Oocytes were held at -100 mV and stepped to depolarizing test potentials for various durations. Under these conditions we failed to observe a substantial persistent current (Figure 3.4B, and not shown). In contrast the inclusion of RNA encoding the ß1 subunit introduced a persistent current (Figure 3.7A).

The persistent sodium current from other organisms has been shown to be sensitive to the drug Riluzole (Urbani and Belluzzi, 2000). To determine whether zebrafish $Na_V1.6$'s persistent sodium current was also sensitive to Riluzole we applied various concentrations of Riluzole to oocytes co-expressing ß1 and $Na_V1.6$. Our results revealed an approximate IC_{50} for Riluzole of 3 μM (Figure 3.7B). At this concentration it had no observable effect on the peak current evoked by membrane depolarization, which was not observed until concentrations beyond 20 μM.

To determine whether the *nav* phenotype could be mimicked by the application of Riluzole we applied various concentrations of Riluzole and assessed touch-evoked behaviors. We found that 3 μM Riluzole was sufficient to phenocopy the *nav* phenotype within several minutes of application (Figure 3.7D). These results implicate a persistent sodium current, potentially contributed by $Na_V1.6$, as essential for the transformation of transient sensory stimuli into prolonged bouts of motor behaviors.

Discussion

We isolated and characterized two alleles of a motor mutant we have named *nav*. Both alleles were found to arise from missense mutations in the gene encoding $Na_V1.6$ which abolished channel activity. We found that *scn8a* was expressed extensively within both the peripheral and central nervous system, consistent with previous reports (Tsai et al., 2001; Novak et al., 2006b; Pineda et al., 2006). To understand how the loss of $Na_V1.6$ results in a lack of touch-evoked swimming in *nav* mutants we undertook an electrophysiological characterization of the circuits that underlie touch-evoked behaviors in zebrafish.

In *nav* mutants, touch-evoked synaptic drive to axial skeletal muscle and primary motor neurons was present, but was of much shorter duration, consistent with the observed motor behaviors in *nav* mutants. Although this finding does not preclude a defect within *nav* skeletal muscle it is unlikely that one exists as skeletal muscle does not appear to express *scn8a*. Therefore if a muscle defect were to exist in *nav* it would most likely be the result of abnormal activity within the central nervous system.

These findings may appear to implicate a problem within motor neurons, an idea supported by the expression of *scn8a* by motor neurons (Tsai et al., 2001; Novak et al., 2006b; Pineda et al., 2006). However a defect at the level of motor neurons alone is not sufficient to account for the *nav* phenotype for the following two reasons. First, it is evident from our recordings that other sodium channels are expressed by motor neurons. Furthermore, expression of *scn8a* was detected in a subset of motor neurons: ventrally projecting primary motor neurons (CaP), and dorsally projecting secondary motor neurons (Pineda et al, 2006). Our recordings were made from all three subtypes of primary motor neurons (RoP, MiP, and CaP), in which we observed similar abrupt patterns of bursting in each subtype. Second, bouts of fictive swimming (of ~500 ms on average) can be sustained in *nav* mutants in response to NMDA. This finding demonstrates that motor neurons are capable of providing sustained drive to skeletal muscle, however they fail to do so in response to touch. Therefore a defect prior to motor neurons is more likely to account for the inability of *nav* mutants to swim following touch. Finally the ability of touch to trigger activity within M cells

demonstrates that, although there is most likely a reduction in number of RBs activated in response to touch and therefore a decrease in the drive to supraspinal elements of the escape network, there still exist sufficient sensory drive to trigger activity in M cells. Artificially triggering activity within M cells has been shown to be sufficient to initiate escape contractions and swimming, however this was done in adult fish and therefore may not be true for the embryonic escape network (Nissanov et al., 1990). These results, coupled with the finding that acute application of Riluzole at concentrations which reduce the persistent sodium current without substantially affecting peak current, are suggestive of at least two models which are not mutually exclusive (Figure 3.8).

The first model supposes that the inability of *nav* mutants to swim in response to touch results from a defect at the level of the sensory neurons (RBs). In this model the residual sodium current contributed by $Na_V1.1$ (Pineda et al., 2005) is sufficient to trigger escape contractions via M cell activation, but not swimming due to a decrease in synaptic drive to additional supraspinal elements necessary for swimming. For ease of discussion the supraspinal element(s) will be referred to as a "Swim neuron". The decrease in synaptic drive to the Swim neuron could result from a decrease in the number of RBs recruited in response to touch due to a loss of $Na_V1.6$, or a reduction in the number of times an RB is capable of spiking in response to touch due to a loss of persistent sodium current contributed by $Na_V1.6$, or some combination of the two. This would be the site of Riluzole action that mimics the *nav* phenotype. This model makes two predictions, both of which are testable. First, an artificial stimulus sufficient to trigger M cell activation should not lead to swimming in wild type embryos. Second, plasmid based rescue of $Na_V1.6$ expression in RBs (Chapter II) should be sufficient to rescue swimming in *nav* mutants, with a duration and frequency at least similar to that observed in NMDA-evoked fictive swimming.

In the second model the persistent sodium current contributed by $Na_V1.6$ is required within the Swim neuron to transform a transient sensory input into a persistent command to the motor network. In this scenario the Swim neuron would be downstream of the M cell, and upstream of motor neurons. In addition, the Swim neuron could be the neuron whose output is substituted for by bath application of NMDA. A similar model has been proposed to explain how transient sensory input in

reticulospinal neurons of lamprey result in the plateau potential upon which repetitive action potentials fire (Di Prisco et al., 1997; Di Prisco et al., 2000). Blockade of the plateau potential results in abbreviated motor activity similar to that observed in *nav*.

In either model, $Na_V1.6$ represents yet another case wherein the contribution of a single gene, or in this case a potential subtle kinetic feature of the protein that it encodes (persistent current), can be held responsible for triggering complex behaviors. To test these models will require cell type specific rescue, coupled with a better understanding of M cells connectivity, and the development of new recording techniques.

Figures

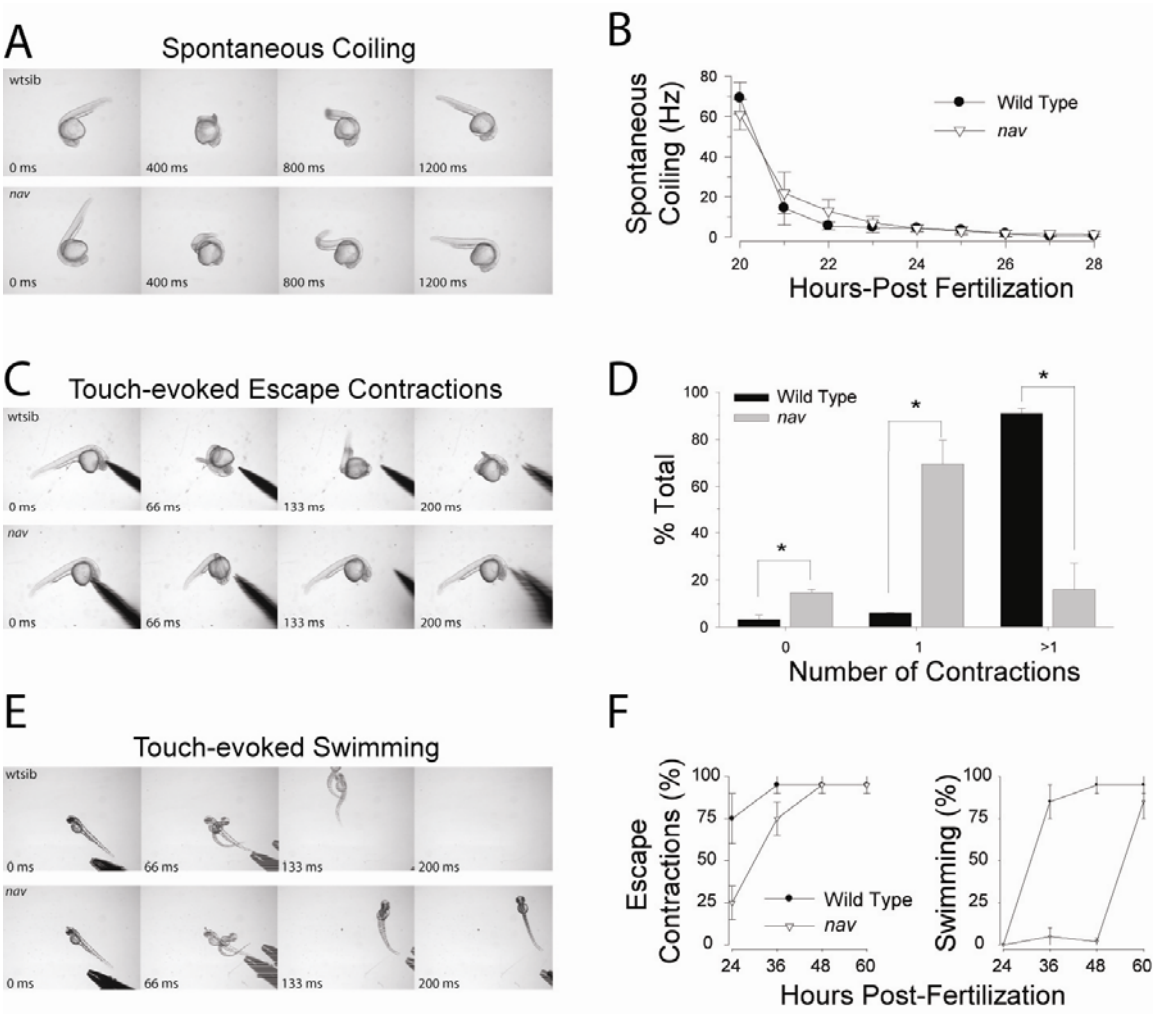

Figure 3.1: Time lapse video analysis of the *nav* mutant phenotype. **(A)** Top: a 24 hpf a wild type sibling exhibiting a single spontaneous coil. Bottom: an aged matched *nav* mutant embryo exhibiting a single spontaneous coil. **(B)** Spontaneous coiling frequency of wild type and *nav* mutant embryos between 20 and 28 hpf. **(C)** Top: a 24 hpf wild type sibling touched on the head responds with multiple escape contractions. Bottom: an aged matched *nav* mutant embryo responds with a single weak contraction. **(D)** Distribution of touch-evoked escape contractions observed in wild type and *nav* mutant embryos. **(E)** Top: a single 48 hpf wild type sibling touched on the tail responds with an escape contraction followed by swimming. Bottom: an single aged matched *nav* mutant embryo responds with an escape contraction but no swimming. **(F)** Progression of *nav* phenotype over the first few days of development compared to wild type.

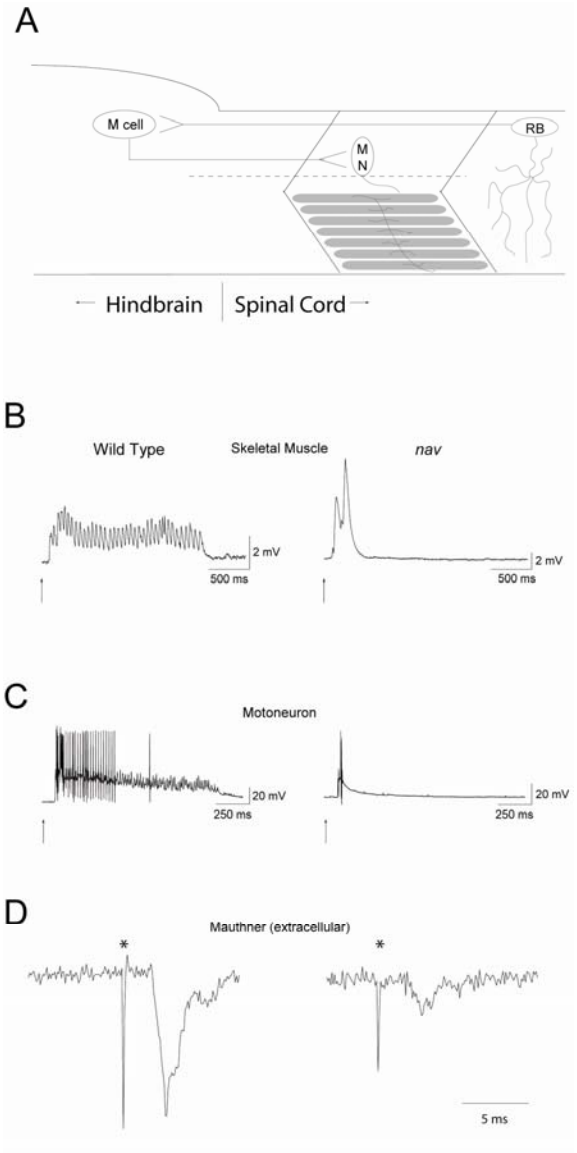

Figure 3.2: In *vivo* electrophysiological characterization of the zebrafish touch-evoked escape circuit. **(A)** A schematic depicting sensory input originating from the activation of the mechanosensitive Rohon-Beard (RB) neurons which project into the hindbrain and lead to the activation of M cells. M cells in turn make monosynaptic connections with motor neurons (MN) innervating axial skeletal muscle. Not shown is sensory input originating from sensory trigeminal. Of note, anatomical studies support the existence of a monosynaptic connection between RBs and M cells, but evidence of a functional connection is lacking. **(B)** Prolonged bouts of touch-evoked fictive swimming is observed in slow twitch skeletal muscle of wild type siblings while an arrhythmic response is recorded in *nav* mutants. Arrows here and in panel C indicate time of stimulus (50 ms). **(C)** Prolonged bouts of touch-evoked bursting in primary motor neurons are observed in wild type sibling but not *nav* mutant embryos. **(D)** Touch-evoked M cell spiking recorded extracellularly from wild type sibling and *nav* mutant embryos. (*) denotes M cell spiking followed by an electromyogram (EMG).

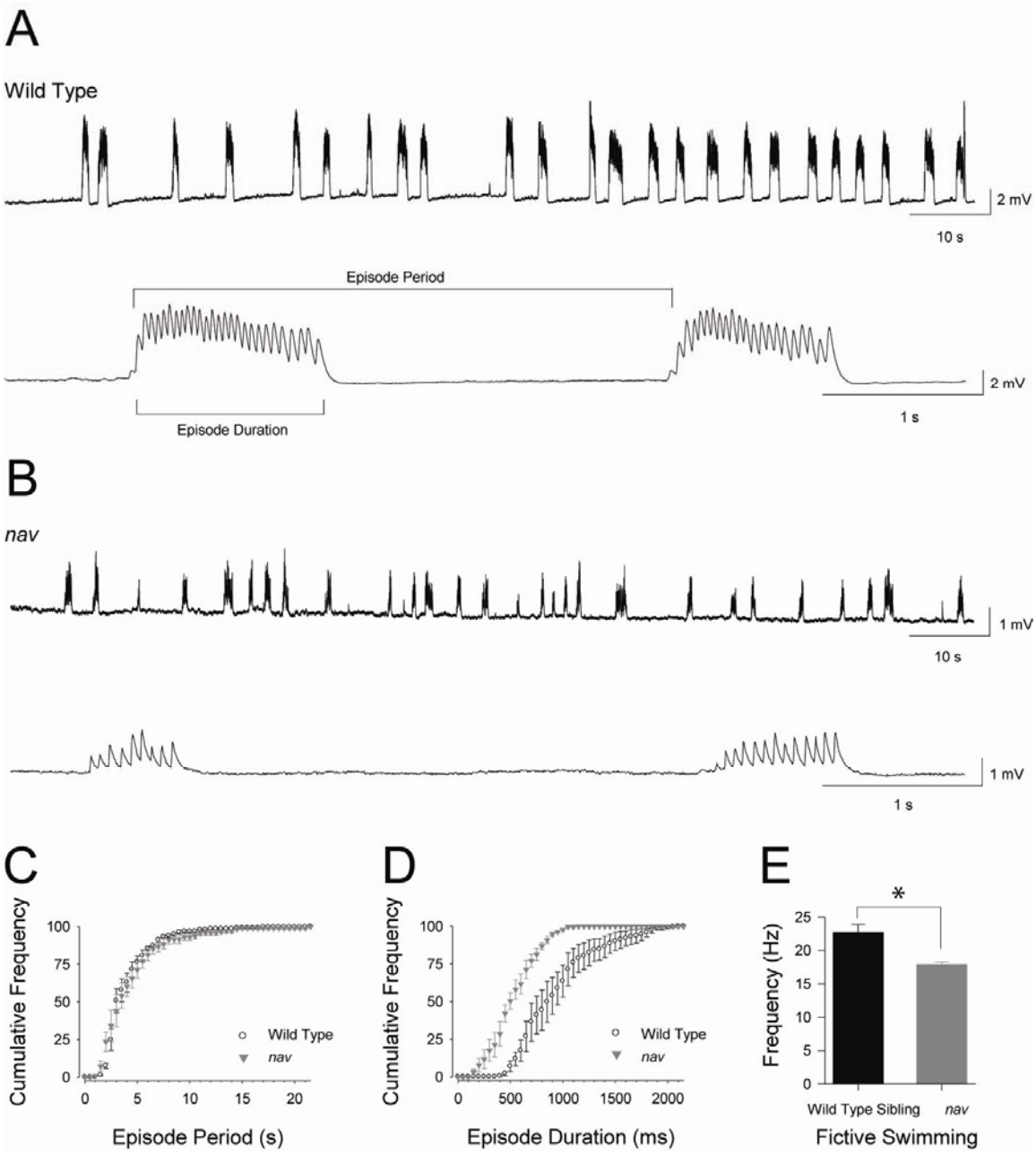

Figure 3.3: *In vivo* characterization of the *nav* locomotor network. **(A)** Top: several minutes of NMDA-evoked fictive swimming from a wild type sibling. Bottom: a faster sweep of two episodes of fictive swimming. **(B)** Top: several minutes of NMDA-evoked fictive swimming from a *nav* mutant. Bottom: a faster sweep of two episodes of fictive swimming. **(C)** Cumulative frequency histograms of episode periods and durations from wild type siblings and *nav* mutant embryos ($n = 5$ for each). **(D)** Fictive swimming frequency of wild type sibling and *nav* mutant embryos (* $p < 0.05$).

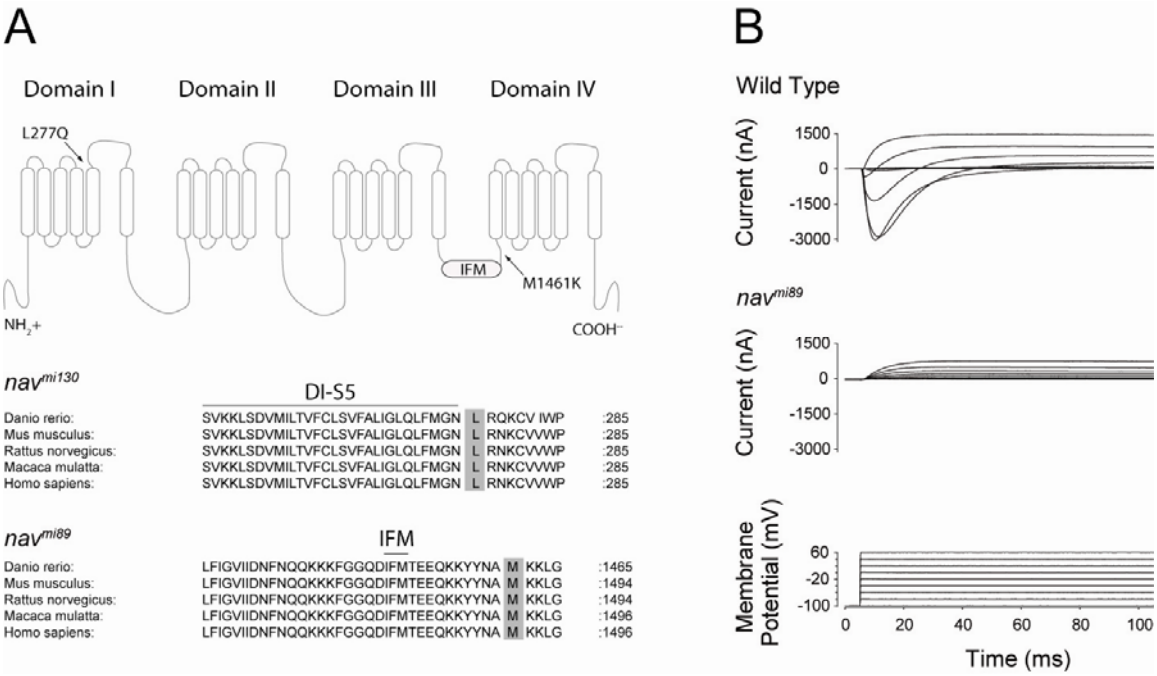

Figure 3.4: Characterization of $Na_V1.6$ from *nav*^{mi130} and *nav*^{mi89}. **(A)** Top: $Na_V1.6$ membrane topology and location of *nav* missense mutations. Bottom: sequence alignment of $Na_V1.6$ from several different species with conserved leucine 277 and methionine 1461 highlighted in gray. Numbers indicate amino acid position within zebrafish $Na_V1.6$. **(B)** Two electrode voltage-clamp recordings made from oocytes injected with either wild type or *nav*^{mi89} RNA. Not shown: results from uninjected oocytes and oocytes injected with *nav*^{mi130} RNA which did not differ from *nav*^{mi89}.

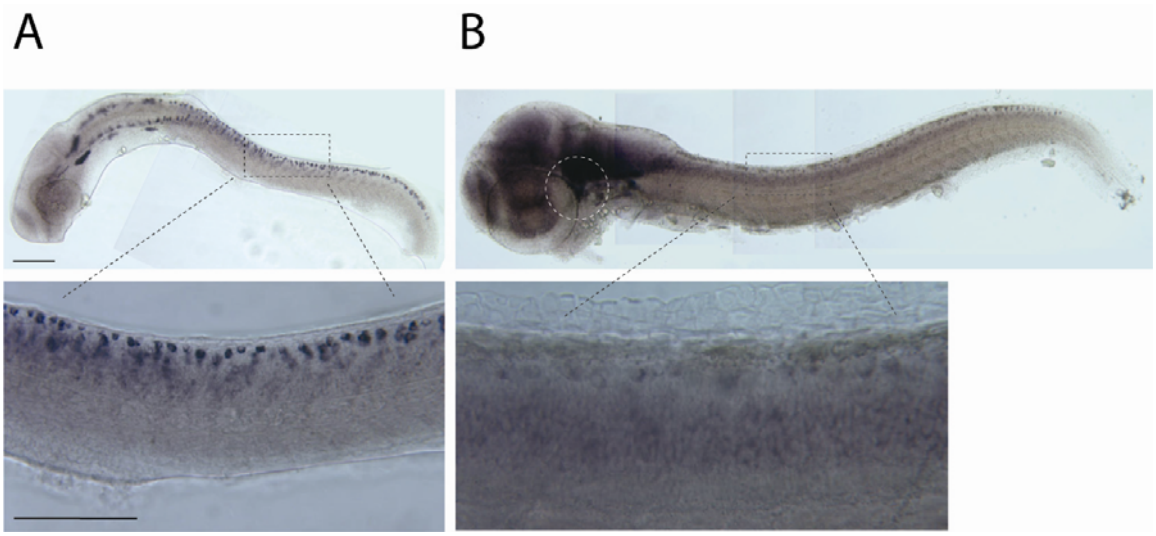

Figure 3.5: Whole-mount *in situ* hybridization of *scn8a*. **(A)** Top: expression of *scn8a* in a 24 hpf embryo. Scale bar 200 µm. Bottom: enlarged image of region indicated above. Scale bar 50 µm. **(B)** Top: expression of *scn8a* in a 48 hpf embryo. Circled area indicates trigeminal ganglia. Bottom: enlarged image of region indicated above.

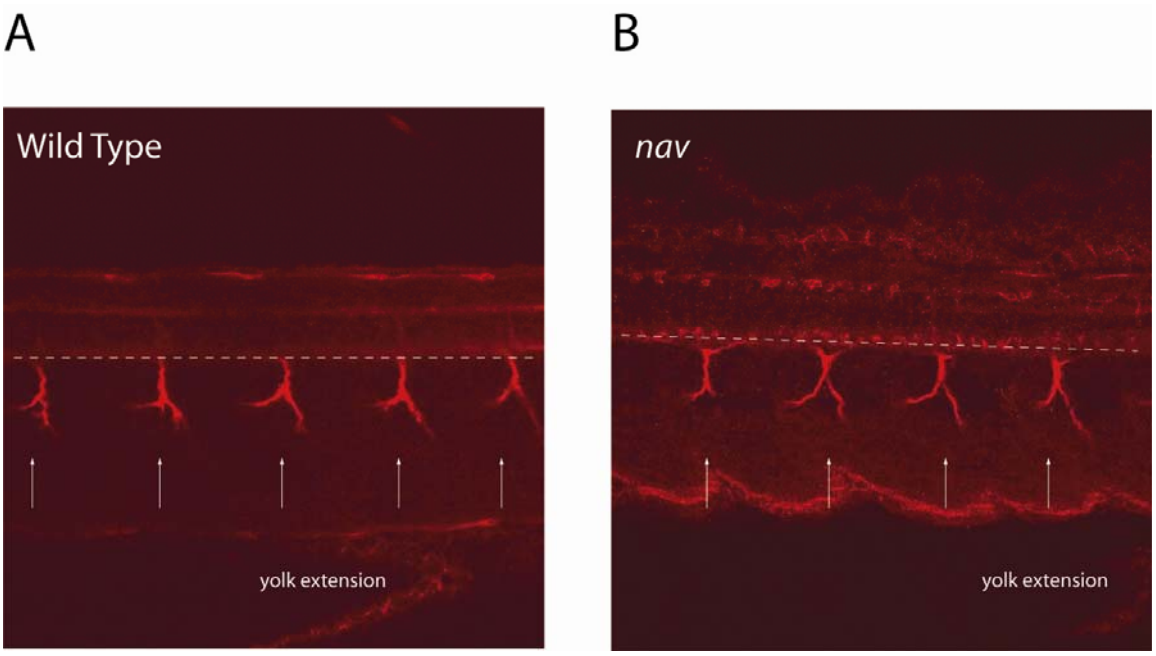

Figure 3.6: Morphological assessment of secondary motor axon projections. Lateral view, dorsal is to the top, rostral is to the left, dashed line indicates ventral spinal cord. The secondary motor axon tracts as labeled with zn-5 were comparable between wild type **(A)** and *nav* mutants **(B)** ~48 hpf**.** Arrows point to secondary motor axon tracts.

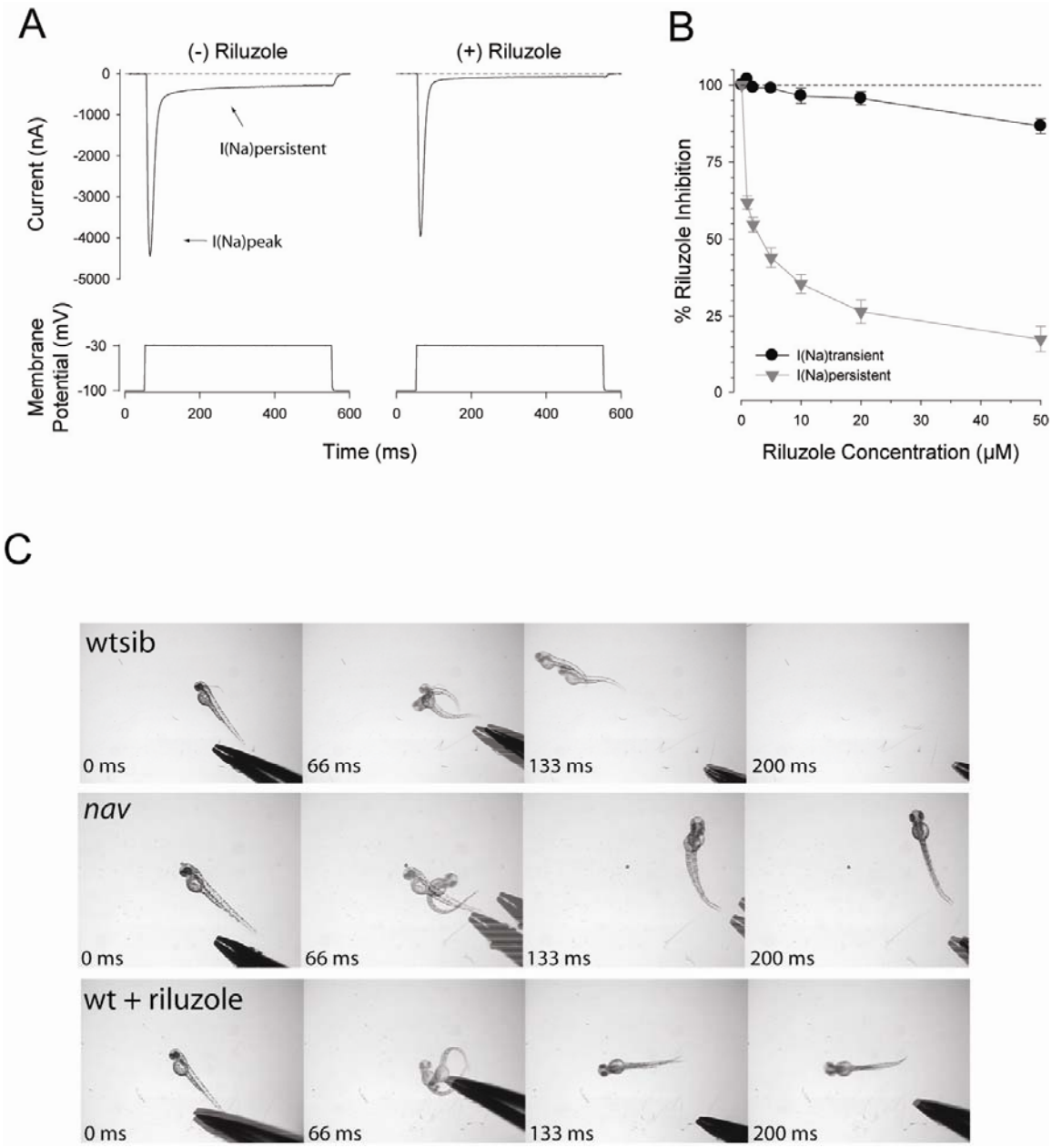

Figure 3.7: Effect of Riluzole on sodium current and touch-evoked behaviors. **(A)** Two electrode voltage clamp recordings made from oocytes expressing $Na_V1.6$ plus ß1 in the absence or presence of Riluzole (50 μM). **(B)** Riluzole block of I (Na) transient verse I (Na) persistent. Values represent the average ± SEM (*n* = 10). **(C)** Application of Riluzole (3 μM) mimicked the *nav* phenotype.

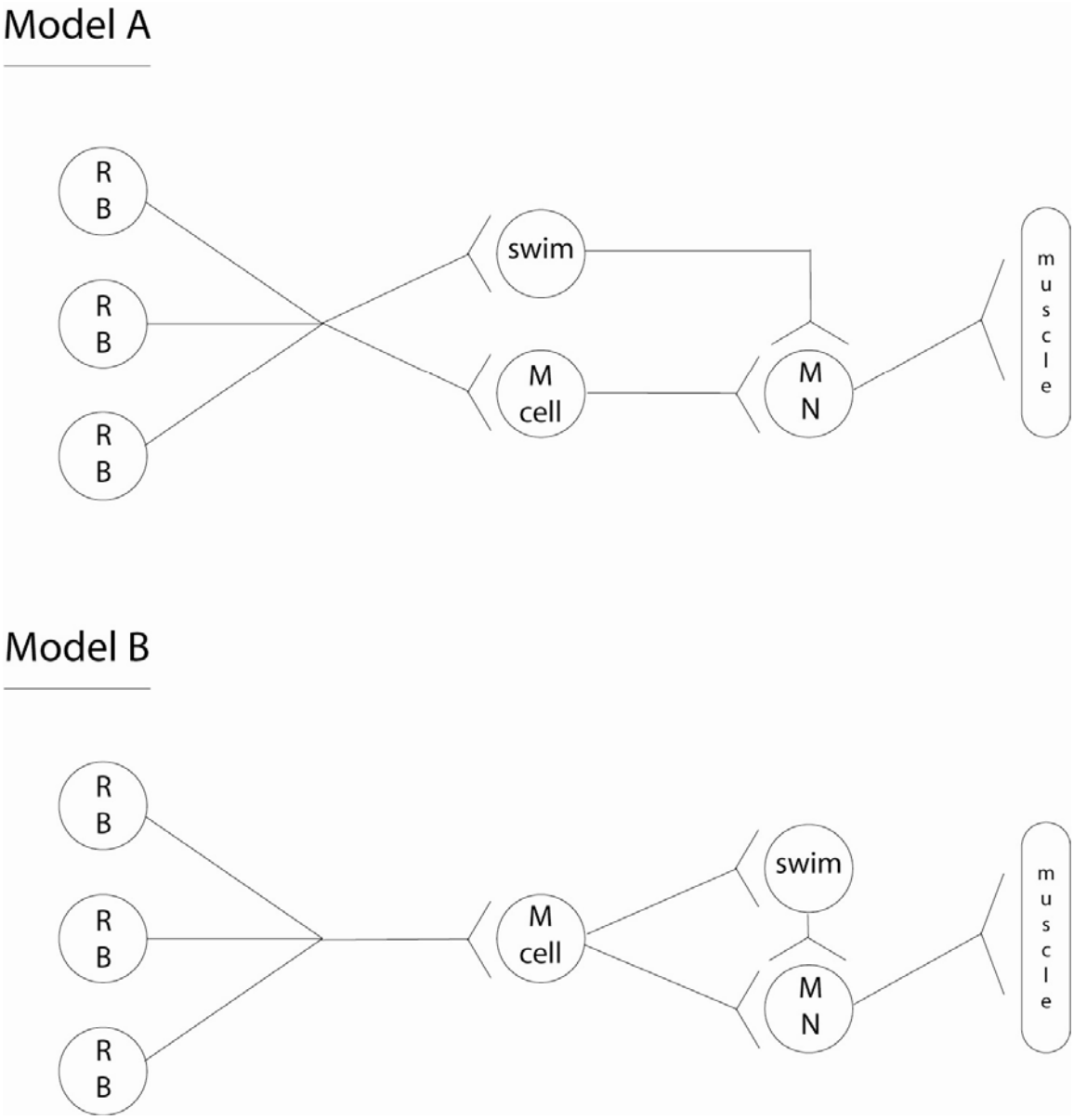

Figure 3.8: Models depicting potential loci of $Na_V1.6$ requirement. **(A)** Rohon-Beard (RB) sensory neurons project to both Mauthner (M) cells and a high threshold "Swim" neuron. Residual sensory input from RBs in the absence of $Na_V1.6$ or blockade of persistent current by Riluzole is sufficient to trigger the low threshold M cells, which in turn drive activity within motor neurons leading to escape contractions. However it is not sufficient to trigger activity within the high threshold Swim neuron. **(B)** In this model the Swim neuron is down stream of M cells, and requires $Na_V1.6$ for sustained drive to motor neurons.

CHAPTER IV

THE CLONING AND CHARACTERIZATION OF TWO FUNCTIONAL P2X RECEPTORS FROM ZEBRAFISH

Summary

P2X receptors are a family of ligand-gated ion channels which open in response to extracellular ATP. Several zebrafish cDNA clones encoding P2X receptors have been reported to produce little or no current when expressed in heterologous systems although their mammalian orthologs produce fully functional homomeric receptors. We isolated additional cDNA clones for all zebrafish P2XR except P2X7, and found variations from the previously reported amino acid sequences for P2X1, P2X2 and P2X 5.1. Unlike the previously reported sequences, the new variants of P2X1 and P2X 5.1 cloned were functional when expressed in *Xenopus* oocytes. However the new P2X2 variant still produced no current. Sequence analysis revealed that zebrafish P2X2 lacked two Lysine residues known to contribute to channel function and therefore we attempted to reconstitute a functional homomeric P2X2 receptor by amino acid substitution, but were unsuccessful.

We next addressed a current hypothesis that P2X signaling is required for myogenesis. Our *in vivo* characterization of P2X5.1 in skeletal muscle revealed the following. P2X5.1 was localized in a manner consistent with membrane localization. Skeletal muscle's responsiveness to ATP required P2X5.1 and antisense knockdown of P2X5.1 did not prevent myogenesis. Therefore we can reject the hypothesis that P2X signaling is necessary for myogenesis.

Introduction

P2X receptors are a family of ligand gated ion channels activated by extracellular ATP (Burnstock, 2007). In mammals the family is comprised of seven members (P2X1-7), each encoded by a different gene. P2X receptors most likely assemble as trimers (Nicke et al., 1998; Stoop et al., 1999), with one member requiring heteromeric assembly (P2X6), and another exhibiting only homomeric assembly (P2X7) (Torres et al., 1999). Despite the presence of P2X receptors in the genomes of many organisms, and their widespread expression pattern in both muscle and neural tissue, only a handful of functions have been attributed to members of this family. Most notably, P2X1 in the neurogenic control of smooth muscle (Mulryan et al., 2000), and the combination of P2X2 and P2X3 in nociception in mice (Cockayne et al., 2000; Souslova et al., 2000), as the post-synaptic receptors of neurons which receive input from taste cells (Finger et al., 2005), and in LTP (Sim et al., 2006). These three examples represent the contribution of only four members of the family, therefore other P2X receptors likely serve roles that are yet to be identified.

The cloning of zebrafish P2X receptors has been reported previously (Boue-Grabot et al., 2000; Egan et al., 2000; Norton et al., 2000; Diaz-Hernandez et al., 2002; Kucenas et al., 2003; Appelbaum et al., 2007). The family is comprised of nine members, each encoded by its own gene. Mammals typically have seven members, but the partial genome duplication known to have occurred in zebrafish resulted in two parologs for P2X3 and P2X4 designated zP2X3.1, zP2X3.2, zP2X4.1 and zP2X4.2 according to established guidelines for nomenclature (www.zfin.org). In addition, the existing literature describes a sequence originally identified and referred to as zP2X514 (Kucenas et al., 2003), later renamed zP2X8 (Appelbaum et al., 2007). However, our analysis indicates that it is most likely a parolog of zP2X5 (Figure 4.1). Many of the first published cDNA sequences failed to form normal or functional receptors when compared to orthologous receptors. As a first step in the use of zebrafish to uncover *in vivo* roles for P2X receptors we recloned all of the zebrafish P2X receptors, with the exception of P2X7 (which is not expressed in the nervous system or in muscle, which are the tissues of interest in our lab).

We uncovered several polymorphisms which may account for several subunits having been reported as non-functional (Kucenas et al., 2003), or exhibiting reduced function (Diaz-Hernandez et al., 2002). Next we characterized the responsiveness of skeletal muscle to applied ATP, and determined through antisense knockdown that the zP2X5.1 is required for this responsiveness. Finally we tested a current hypothesis that signaling through P2X receptors is necessary for myogenesis.

Materials and Methods

Animal Care and Use

Zebrafish were bred and raised according to approved guidelines set forth by the University Committee on Use and Care of Animals, University of Michigan. Developmental staging of embryos was performed either by counting somites prior to 24 hours post-fertilization (hpf), or by assessing the migration of the lateral line primordia as described previously (Kimmel et al., 1995).

Cloning of zebrafish P2X receptors

5' and 3' RACE ready cDNA (GeneRacer kit, Invitrogen, Carlsbad, CA) was synthesized from total RNA extracted from the AB background at 48 hpf using TRIzol® Reagent (Invitrogen, Carlsbad, CA). P2X receptors were PCR amplified (Pfu Turbo Polymerase, Stratagene, La Jolla, CA) using RACE primers and internal primers raised against published P2X sequences (Kucenas et al., 2003). PCR products were A-tailed using Taq DNA Polymerase (Promega, Madison, WI) and subcloned into pGEM-Teasy (Promega, Madison, WI). Five individual clones for each zP2X receptor were sequenced and compared. Based on our sequence analysis the following primers were used to clone full length transcripts for $zP2X_{1\text{-}5.2}$:

zP2X1	forward, 5'- ACACTGTGAAGACAGACTGAAGGAT-3'
	reverse, 5'- TCACTCCTTCTGTGACTCGCTGTCT-3'
zP2X2	forward, 5'- TTCACTTCACAGGAGCTTTATTTGT-3'
	reverse, 5'- GATTCAAATATGACATTTTATGATG-3'
zP2X3.1	forward, 5'- ATGGCTCCCAGAGTGCTGGGCT-3'
	reverse, 5'- TCACTCCTGACGCCCAATAGAA-3'
zP2X3.2	forward, 5'- ATGCAGCAGTGCTCTGGAAAAAT-3'
	reverse, 5'- TTAGCTGTAACGTTCGATGGAAA-3'
zP2X4.1	forward, 5'- GTGGAAGTGATTTAATGTTTAAGTCG-3'
	reverse, 5'- CTATTTGTCTTCGTTGTGTAAAAGTC-3'
zP2X4.2	forward, 5'- ACAATGGGCTGTTCTGCTTATTG-3'
	reverse, 5'- ATCAAGGAGTCCCGTATGAGCTC-3'

zP2X5.1	forward, 5'- AGAGCTGCTTCCAGGCTGTCATT-3'
	reverse, 5'- TTCTACTGGTGGCGTGCTGCTCT-3’
zP2X5.2	forward, 5'- ATGGCTCGACGGTGCAGTAATCC-3'
	reverse, 5'- ATTTCAGTGACTGAACTTTCTTTTC-3’

Electrophysiological characterization of P2X receptors expressed by *Xenopus* oocytes

Capped RNA encoding each zP2X receptor was synthesized using the mMESSAGE mMACHINE® T7 kit (Ambion, Austin, TX). RNA (5 ng) diluted to a volume of 50 nl was injected into stage V-VI defolliculated *Xenopus laevis* oocytes using a Nanoinject II system (Drummond Scientific Company, Broomall, PA). Oocytes were maintained in Barth's solution at 17 °C for 48-72 hrs before electrophysiological characterization. Two-electrode voltage-clamp recordings were made with an NPI Electronics (Tamm, Germany) TurboTec 3 amplifier at room temperature (22° C). The external recording solution was as follows (in mM): 90 NaCl, 1 KCl, 1.7 $MgCl_2$, and 10 HEPES, pH 7.6. In some experiments 2 $MgCl_2$ was replaced with 2 $CaCl_2$. Electrodes pulled from Borosilicate glass had resistances of ~0.5 MΩ and contained 3M KCl. Oocytes were held at -50 mV while ATP diluted from a stock solution (100 mM) in external solution was applied to each oocyte using a BPS-8 solution switcher (ALA Scientific Instruments, Westbury, NY). Data acquisition was controlled by pClamp 8 software using a Digidata 1322A interface (Axon Instruments, Union City, CA). The initial data analysis was done in pClamp, and current-voltage relationships were fit using functions included in Sigma Plot 9.0 (SPSS, Chicago, IL).

Morpholino injections and behavioral experiments

An antisense morpholino oligonucleotide (MO) (Gene Tools, Philomath, OR) was synthesized against the following sequence for zebrafish P2X5.1: 5’- TTGACACAGGAGCATGGCTCAGACC -3’. The underlined area designates the codon for the initial methionine. Embryos for morpholino injections were obtained from crosses of AB parents. P2X5 morpholino diluted from a stock concentration of 2 mM to the indicated concentration in 5 nl of water containing 0.1% phenol red and 1X

Deinhardts solution was injected into embryos between the one and four cell stage using a Nanoinject II system (Drummond Scientific Company, Broomall, PA). Thereafter morpholino injected embryos (morphants) were raised in a 28.5 ^{0}C water bath. Prior to the beginning of an experiment embryos were dechorionated with pronase and staged as described above. Locomotor behaviors were recorded (30 Hz) using a Panasonic CCD camera (wv-BP330) mounted to a Leica stereomicroscope at 10 X magnification. Images were captured and analyzed off-line using Scion Image (www.scioncorp.com). Touch-evoked behaviors were elicited by touching the head, yolk sac, trunk or tail region up to 3 times with a pair of No. 5 forceps.

Whole-mount *in situ* hybridization

In situ hybridization was performed using variations of a previously described approach (Westerfield, 1993). Template was prepared by cutting 1.2 µg of plasmid DNA and Phenol/Chloroform precipitated by the following method. Following a 1-2 hr digest 2 mg of Protinase K plus SDS to a final concentration of 0.5% was added and incubated at 50 ^{0}C for 30 minutes. Thereafter 200µl ddH_20, 8µl 5M NaCl, 1µl glycogen was added and mixture vortexed. Then 100µls Phenol and 100µl Chloroform were added and mixture vortexed. The mixture was then centrifuged at 14,000 rpm for 5 minutes at room temperature. The top phase was transferred to a fresh eppendorf tube and 200µl of Chloroform was added. The mixture was vortexed and centrifuged as before with the top phase again transferred to a fresh eppendorf tube followed by the addition of ice cold 100% ethanol (600µl). The mixture was placed in -80 ^{0}C for 30 minutes and then centrifuge at 4 ^{0}C for 20 minutes at 140,000 rpm. Supernatant was removed and precipitated template was resuspended in DEPC-H_2O. Riboprobes were synthesized and sheared to ~600bp. Probe integrity was checked by gel electrophoresis. Embryos were reared in 1-phenyl-2-thiourea (PTU) beginning ~22 hpf to prevent pigmentation and fixed with 4% paraformaldehyde in PBS for one hour at room temperature (22 ^{0}C). Embryos were then dehydrated with an increasing percentage of methanol in PBS and stored at -20 ^{0}C for 30 minutes. Thereafter embryos were rehydrated by decreasing the percentage of methanol in PBST (PBS containing 0.1% Tween) and incubated at 37 ^{0}C with Proteinase K for 12 minutes to increase the penetration of riboprobes. Antisense

and sense control riboprobes (5 µg/ml) were hybridized for ~16 hours at 65 °C. Anti-DIG antibody conjugated to alkaline phosphatase (Roche Products, Welwyn Garden City, UK) was bound overnight at 4 ^{0}C followed by chromogenic detection using a NBT/BCIP stock solution (Roche Products, Welwyn Garden City, UK). The chromogenic reaction was quenched at various time points for both antisense and sense control conditions. P2X receptor specific staining was considered specific when corresponding staining was absent in sense control.

Whole-cell voltage clamp recordings from skeletal muscle

All reagents and drugs were purchased from Sigma-Aldrich, St. Louis, MO. Electrophysiological recording were obtained from axial skeletal muscle as previously described (Ribera and Nusslein-Volhard, 1998; Buss and Drapeau, 2000). In brief embryos and larvae were anesthetized in 1X Evans recording solution (in mM): 134 NaCl, 2.9 KCl, 2.1 $CaCl_2$, 1.2 $MgCl_2$, 10 glucose, 10 HEPES, pH 7.8, containing 0.02% tricaine and pinned to a 35 mm dish coated with Sylgard® through the notochord using 25 µm tungsten wires. The skin overlying the trunk and tail was removed with fine No.5 forceps. The bath solution (1X Evans) containing 5µM d-tubocurarine was continuously exchanged at ~1 ml/min throughout the recording session. The internal recording solution contained (in mM): 116 K-gluconate, 16 KCl, 2 $MgCl_2$, 10 HEPES, 10 EGTA, at pH 7.2 with 0.1% SulforhodamineB for muscle cell type identification. Electrodes pulled from Borosilicate glass had resistances of 6-10 MΩ when filled with internal recording solution. Recordings were made with an Axopatch 200B amplifier (Axon Instruments, Union City, CA) low passed filtered at 5 kHz and sampled at 10 kHz. The application of ATP (10 psi, 50 ms) was controlled by a Picospritzer II (Parker Hannifin, Fairfield, NJ). Data acquisition was controlled by pClamp 8.2 software using a Digidata 1322A interface. The initial data analysis was done in pClamp 9.2, and traces were plotted using Sigma Plot 9.0.

Results

Cloning of P2X1, P2X2 and P2X5.1 from zebrafish uncovers three new variants

Using RNA extracted from embryos during the first and second day of development as template we recloned all the zP2X receptors except zP2X7. We uncovered polymorphisms at the amino acid level within zP2X1, zP2X2 and zP2X5.1 sequences, and refer to them by the terminology zP2X1^{MI}, zP2X2^{MI} and zP2X5.1^{MI}. Given that these three P2X receptors were reported to either be non-functional, or to produce extremely small currents (Diaz-Hernandez et al., 2002; Kucenas et al., 2003) we assessed whether the variants we identified could produce responses to ATP. Each zP2X receptor variant was expressed by *Xenopus* oocytes and exposed to ATP under two-electrode voltage-clamp. zP2X2^{MI} produced no ATP activated current, but both zP2X1^{MI} and zP2X5.1^{MI} formed functional homomeric receptors, and were therefore examined in more detail.

Serine 239 is necessary for zP2X1 channel activity

The amino acid sequence of the clone we identified, zP2X1^{MI} differed from the previously reported sequence at three positions. Application of ATP to *Xenopus* oocytes injected with RNA encoding zP2X1^{MI} evoked an inward current that rapidly desensitized (Figure 4.2B). Repeated application revealed that the channel required several minutes to recover making the estimation of an EC_{50} for ATP problematic. This profile is consistent with the reported activity of P2X1 from other species (Rettinger and Schmalzing, 2004). To explore why zP2X1^{MI} was functional we aligned zP2X1^{M} with the previously identified zebrafish P2X1, and P2X1 sequences from many different species which revealed that serine 239 was a highly conserved amino acid (Figure 4.2A). Substitution of serine 239 with a tyrosine, as in the first cDNA clone reported was sufficient to abolish responsiveness to ATP (Figure 4.2C). Furthermore substitution of serine 239 with an alanine (Figure 4.2D), or a cysteine, the amino acid most chemically similar to serine, (Figure 4.2E) all produced non-functional receptors. Finally, replacing the alanine found at the homologous position within rat P2X2 with a tyrosine was also sufficient to abolish function (Figure 4.2F).

Although zP2X1^{MI} also differed at two other sites (I153M and K216N) we did not explore the functional significance of these differences as I153M represents a conserved substitution, and position 216 is occupied by a variety of residues in P2X1 receptors from other species. From these findings we conclude that the loss of serine at position 239 or the inclusion of a tyrosine at the analogous position in P2X2 is sufficient to abolish channel activity.

zP2X2 does not function as a homomeric receptor

The first reported cDNA clone encoding zP2X2 had 11 cysteines in the extracellular domain, in contrast to the 10 that characterize most members of the family. However, disruption of the normal network of disulfide bonds was not the sole reason that this clone could not produce functional homomeric receptors, as zP2X2^{MI} possessed only the 10 canonical cysteines and was still non-functional (Figure 4.3C). Another striking feature of zP2X2 is the sequence EMR at positions 70-72, which is normally occupied by the highly conserved KXK motif. In hP2X1, rP2X2, and rP2X4, mutation of either of these two highly conserved lysines severely impaired ATP potency (Wilkinson et al., 2006; Marquez-Klaka et al., 2007). Replacing E70 and R72 of zP2X2^{MI} with lysines (producing the sequence KMK) was insufficient to endow this subunit with the ability to respond to ATP when it was expressed alone in oocytes (Figure 4.3D).

zP2X5 forms a functional receptor with megapore-like characteristics

The initial identification and characterization of zP2X5.1 reported that when this cDNA was expressed in HEK293 cells under the control of a promoter that gave robust expression of other P2X receptors, the whole-cell current responses were typically <20 pA (Diaz-Hernandez et al., 2002). When expressed in oocytes this isoform (AF500300) failed to generate currents above background. The amino acid sequence of clone we identified, zP2X5.1^{MI} differed from AAM74150 at 9 positions. Among these were a string of six consecutive amino acids just prior to the second transmembrane domain, which did not match the sequence predicted for this region in the Zv7 zebrafish genome. Upon closer examination of the nucleotide sequence

encoding AAM74150, it appears that a nucleotide insertion at position 848, followed a nucleotide deletion at position 862, accounts for an in frame six amino acid substitution at positions 283 through 288 (Figure 4.4).

When zP2X5.1^{MI} was expressed and studied in our normal recording solution the responses exhibited a rapidly desensitizing component (I_1), followed by an entry into a long-lasting secondary phase (I_2), which reached its peak many seconds after the ATP had been washed away (Figure 4.3B). The nature of the I_2 phase of the response was reminiscent of the "megapore" state reported for other members of the P2X family (Surprenant et al., 1996). We therefore analyzed this I_2 state further.

The megapore state is characterized by: (1) sensitivity to calcium (2) a high relative permeability for the large cation NMDG, which is impermeable during the time the channels are in the I_1 state. We found that the inclusion of 2 mM $Ca2^+$ in the recording solution blocked entry into the I_2 state (Figure 4.3C), and that replacement of $MgCl_2$ with $CaCl_2$ at the peak of I_2 resulted in a rapid exit from the I_2 state (Figure 4.3D). In addition, substantial inward current remained when NMDG was substituted for sodium in the extracellular solution (not shown). From these findings we conclude that the I_2 state exhibited by zebrafish zP2X5.1^{MI} is "megapore-like".

Localization of P2X5

The existence of an ion channel sensitive to ATP in skeletal muscle was first suggested many years ago (Kolb and Wakelam, 1983). Subsequent studies confirmed the existence of ATP sensitive ion channels in avian skeletal muscle, but argued that the single channel currents had a very low unitary conductance compared to the initial report (Hume and Honig, 1986; Thomas and Hume, 1990b). Following the cloning of the P2X family the expression of multiple P2X receptors by skeletal muscle has been demonstrated in several different organisms (Meyer et al., 1999; Ruppelt et al., 2001; Ryten et al., 2001; Soto et al., 2003). Several roles for P2X receptors in muscle have been proposed including regulating myogenesis during development (Ryten et al., 2001) and regeneration following injury (Ryten et al., 2002; Ryten et al., 2004), and regulating the contractility of muscle fibers (Sandona et al., 2005).

We used whole mount *in situ* hybridization to explore the subunits expressed by zebrafish skeletal muscle during the first two days of development which revealed the expression only one subunit, zP2X5.1 by skeletal muscle (Figure 4.5A). Lacking an antibody for zebrafish zP2X5.1 we examined the localization of P2X5.1 by tagging it with EGFP and placing it under control of the heat-shock protein 70 promoter (hsp70:zP2X5-EGFP). Wild type embryos were injected with the plasmid encoding hsp70:P2X5-EGFP, or with hsp70:EGFP as a control, at the one to four cell stage and raised at 28.5^0 C until 48 hours post-fertilization (hpf) at which time they were "heat-shocked" at 37^0 C for 30 minutes. In both control and experimental animals expression 2-3 hours after heat shock was highly mosaic. However in animals injected with hsp70:EGFP the expression of EGFP within muscle fibers was ubiquitous, while the fluorescence in animals injected with hsp70:P2X5-EGFP could be observed in a pattern consistent with membrane localization (Figure 4.5B). This finding indicates that P2X5 most likely is found on the plasma membrane of skeletal muscle.

P2X signaling is not required for myogenesis or for swimming

Two lines of evidence have suggested that P2X signaling may play an essential role in myogenesis. On study was conducted on the C2C12 cell line (Araya et al., 2004), and another was conducted on satellite cells, which are a population of myogenic precursors triggered to proliferate and then differentiate in response to injury *in vivo* (Ryten et al., 2002). In both studies blocking purinergic signaling through P2X receptors disrupted the differentiation of myogenic precursors. These findings, coupled with the fact that P2X receptors are expressed during development by myogenic precursors in multiple organisms, has lead to the hypothesis that P2X receptors might contribute to early myogenesis. However these reports have also indicated that myogenic precursors also express multiple P2X receptor subunits making the examination P2X receptor function by knockout problematic. Given that zebrafish appear to only express one P2X receptor in muscle we tested the hypothesis that P2X receptor signaling is required for myogenesis in zebrafish through the use of an antisense morpholino. We found that the injection of a morpholino that targeted

the 5'start site of P2X5 had no observable effect on muscle morphology in injected embryos (morphants) (Figure 4.6A). The failure to alter muscle morphology was not because the morpholino was ineffective. Muscle fibers from uninjected embryos held at -60 mV responded to applied ATP (100 μM) with a transient inward current peaking at about -150 pA and lasting ~1-2 s, followed by a sustained outward current lasting tens of seconds (Figure 4.6B-E). In contrast the injection of the P2X5.1 morpholino at 100 nM decreased the average ATP response to less than half of the control, and complete loss of ATP responsiveness achieved at 200 nM. These results demonstrate that P2X5.1 is required muscle ATP responsiveness at this developmental stage, and that P2X signaling is not required for myogenesis.

Finally ATP is known to be packaged in most, if not all synaptic vesicles. This finding coupled with the presence of P2X receptors on the membranes of muscle suggested the possibility that there might be a purinergic as well as a cholinergic component to the synaptic responses at the neuromuscular junction (NMJ). To examine this issue at the zebrafish NMJ we assessed synaptic communication in the absence of P2X signaling behaviorally by assaying the ability of embryos to swim following injection of the zP2X5.1 morpholino to (200 nM). A swim was stimulated in control embryos by touching the head or tail with a pair of forceps to induce touch-evoked escape contractions and swimming. Touch was found to induce similar responses in P2X5.1 morphants (Figure 4.7F), indicating that sufficient synaptic communication persists in the absence of P2X signaling to result in muscle contractions.

Discussion

The zebrafish family of P2X receptors is comprised of nine members, one copy of P2X1, P2X2 and P2X7, and two parolog copies of P2X3, P2X4 and P2X5. There is no evidence in the genome for a P2X6. It should be noted that in mammals, P2X5 and P2X6 are the most closely related subunits (see Figure 4.1) but the phylogenetic analysis indicates that zP2X5.2 (zP2X8) is much more closely related to other P2X5 sequences than to the mammalian P2X6 sequences. As the versions of zP2X1 and zP2X5.1 that we cloned readily produce currents in *Xenopus* oocytes, eight of these nine have now been shown to form functional homomeric receptors sensitive to ATP. The exception is zP2X2. The apparent explanation is that this subunit lacks two highly conserved lysine residues believed to form part of the ATP binding site of P2X receptors (Ennion et al., 2000; Jiang et al., 2000). However, there must be other differences from mammalian P2X2 receptors as well, since substitution of EMR with KMK failed to result in ATP induced currents above background. When zP2X2 is co-expressed with zP2X3.1 it has been reported to be incorporated into heteromeric complexes responsive to ATP (Kucenas et al., 2003). The overlapping expression pattern of zP2X2 with other zP2X receptors in zebrafish is consistent with the idea that it can only play a role when co-assembled with another subunit. As any trimeric complex containing zP2X2 would have a non-functional ATP binding site, this suggests that fewer than three ATP molecules are sufficient to activate the channel *in vivo*.

We found that embryonic zebrafish muscle expresses zP2X5.1, and that this protein produces functional channels that can enter the megapore state when experimental conditions are suitable. However, as 2 mM calcium was sufficient to suppress entry into this state, it may not be physiologically relevant under most conditions. The simplest interpretation of our ability to completely suppress ATP-evoked current with a morpholino designed specifically for P2X5.1 is that this is the only P2X receptor expressed at this developmental stage. However, the morpholino result is also consistent with the idea that zP2X5.1 is essential to move other zP2X subunits also expressed in muscle cells to the surface. Consistent with the idea that

zP2X5.1 is indeed the only P2X receptor of muscle at this stage is our failure to see a detectable signal with *in situ* studies using probes directed against all of the other P2X receptors (except that we did not test P2X7, which is not expressed in muscle in any species in which the issue has been explored).

The fact that morphant animals are morphologically normal, and can swim away from a tactile stimulus, at a time when the muscle fibers are completely unresponsive to ATP, indicates that P2X signaling cannot be playing an essential role at the age these animals were assayed. Although it remains possible that the concentration of morpholino that we injected did not suppress ATP signaling earlier in development, it seems more likely that the hypothesis that P2X mediated signaling plays an essential role in the development of muscle is likely not the case for embryonic development in zebrafish.

Figures

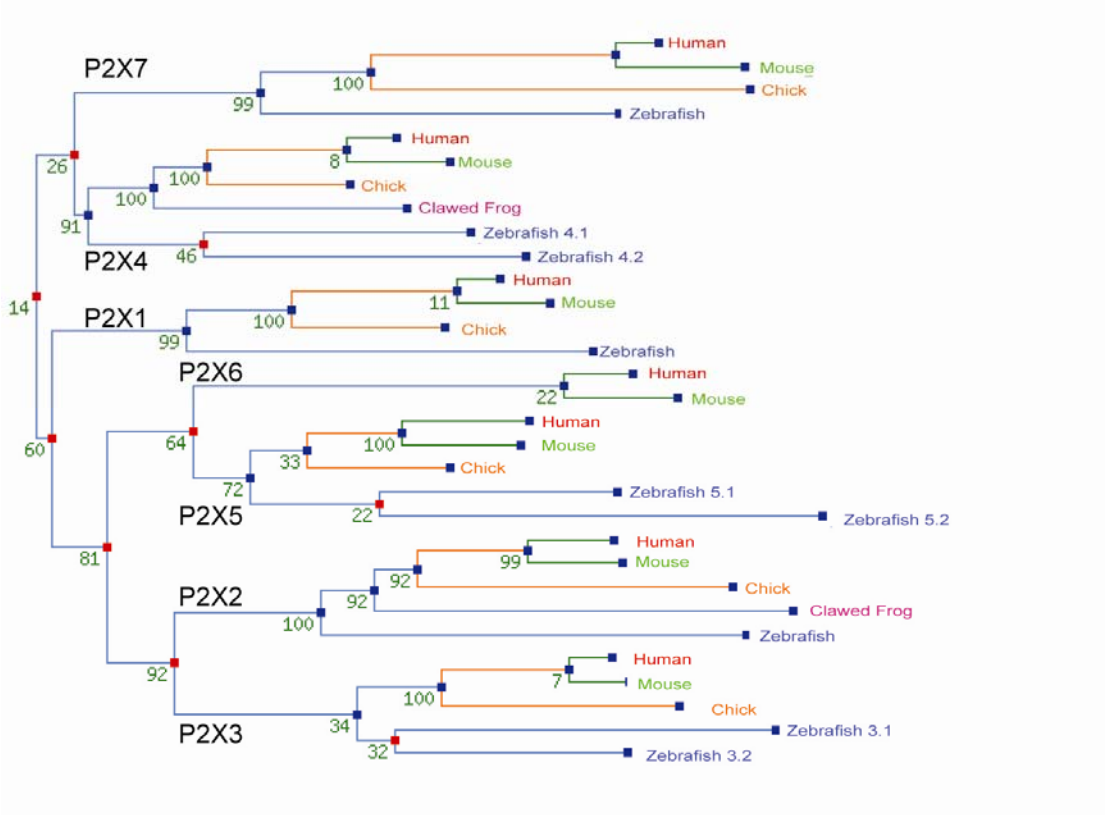

Figure 4.1: Phylogenic analysis of the zP2X receptor family. A tree showing the relationships among all chordate P2X receptors. Of note the previously identified zP2X514/P2X8 receptor is consistent with that of a parolog of zP2X5.1, numbers indicate confidence level.

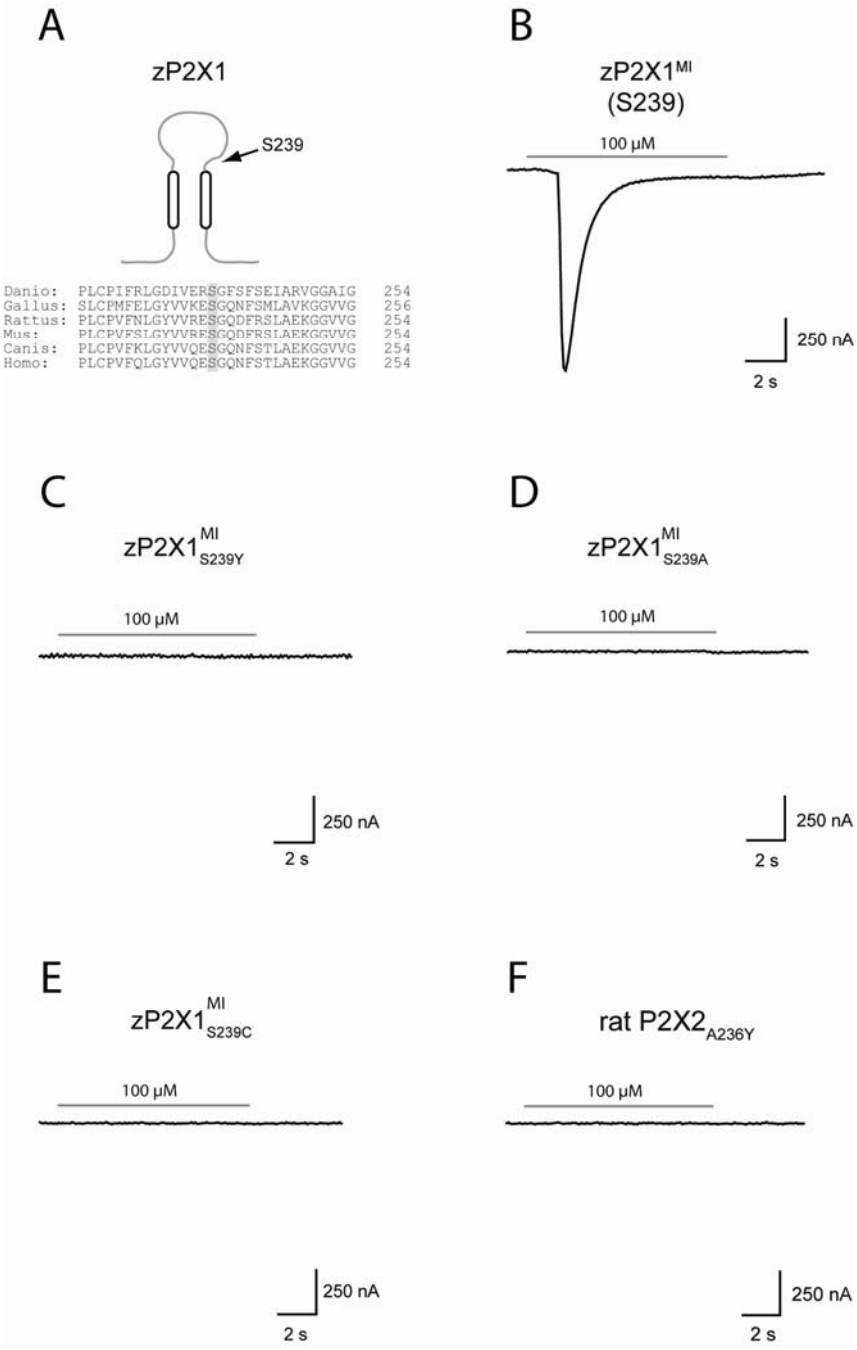

Figure 4.2: Characterization of the newly identified zP2X1^{MI}. **(A)** Sequence alignment of P2X1 receptors from different species indicates that serine 239 is a conserved residue. **(B)** zP2X1^{MI} forms a channel responsive to ATP, bar indicates here and in the following traces the application of 100 µM ATP. **(C)** Replacement of serine 239 with a tyrosine (S238Y) is sufficient to abolish responsiveness of zP2X1^{MI} to ATP. **(D-E)** Substitution of S239 with either an alanine or a cysteine also abolishes responsiveness to ATP. **(F)** The substitution of a tyrosine at the analogous residue in rat P2X2 (A236) was also sufficient to abolish rat P2X2's responsiveness to ATP.

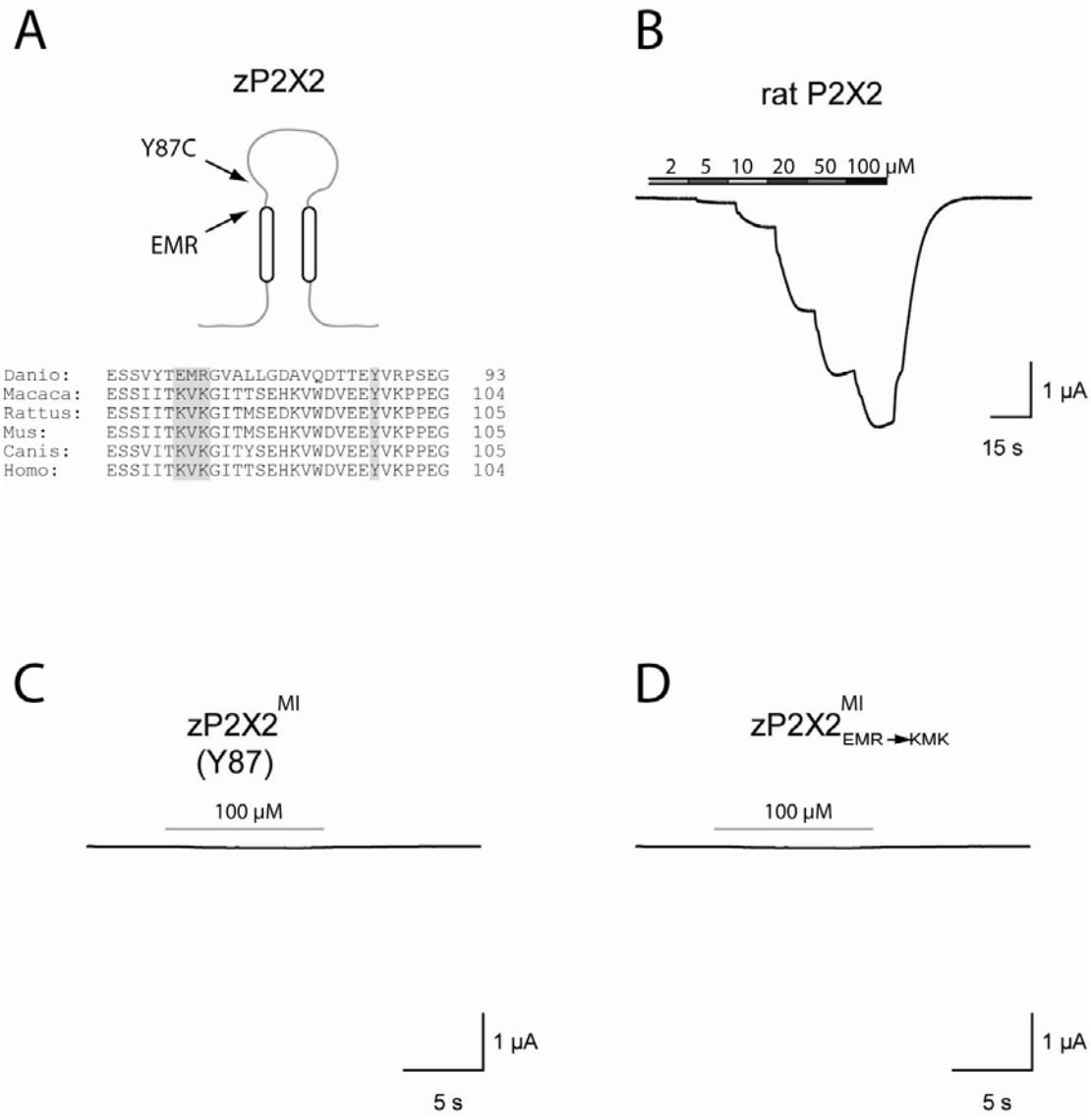

Figure 4.3: Characterization of the newly identified zP2X2^{MI}. **(A)** Membrane topology and sequence alignment of zebrafish P2X2 in relation to other P2X receptors from different species. Highlighted is the Y87C polymorphism and EMR motif found in place of the KXK motif which has been implicated in the binding of ATP. **(B)** For comparison the application of 100 µM ATP to an oocyte expressing rat P2X2 exhibits a dose dependent inward current. **(C)** The newly identified zP2X2^{MI} fails to respond to applied ATP. **(D)** Alterations of residues 70-73 from EMR to KVK is not sufficient to reconstitute sensitivity to ATP.

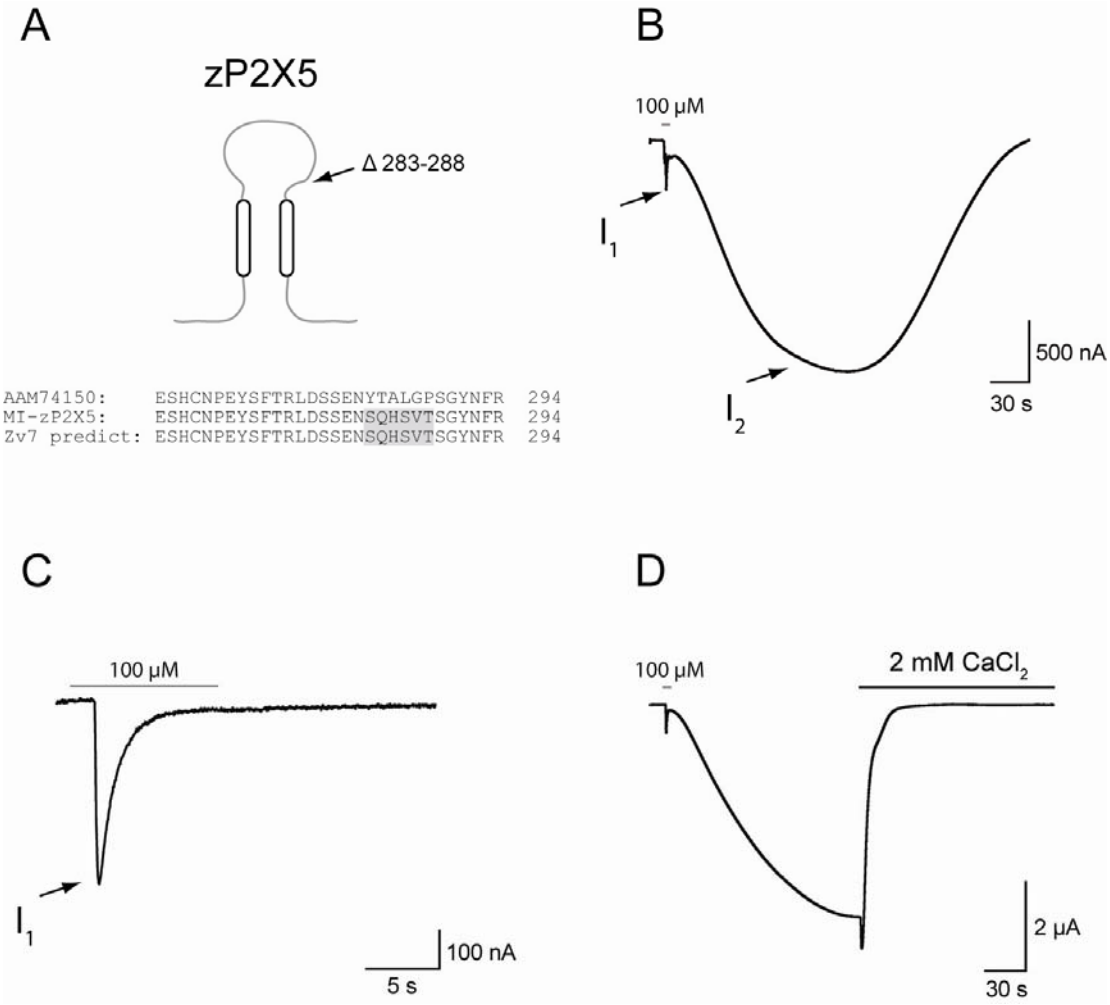

Figure 4.4: Characterization of the newly identified zP2X5^{MI}. **(A)** Sequence comparison between published zP2X5 (AAM74150), and that of our zP2X5 receptor in addition to the predicted genome sequence. **(B)** zP2X5 forms a functional channel responsive to ATP, which exhibits megapore-like characteristics. Bar indicates here and in the following traces the application of 100 μM ATP. **(C)** Entry into the I_2 state is blocked by the inclusion of $CaCl_2$ in the recording solution. **(D)** Rapid exit from the I_2 state occurs when recording solution containing 1.7 mM $MgCl_2$ is changed to 2 mM $CaCl_2$.

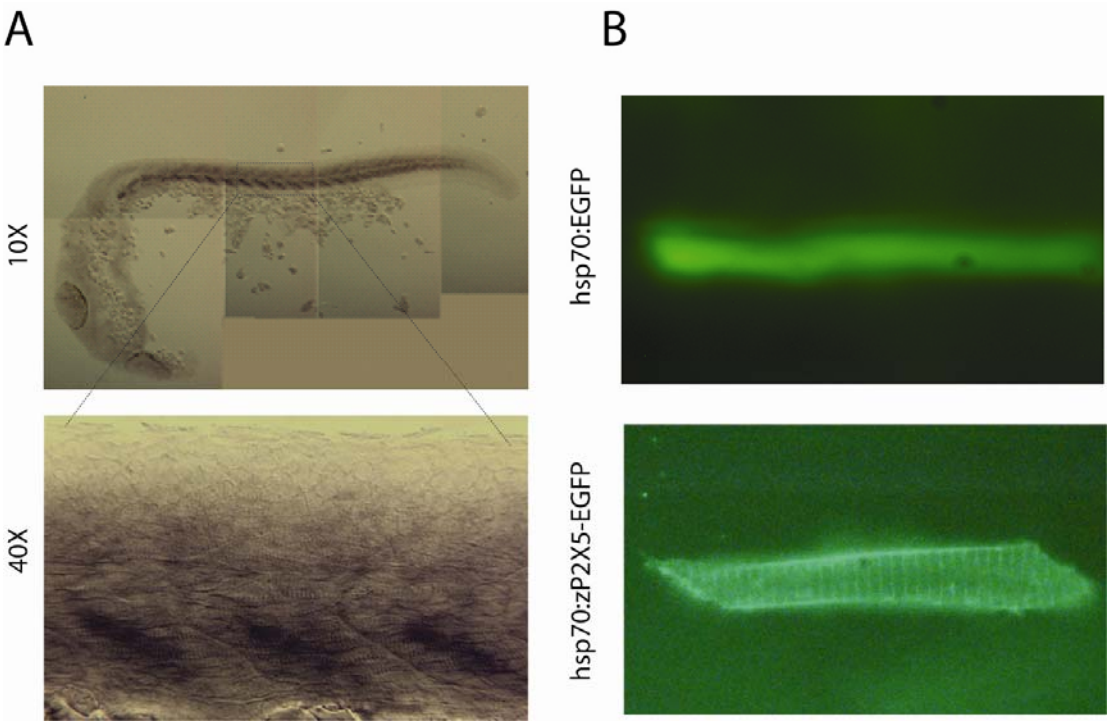

Figure 4.5: Expression analysis of zP2X5. **(A)** Whole-mount in situ hybridization from 24 hpf embryo reveals expression within the somites of the trunk and tail (top). Closer examination indicates labeling of axial skeletal muscle (bottom). **(B)** EGFP expression under the control of the hsp70 promoter (top) and when fused to the C-terminus zP2X5 indicates a pattern consistent with membrane localization in 48 hpf embryos.

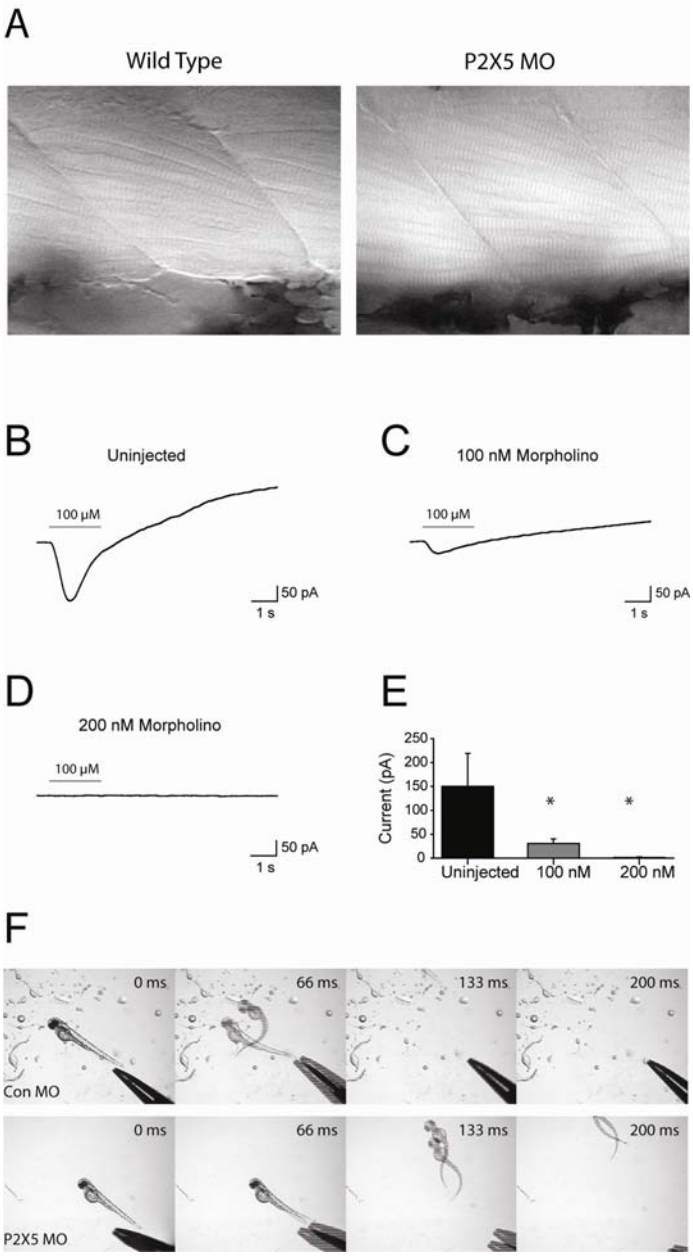

Figure 4.6: Morphology and responsiveness of skeletal muscle to ATP. **(A)** Left: image of axial skeletal muscle above the yolk extension from an uninjected 48 hpf embryo. Right: image of axial skeletal muscle above the yolk extension from a 48 hpf zP2X5.1 morpholino injected embryo. **(B)** In response to the application of ATP (100 µM) a muscle fiber voltage clamped at -60 mV responds with a transient (1-2 s) inward current followed by a prolonged outward current. **(C-E)** Injection of a morpholino against zP2X5.1 results in a dose-dependent reduction of ATP induced currents with complete blockade achieved by 200 nM. Values represent the average ± the SD, $n = 10$ (1 fiber per fish). **(F)** A loss of P2X5.1 in axial skeletal muscle does not abolish synaptic communication at the neuromuscular junction as assayed behaviorally.

CHAPTER V

CONCLUSION

Summary

The aim of this thesis was to use forward and reverse genetics to explore the contribution of unknown and known genes to the touch-evoked escape behaviors of zebrafish (*Danio rerio*).

A forward genetic screen identified two mutants that displayed abnormal touch-evoked escape behaviors. The first mutant *touchdown* (*tdo*) lacked sensitivity to light touch, but responded to noxious stimuli. *tdo* mutants were shown to result from mutations in the gene encoding for TRPM7, an ion channel with an attached kinase. A combination of electrophysiological and molecular techniques revealed that ion channel function was sufficient to restore sensitivity to light touch within excitable mechanosensitive neurons. Therefore TRPM7 is a candidate for a vertebrate mechanoreceptor responsible for sensitivity to light touch.

The second mutant identified from our forward genetic screen *non-active* (*nav*) initiated escape contractions, but failed to swim in response to touch. *nav* mutants were shown to result from mutations in the gene encoding $Na_V1.6$ that abolished channel activity. Electrophysiological recordings revealed that $Na_V1.6$ is required to turn on a locomotor network capable of generating rudimentary swimming. Furthermore the requirement of $Na_V1.6$ to turn this network might be its contribution of a persistent sodium current which is known to facilitate repetitive firing in other neurons.

Finally the cloning and characterization of the ATP-gated P2X receptor subunits P2X1 through P2X5.2 from zebrafish demonstrated that two subunits (P2X1 and P2X5.1) form functional homomeric receptors in contrast to previous reports. The use of reverse genetics (antisense knockdown) allowed the rejection of the hypothesis that signaling through P2X receptors is essential for myogenesis.

Conclusions drawn from thesis

Your muscle is not sensitive to sound. Neither are the motor neurons which innervate your muscle, nor the interneurons which drive your motor neurons, nor even the neurons which are post synaptic to the hair cells in your ear. However we all have experienced that a loud sound can make you jump.

What mediates this behavioral response is of course a circuit of cells. The virtue of screening for simple behaviors such as touch-evoked escape behaviors is that one simultaneously screens at all levels at once. The vice is that mutations at different level may resemble each other. Therein lies the advantage of coupling *in vivo* electrophysiology with forward genetics. A well trained electrophysiologist can often determine within one week the level of defect within the touch-evoked escape circuit (muscle vs. nervous system). However even with this advantage I was unable to pinpoint the exact loci of defect for either the TRPM7 or $Na_V1.6$ mutation. Furthermore it is still unclear what role(s) P2X receptors serve in zebrafish, but several hypotheses can be proposed.

TRPM7

It is abundantly clear that TRPM7 is required by mechanosensitive cells for sensitivity to light touch, and the ability to evoke swimming following the application of noxious stimuli. One straightforward hypothesis is that TRPM7 is the pore conducting portion of the mechanotransduction complex responsible for sensitivity to light touch. The belief that TRPM7 could be the pore portion stems from the findings that the non-conducting $TRPM7_{E1026K}$ version failed to rescue touch-evoked behaviors, whereas the $TRPM7_{E1026Q}$ version which essentially renders TRPM7 a monovalent cation channel was sufficient. Therefore it appears that TRPM7 is required for membrane depolarization,

and not as an accessory subunit in a macromolecular complex similar to the MEC mechanotransduction complex found in *C. elegans*. However the only evidence we have at this time that TRPM7 is sensitive to mechanical stimuli are the recordings from TRPM7-EGFP transfected HEK cells following membrane stretch induced by displacement of the recording electrode which results in a "gating-like" current. Analysis of the S4 region of TRPM7 did reveal three charged amino acids which potentially could account for this gating current. The question however is why did we not observe a more prolonged ionic current in response to membrane stretch? Several possibilities exist and include that HEK cells lack some critical co-factor essential for translating gating movements into channel openings. Alternatively HEK cells could possess some factor that blocks the translation of gating movements into channel opening. In either case it was not possible to reconstitute a mechanotransduction complex *in vitro*, which has been a problem in this field as a whole for solving the identity of mechanoreceptors by techniques such as expression cloning that have been so successful in the identification of other receptors.

It is also possible that TRPM7 does not contribute the pore forming region of the mechanotransduction complex. A recurring issue raised by Colquhoun is the distinction between gating and conductance, as electrophysiologists often measure gating as a function of conductance (Colquhoun, 1998). What is clear from the $TRPM7_{E1026K}$ mutation is that there is no conductance (Li et al., 2007), however this mutation may actually affect gating and not conductance. Further recordings from HEK cells expressing $TRPM7_{E1026K}$ could resolve this issue.

Another possible role for TRPM7 is that it is required within synaptic vesicles at the axon terminals of mechanosensitive neurons for the release of transmitter, similar to a role that has been demonstrated for cholinergic synapses in mice (Krapivinsky et al., 2006). Although our recordings from the zebrafish neuromuscular junction contradict the model put forth for mammalian TRPM7 in cholinergic synaptic vesicles it is possible that TRPM7 promotes the transmitter at a central synapse. Consistent with this possibility is the fact that Acetylcholine and Glutamate (the most likely transmitter released by mechanosensitive neurons) are both negatively charged transmitters. Our recent ability to record from RBs within the spinal cord and extracellularly from M cells opens up the

possibility of performing paired recordings to resolve this issue. A potential concern is that that although inducing an action potential within a single RB in *Xenopus* was sufficient to induce bursting in ventral nerve roots (Clarke et al., 1984), it is unclear whether this activity is mediated by M cells. Furthermore a single RB may not be sufficient to trigger activity within ventral nerve roots or M cells in zebrafish.

If TRPM7 were a vertebrate mechanoreceptor responsible for sensitivity to light touch then the finding that *tdo* mutants fail to swim in response to noxious stimuli, but do so when TRPM7 was restored within mechanosensitive neurons suggests that somatosensory feedback is essential for triggering swimming. This proposes a model wherein touch delivered to the skin of the fish activates TRPM7 containing neurons which then triggers escape contractions. The bending of the fish then activates additional TRPM7 containing neurons which then en mass trigger swimming. A similar model for the ortholog of TRPN1 in *C. elegans* (TRP-4) has been proposed to account for the finding that worms deficient in TRP-4 exhibit abnormal body bending during locomotion (Li et al., 2006). However these models are in opposition to the common observation of many other sensory-motor systems wherein the triggering of a behavior occurs in the absence of sensory feedback.

Finally *tdo* mutants exhibit sensitivity to light touch until ~ 48 hpf, and begin to recover around 72 hpf. Given that the morpholino used was raised against sequence obtained for both maternal inherited mRNA, and embryonic mRNA encoding TRPM7 there must be an additional mechanoreceptor for sensitivity to light touch within the first two days. Furthermore the recovery around 72 hpf is commensurate with the replacement of RBs with the more common sensory neurons belonging to the dorsal root ganglia (Williams et al., 2000). While this may appear to suggest that TRPM7 is only required transiently by a transient population of mechanosensitive neurons, the absence of evidence suggesting that neurons within the trigeminal are also replaced instead argues that TRPM7 is required transiently for sensitivity to light touch. As a whole it appears that TRPM7 could be a vertebrate mechanoreceptor for sensitivity to light touch, but others must exist.

If TRPM7 is not a mechanoreceptor and is actually required for the release of transmitter then the loss of TRPM7 may result in a reduction of synaptic drive to

supraspinal elements essential to evoke escape contractions in response to touch, and the ability of noxious stimuli to induce swimming. This model is also consistent with a potential requirement of the voltage-gated sodium channel $Na_V1.6$ in triggering swimming (see below).

$Na_V1.6$

The finding that mutations in the gene encoding for $Na_V1.6$, which abolished channel activity, lead to the motor mutant *nav* (*non-active*) was not surprising. Mutations in the sodium channels (Meisler et al., 2002) and in $Na_V1.6$ in particular (Meisler et al., 2004) have been known to affect motor function . What was interesting is that $Na_V1.6$ exhibits a persistent current and appears to serve two roles within the touch-evoked escape circuit. First $Na_V1.6$ appears to be required within the locomotor network to generate "normal" patterns of fictive swimming. Second $Na_V1.6$ is required to activate the rudimentary locomotor network found in *nav* mutants. I will discuss these two findings independently starting with the activation defect first.

The inability of touch to activate the rudimentary locomotor network found in *nav* mutants is suggestive of a defect within the sensory neurons. Consistent with this hypothesis $Na_V1.6$ is expressed within RB and has been found to contribute the majority of the voltage-gated sodium current (Pineda et al., 2005). Furthermore RBs from *Xenopus* tadpoles were found to fire multiple action potentials in response to tactile stimulation delivered to the skin (Roberts and Hayes, 1977). Together these findings indicate that supraspinal drive from RBs in *nav* mutants could be defective in two ways. First the loss of $Na_V1.6$ might result in fewer RBs being recruited in response to touch. Second the number of times an RB fires in response to touch might be reduced due a loss of $Na_V1.6$'s persistent current. However inconsistent with a defect at the level of sensory neurons is also the finding from *Xenopus* that triggering a single RB to spike via depolarizing current injections was sufficient to trigger ventral root bursting (Clarke et al., 1984). This would suggest that the residual voltage-gated sodium current in *nav*, which is capable of activating supraspinal elements and triggering escape contractions, should be sufficient to trigger swimming but doesn't. Furthermore the activation of M cells in response to touch, a phenomenon which is sufficient to evoke both escape

contractions and swimming in more adult fish (Nissanov et al., 1990), indicates that sufficient sensory input is reaching the supraspinal elements of the escape circuit. This implies that a defect downstream of sensory neurons within the neurons responsible for activating the locomotor network responsible for swimming (Swim neuron) is one loci of defect in *nav*. This model makes the following recently testable hypothesis: selective restoration of $Na_V1.6$ within mechanosensitive neurons by plasmid based methods (similar to TRPM7) should not rescue touch-evoked swimming of durations consistent with NMDA-evoked fictive swimming. If plasmid based methods were to rescue touch-evoked swimming in *nav* then the circuits between *Xenopus* and zebrafish are simply different. In addition to identifying the loci of the defect it would also suggest that persistent sensory input is essential for triggering swimming, but not escape contractions. This is an intriguing model considering that noxious stimuli can trigger escape contractions but not swimming in *tdo* mutants. Collectively this would imply that escape contractions can be dissociated from swimming, which is unclear within the context of touch-evoked escape behaviors in zebrafish.

With respect to the locomotor defect in *nav,* if we assume that NMDA activates the locomotor network responsible for swimming similar to sensory stimuli, and that there is not an alteration within the locomotor network as a result of decreased synaptic drive from mechanosensitive neurons, then there is at least one additional defect within *nav* mutants. The finding that the *nav* locomotor network generates a bout of fictive swimming as often wild types, but that the bouts are of both shorter duration and lower fictive swimming frequency demonstrates that the locomotor network is not capable of generating sustained high frequency activity. As $Na_V1.6$ does exhibit a persistent sodium current, and the application of Riluzole does mimic the *nav* phenotype it would be reasonable to suspect that the contribution $Na_V1.6$'s persistent current is essential for prolonged activity within zebrafish's locomotor network in response to NMDA. Further insight would be garnered by recording NMDA-evoked fictive swimming in the presence of Riluzole. If the concentration of Riluzole sufficient to mimic the *nav* phenotype fails to replicate the pattern of NMDA-evoked fictive swimming observed in *nav* then the effect due to a loss of $Na_V1.6$ on the locomotor network might be a consequence of decreased synaptic drive from sensory neurons during development.

Whether the defect is at the level of sensory neurons, interneurons or both the finding that a locomotor network capable of generating rudimentary fictive swimming was present in *nav* indicates that $Na_V1.6$ is required to transform a transient sensory stimulus into a prolonged motor output, which is surprising.

Zebrafish P2X receptors

The first evidence that ATP could activate an ion channel in a transmitter like fashion was shown in skeletal muscle (Kolb and Wakelam, 1983; Hume and Honig, 1986). Since this time a member of the ATP gated ion channel family has been cloned from muscle (Valera et al., 1994) and the family has grown to include typically seven members in mammals (North, 2002). However what has not been solved is the role of P2X signaling within muscle. Our ability to reject the hypothesis that signaling via P2X receptors is essential to myogenesis during development although disappointing, it does present new hypotheses.

Blockade of P2X receptor signaling in satellite cells was shown to block exit from a proliferative state. However this was achieved with the use of pharmacological agents that may also have affected members of the P2Y receptor family. Therefore there may be a parallel pathway with the contribution of G-protein coupled receptor signaling. Furthermore it would be worth investigating whether artificially activating P2X receptor signaling through rearing embryos in media supplemented with ATP (or a more stable agonist) could induce early differentiation. Although this would also activate additional receptors sensitive to ATP and its metabolites, any effect observed could then be tested for a P2X component by the inclusion of the P2X5.1 morpholino which blocks P2X responses in skeletal muscle.

Alternatively it may just be that regeneration does not recapitulate development. In this scenario expression of P2X receptors during development is not detrimental to the development of an organism and is therefore allowed to exist. The defect may then manifest itself during regeneration which is unfortunately out of the realm of testing with current antisense technology in zebrafish and would therefore be best addressed with pharmacological methods.

Overview

If TRPM7 holds up as a vertebrate mechanoreceptor for light touch then one could use it as a background for the study of other sensory modalities such as nociception, devoid of contaminating influences from light touch. In humans there is also a link between TRPM7 and hypomagnesemia with secondary hypocalcemia (Chubanov et al., 2004). Given that the pigmentation defect associated with *tdo* has been reported to be rescued by simply rearing mutant embryos in media with elevated magnesium (Elizondo et al., 2005), suggests that zebrafish *tdo* mutants might useful as a model for this disorder. In addition the permeability of zebrafish to compounds can be increased by the inclusion of minimal DMSO (0.1%).

With respect to *nav*, the number of mutations associated with $Na_V1.6$, and with sodium channels as a whole, is ever increasing. Given the feasibility of RNA based rescue, coupled with *in vivo* patch-clamping in zebrafish could facilitate the use of *nav* mutants as a backdrop to study the effects of human mutations *in vivo* without the need of knockins (gene replacement).

As an instrument of instruction for undergraduate students the use of zebrafish in the classroom has only begun. With the stable of identified motor mutants that result from electrogenic proteins only increasing, and the relative ease of extracellular and two-electrode voltage clamp electrophysiology (already utilized in some lab courses) zebrafish motor mutants could be used in a teaching lab in a "solve your mutant" manner. Students could start with critical review of the literature for a set of mutants. Then be handed several breeding pairs for a mutant (unknown to them) and then be asked to phenotype their mutant, behaviorally and physiologically including extracellular recordings and response to caffeine and KCl. From this they could be asked to write a midterm paper where they which mutant they believe they have, and why they think it's not another mutant. After which they would map their mutant, identify candidates and clone the gene (either cDNA or genomic), followed by RNA based rescue and/or morpholino knockdown to confirm the identity of their mutant. The consequence of the mutation would then be examined in oocytes, followed by a review of the literature to determine whether their mutant might have any therapeutic value to the study of human disorders.

As an instrument of instruction for graduate students forward genetic screens are an excellent tool. They supply the hope of finding something completely novel, whether a new gene or a new role for a known gene. In addition the art of formulating testable hypothesis is molded in the absence of the gene through the countless iterations of, "If it were X gene, then if we did Y, we might expect to see Z." This process does not end once the gene is identified, as we have seen with the *tdo* and *nav* mutants, because one would like to know what the protein is doing within the cells that give rise to the behavior. Hence the title of my thesis. As one truly goes, "From Behavior to Genes, and Back Again"

References:

Aarts M, Iihara K, Wei WL, Xiong ZG, Arundine M, Cerwinski W, MacDonald JF, Tymianski M (2003) A key role for TRPM7 channels in anoxic neuronal death. Cell 115:863-877.

Agranoff BW, Klinger PD (1964) Puromycin Effect on Memory Fixation in the Goldfish. Science 146:952-953.

Al-Anzi B, Tracey WD, Jr., Benzer S (2006) Response of Drosophila to wasabi is mediated by painless, the fly homolog of mammalian TRPA1/ANKTM1. Curr Biol 16:1034-1040.

Appelbaum L, Skariah G, Mourrain P, Mignot E (2007) Comparative expression of p2x receptors and ecto-nucleoside triphosphate diphosphohydrolase 3 in hypocretin and sensory neurons in zebrafish. Brain Res 1174:66-75.

Araya R, Riquelme MA, Brandan E, Saez JC (2004) The formation of skeletal muscle myotubes requires functional membrane receptors activated by extracellular ATP. Brain Res Brain Res Rev 47:174-188.

Arduini BL, Henion PD (2004) Melanophore sublineage-specific requirement for zebrafish touchtone during neural crest development. Mech Dev 121:1353-1364.

Armstrong CM, Bezanilla F (1973) Currents related to movement of the gating particles of the sodium channels. Nature 242:459-461.

Armstrong CM, Bezanilla F (1977) Inactivation of the sodium channel. II. Gating current experiments. J Gen Physiol 70:567-590.

Bautista DM, Siemens J, Glazer JM, Tsuruda PR, Basbaum AI, Stucky CL, Jordt SE, Julius D (2007) The menthol receptor TRPM8 is the principal detector of environmental cold. Nature 448:204-208.

Bautista DM, Jordt SE, Nikai T, Tsuruda PR, Read AJ, Poblete J, Yamoah EN, Basbaum AI, Julius D (2006) TRPA1 mediates the inflammatory actions of environmental irritants and proalgesic agents. Cell 124:1269-1282.

Beneski DA, Catterall WA (1980) Covalent labeling of protein components of the sodium channel with a photoactivable derivative of scorpion toxin. Proc Natl Acad Sci U S A 77:639-643.

Bernhardt RR, Chitnis AB, Lindamer L, Kuwada JY (1990) Identification of spinal neurons in the embryonic and larval zebrafish. J Comp Neurol 302:603-616.

Bo X, Jiang LH, Wilson HL, Kim M, Burnstock G, Surprenant A, North RA (2003) Pharmacological and biophysical properties of the human P2X5 receptor. Mol Pharmacol 63:1407-1416.

Boue-Grabot E, Akimenko MA, Seguela P (2000) Unique functional properties of a sensory neuronal P2X ATP-gated channel from zebrafish. J Neurochem 75:1600-1607.

Buchthal F, Folkow B (1944) Close arterial injection of adenosine triphosphate and inorganic triphosphate into frog muscle. Acta Physiol Scand 8:312–316.

Burnstock G (1972) Purinergic nerves. Pharmacol Rev 24:509–581.

Burnstock G (2007) Physiology and pathophysiology of purinergic neurotransmission. Physiol Rev 87:659-797.

Buss RR, Drapeau P (2000) Physiological properties of zebrafish embryonic red and white muscle fibers during early development. J Neurophysiol 84:1545-1557.
Buss RR, Drapeau P (2001) Synaptic drive to motoneurons during fictive swimming in the developing zebrafish. J Neurophysiol 86:197-210.
Buss RR, Drapeau P (2002) Activation of embryonic red and white muscle fibers during fictive swimming in the developing zebrafish. J Neurophysiol 87:1244-1251.
Catterall WA, Goldin AL, Waxman SG (2005a) International Union of Pharmacology. XLVII. Nomenclature and structure-function relationships of voltage-gated sodium channels. Pharmacol Rev 57:397-409.
Catterall WA, Perez-Reyes E, Snutch TP, Striessnig J (2005b) International Union of Pharmacology. XLVIII. Nomenclature and structure-function relationships of voltage-gated calcium channels. Pharmacol Rev 57:411-425.
Chahine M, Deschenes I, Trottier E, Chen LQ, Kallen RG (1997) Restoration of fast inactivation in an inactivation-defective human heart sodium channel by the cysteine modifying reagent benzyl-MTS: analysis of IFM-ICM mutation. Biochem Biophys Res Commun 233:606-610.
Chen C, Westenbroek RE, Xu X, Edwards CA, Sorenson DR, Chen Y, McEwen DP, O'Malley HA, Bharucha V, Meadows LS, Knudsen GA, Vilaythong A, Noebels JL, Saunders TL, Scheuer T, Shrager P, Catterall WA, Isom LL (2004) Mice lacking sodium channel beta1 subunits display defects in neuronal excitability, sodium channel expression, and nodal architecture. J Neurosci 24:4030-4042.
Chen YH, Huang FL, Cheng YC, Wu CJ, Yang CN, Tsay HJ (2008) Knockdown of zebrafish Nav1.6 sodium channel impairs embryonic locomotor activities. J Biomed Sci 15:69-78.
Chong M, Drapeau P (2007) Interaction between hindbrain and spinal networks during the development of locomotion in zebrafish. Dev Neurobiol 67:933-947.
Chopra SS, Watanabe H, Zhong TP, Roden DM (2007) Molecular cloning and analysis of zebrafish voltage-gated sodium channel beta subunit genes: implications for the evolution of electrical signaling in vertebrates. BMC Evol Biol 7:113.
Chubanov V, Waldegger S, Mederos y Schnitzler M, Vitzthum H, Sassen MC, Seyberth HW, Konrad M, Gudermann T (2004) Disruption of TRPM6/TRPM7 complex formation by a mutation in the TRPM6 gene causes hypomagnesemia with secondary hypocalcemia. Proc Natl Acad Sci U S A 101:2894-2899.
Clapham DE (2003) TRP channels as cellular sensors. Nature 426:517-524.
Clarke JD, Hayes BP, Hunt SP, Roberts A (1984) Sensory physiology, anatomy and immunohistochemistry of Rohon-Beard neurones in embryos of Xenopus laevis. J Physiol 348:511-525.
Cockayne DA, Hamilton SG, Zhu QM, Dunn PM, Zhong Y, Novakovic S, Malmberg AB, Cain G, Berson A, Kassotakis L, Hedley L, Lachnit WG, Burnstock G, McMahon SB, Ford AP (2000) Urinary bladder hyporeflexia and reduced pain-related behaviour in P2X3-deficient mice. Nature 407:1011-1015.
Colbert HA, Bargmann CI (1995) Odorant-specific adaptation pathways generate olfactory plasticity in C. elegans. Neuron 14:803-812.
Colquhoun D (1998) Binding, gating, affinity and efficacy: the interpretation of structure-activity relationships for agonists and of the effects of mutating receptors. Br J Pharmacol 125:924-947.

Connors BW, Prince DA (1982) Effects of local anesthetic QX-314 on the membrane properties of hippocampal pyramidal neurons. J Pharmacol Exp Ther 220:476-481.
Corey DP, Garcia-Anoveros J, Holt JR, Kwan KY, Lin SY, Vollrath MA, Amalfitano A, Cheung EL, Derfler BH, Duggan A, Geleoc GS, Gray PA, Hoffman MP, Rehm HL, Tamasauskas D, Zhang DS (2004) TRPA1 is a candidate for the mechanosensitive transduction channel of vertebrate hair cells. Nature 432:723-730.
Cornell RA, Yemm E, Bonde G, Li W, d'Alencon C, Wegman L, Eisen J, Zahs A (2004) Touchtone promotes survival of embryonic melanophores in zebrafish. Mech Dev 121:1365-1376.
Cox JJ, Reimann F, Nicholas AK, Thornton G, Roberts E, Springell K, Karbani G, Jafri H, Mannan J, Raashid Y, Al-Gazali L, Hamamy H, Valente EM, Gorman S, Williams R, McHale DP, Wood JN, Gribble FM, Woods CG (2006) An SCN9A channelopathy causes congenital inability to experience pain. Nature 444:894-898.
Crill WE (1996) Persistent sodium current in mammalian central neurons. Annu Rev Physiol 58:349-362.
Cui WW, Low SE, Hirata H, Saint-Amant L, Geisler R, Hume RI, Kuwada JY (2005) The zebrafish shocked gene encodes a glycine transporter and is essential for the function of early neural circuits in the CNS. J Neurosci 25:6610-6620.
Davis TH, Chen C, Isom LL (2004) Sodium channel beta1 subunits promote neurite outgrowth in cerebellar granule neurons. J Biol Chem 279:51424-51432.
de Bono M, Tobin DM, Davis MW, Avery L, Bargmann CI (2002) Social feeding in Caenorhabditis elegans is induced by neurons that detect aversive stimuli. Nature 419:899-903.
Devoto SH, Melancon E, Eisen JS, Westerfield M (1996) Identification of separate slow and fast muscle precursor cells in vivo, prior to somite formation. Development 122:3371-3380.
Di Prisco GV, Pearlstein E, Robitaille R, Dubuc R (1997) Role of sensory-evoked NMDA plateau potentials in the initiation of locomotion. Science 278:1122-1125.
Di Prisco GV, Pearlstein E, Le Ray D, Robitaille R, Dubuc R (2000) A cellular mechanism for the transformation of a sensory input into a motor command. J Neurosci 20:8169-8176.
Diaz-Hernandez M, Cox JA, Migita K, Haines W, Egan TM, Voigt MM (2002) Cloning and characterization of two novel zebrafish P2X receptor subunits. Biochem Biophys Res Commun 295:849-853.
Downes GB, Granato M (2006) Supraspinal input is dispensable to generate glycine-mediated locomotive behaviors in the zebrafish embryo. J Neurobiol 66:437-451.
Doyle DA, Morais Cabral J, Pfuetzner RA, Kuo A, Gulbis JM, Cohen SL, Chait BT, MacKinnon R (1998) The structure of the potassium channel: molecular basis of K+ conduction and selectivity. Science 280:69-77.
Drapeau P, Ali DW, Buss RR, Saint-Amant L (1999) In vivo recording from identifiable neurons of the locomotor network in the developing zebrafish. J Neurosci Methods 88:1-13.

Drew LJ, Rohrer DK, Price MP, Blaver KE, Cockayne DA, Cesare P, Wood JN (2004) Acid-sensing ion channels ASIC2 and ASIC3 do not contribute to mechanically activated currents in mammalian sensory neurones. J Physiol 556:691-710.
Eaton RC, Farley RD (1975) Mauthner neuron field potential in newly hatched larvae of the zebra fish. J Neurophysiol 38:502-512.
Eaton RC, Emberley DS (1991) How stimulus direction determines the trajectory of the Mauthner-initiated escape response in a teleost fish. J Exp Biol 161:469-487.
Eaton RC, DiDomenico R, Nissanov J (1988) Flexible body dynamics of the goldfish C-start: implications for reticulospinal command mechanisms. J Neurosci 8:2758-2768.
Egan TM, Cox JA, Voigt MM (2000) Molecular cloning and functional characterization of the zebrafish ATP-gated ionotropic receptor P2X(3) subunit. FEBS Lett 475:287-290.
Eisen JS, Myers PZ, Westerfield M (1986) Pathway selection by growth cones of identified motoneurones in live zebra fish embryos. Nature 320:269-271.
Elizondo MR, Arduini BL, Paulsen J, MacDonald EL, Sabel JL, Henion PD, Cornell RA, Parichy DM (2005) Defective skeletogenesis with kidney stone formation in dwarf zebrafish mutant for trpm7. Curr Biol 15:667-671.
Ennion S, Hagan S, Evans RJ (2000) The role of positively charged amino acids in ATP recognition by human P2X(1) receptors. J Biol Chem 275:29361-29367.
Fein AJ, Meadows LS, Chen C, Slat EA, Isom LL (2007) Cloning and expression of a zebrafish SCN1B ortholog and identification of a species-specific splice variant. BMC Genomics 8:226.
Finger TE, Danilova V, Barrows J, Bartel DL, Vigers AJ, Stone L, Hellekant G, Kinnamon SC (2005) ATP signaling is crucial for communication from taste buds to gustatory nerves. Science 310:1495-1499.
Fountain SJ, Cao L, Young MT, North RA (2008) Permeation properties of a P2X receptor in the green algae ostreococcus tauri. J Biol Chem.
Fountain SJ, Parkinson K, Young MT, Cao L, Thompson CR, North RA (2007) An intracellular P2X receptor required for osmoregulation in Dictyostelium discoideum. Nature 448:200-203.
Gahtan E, Sankrithi N, Campos JB, O'Malley DM (2002) Evidence for a widespread brain stem escape network in larval zebrafish. J Neurophysiol 87:608-614.
Goodman MB (2006) Mechanosensation. WormBook:1-14.
Granato M, van Eeden FJ, Schach U, Trowe T, Brand M, Furutani-Seiki M, Haffter P, Hammerschmidt M, Heisenberg CP, Jiang YJ, Kane DA, Kelsh RN, Mullins MC, Odenthal J, Nusslein-Volhard C (1996) Genes controlling and mediating locomotion behavior of the zebrafish embryo and larva. Development 123:399-413.
Haffter P, Nusslein-Volhard C (1996) Large scale genetics in a small vertebrate, the zebrafish. Int J Dev Biol 40:221-227.
Haffter P, Granato M, Brand M, Mullins MC, Hammerschmidt M, Kane DA, Odenthal J, van Eeden FJ, Jiang YJ, Heisenberg CP, Kelsh RN, Furutani-Seiki M, Vogelsang E, Beuchle D, Schach U, Fabian C, Nusslein-Volhard C (1996) The identification of genes with unique and essential functions in the development of the zebrafish, Danio rerio. Development 123:1-36.

Harty TP, Dib-Hajj SD, Tyrrell L, Blackman R, Hisama FM, Rose JB, Waxman SG (2006) Na(V)1.7 mutant A863P in erythromelalgia: effects of altered activation and steady-state inactivation on excitability of nociceptive dorsal root ganglion neurons. J Neurosci 26:12566-12575.

Higashijima S, Hotta Y, Okamoto H (2000) Visualization of cranial motor neurons in live transgenic zebrafish expressing green fluorescent protein under the control of the islet-1 promoter/enhancer. J Neurosci 20:206-218.

Hillle B (2001) Ion channels of Excitable Membranes. 3rd ed., Sinauer Associates, Inc.

Hirata H, Saint-Amant L, Downes GB, Cui WW, Zhou W, Granato M, Kuwada JY (2005) Zebrafish bandoneon mutants display behavioral defects due to a mutation in the glycine receptor beta-subunit. Proc Natl Acad Sci U S A 102:8345-8350.

Hirata H, Saint-Amant L, Waterbury J, Cui W, Zhou W, Li Q, Goldman D, Granato M, Kuwada JY (2004) accordion, a zebrafish behavioral mutant, has a muscle relaxation defect due to a mutation in the ATPase Ca2+ pump SERCA1. Development 131:5457-5468.

Hirata H, Watanabe T, Hatakeyama J, Sprague SM, Saint-Amant L, Nagashima A, Cui WW, Zhou W, Kuwada JY (2007) Zebrafish relatively relaxed mutants have a ryanodine receptor defect, show slow swimming and provide a model of multi-minicore disease. Development 134:2771-2781.

Hodgkin AL, Huxley AF (1952) Currents carried by sodium and potassium ions through the membrane of the giant axon of Loligo. J Physiol 116:449-472.

Hotson JR, Prince DA, Schwartzkroin PA (1979) Anomalous inward rectification in hippocampal neurons. J Neurophysiol 42:889-895.

Hukriede NA, Joly L, Tsang M, Miles J, Tellis P, Epstein JA, Barbazuk WB, Li FN, Paw B, Postlethwait JH, Hudson TJ, Zon LI, McPherson JD, Chevrette M, Dawid IB, Johnson SL, Ekker M (1999) Radiation hybrid mapping of the zebrafish genome. Proc Natl Acad Sci U S A 96:9745-9750.

Hume RI, Honig MG (1986) Excitatory action of ATP on embryonic chick muscle. J Neurosci 6:681-690.

Hume RI, Thomas SA (1988) Multiple actions of adenosine 5'-triphosphate on chick skeletal muscle. J Physiol 406:503-524.

Isom LL (2001) Sodium channel beta subunits: anything but auxiliary. Neuroscientist 7:42-54.

Isom LL, Ragsdale DS, De Jongh KS, Westenbroek RE, Reber BF, Scheuer T, Catterall WA (1995) Structure and function of the beta 2 subunit of brain sodium channels, a transmembrane glycoprotein with a CAM motif. Cell 83:433-442.

Isom LL, De Jongh KS, Patton DE, Reber BF, Offord J, Charbonneau H, Walsh K, Goldin AL, Catterall WA (1992) Primary structure and functional expression of the beta 1 subunit of the rat brain sodium channel. Science 256:839-842.

Jiang LH, Rassendren F, Surprenant A, North RA (2000) Identification of amino acid residues contributing to the ATP-binding site of a purinergic P2X receptor. J Biol Chem 275:34190-34196.

Jiang Y, Ruta V, Chen J, Lee A, MacKinnon R (2003a) The principle of gating charge movement in a voltage-dependent K+ channel. Nature 423:42-48.

Jiang Y, Lee A, Chen J, Ruta V, Cadene M, Chait BT, MacKinnon R (2003b) X-ray structure of a voltage-dependent K+ channel. Nature 423:33-41.

Jontes JD, Buchanan J, Smith SJ (2000) Growth cone and dendrite dynamics in zebrafish embryos: early events in synaptogenesis imaged in vivo. Nat Neurosci 3:231-237.
Kimchi T, Xu J, Dulac C (2007) A functional circuit underlying male sexual behaviour in the female mouse brain. Nature 448:1009-1014.
Kimmel CB, Hatta K, Metcalfe WK (1990) Early axonal contacts during development of an identified dendrite in the brain of the zebrafish. Neuron 4:535-545.
Kimmel CB, Ballard WW, Kimmel SR, Ullmann B, Schilling TF (1995) Stages of embryonic development of the zebrafish. Dev Dyn 203:253-310.
Kindt KS, Viswanath V, Macpherson L, Quast K, Hu H, Patapoutian A, Schafer WR (2007) Caenorhabditis elegans TRPA-1 functions in mechanosensation. Nat Neurosci 10:568-577.
Kolb HA, Wakelam MJ (1983) Transmitter-like action of ATP on patched membranes of cultured myoblasts and myotubes. Nature 303:621-623.
Korn H, Faber DS (2005) The Mauthner cell half a century later: a neurobiological model for decision-making? Neuron 47:13-28.
Krapivinsky G, Mochida S, Krapivinsky L, Cibulsky SM, Clapham DE (2006) The TRPM7 ion channel functions in cholinergic synaptic vesicles and affects transmitter release. Neuron 52:485-496.
Kucenas S, Li Z, Cox JA, Egan TM, Voigt MM (2003) Molecular characterization of the zebrafish P2X receptor subunit gene family. Neuroscience 121:935-945.
Kuwada JY, Bernhardt RR, Chitnis AB (1990) Pathfinding by identified growth cones in the spinal cord of zebrafish embryos. J Neurosci 10:1299-1308.
Kwan KY, Allchorne AJ, Vollrath MA, Christensen AP, Zhang DS, Woolf CJ, Corey DP (2006) TRPA1 contributes to cold, mechanical, and chemical nociception but is not essential for hair-cell transduction. Neuron 50:277-289.
Li M, Du J, Jiang J, Ratzan W, Su LT, Runnels LW, Yue L (2007) Molecular determinants of Mg2+ and Ca2+ permeability and pH sensitivity in TRPM6 and TRPM7. J Biol Chem 282:25817-25830.
Li Q, Shirabe K, Kuwada JY (2004) Chemokine signaling regulates sensory cell migration in zebrafish. Dev Biol 269:123-136.
Li W, Feng Z, Sternberg PW, Xu XZ (2006) A C. elegans stretch receptor neuron revealed by a mechanosensitive TRP channel homologue. Nature 440:684-687.
Liedtke W, Tobin DM, Bargmann CI, Friedman JM (2003) Mammalian TRPV4 (VR-OAC) directs behavioral responses to osmotic and mechanical stimuli in Caenorhabditis elegans. Proc Natl Acad Sci U S A 100 Suppl 2:14531-14536.
Liedtke W, Choe Y, Marti-Renom MA, Bell AM, Denis CS, Sali A, Hudspeth AJ, Friedman JM, Heller S (2000) Vanilloid receptor-related osmotically activated channel (VR-OAC), a candidate vertebrate osmoreceptor. Cell 103:525-535.
Liu KS, Fetcho JR (1999) Laser ablations reveal functional relationships of segmental hindbrain neurons in zebrafish. Neuron 23:325-335.
Marquez-Klaka B, Rettinger J, Bhargava Y, Eisele T, Nicke A (2007) Identification of an intersubunit cross-link between substituted cysteine residues located in the putative ATP binding site of the P2X1 receptor. J Neurosci 27:1456-1466.
Matsushita M, Kozak JA, Shimizu Y, McLachlin DT, Yamaguchi H, Wei FY, Tomizawa K, Matsui H, Chait BT, Cahalan MD, Nairn AC (2005) Channel function is

dissociated from the intrinsic kinase activity and autophosphorylation of TRPM7/ChaK1. J Biol Chem 280:20793-20803.
McDearmid JR, Drapeau P (2006) Rhythmic motor activity evoked by NMDA in the spinal zebrafish larva. J Neurophysiol 95:401-417.
McKemy DD, Neuhausser WM, Julius D (2002) Identification of a cold receptor reveals a general role for TRP channels in thermosensation. Nature 416:52-58.
Meisler MH, Plummer NW, Burgess DL, Buchner DA, Sprunger LK (2004) Allelic mutations of the sodium channel SCN8A reveal multiple cellular and physiological functions. Genetica 122:37-45.
Meisler MH, Kearney JA, Sprunger LK, MacDonald BT, Buchner DA, Escayg A (2002) Mutations of voltage-gated sodium channels in movement disorders and epilepsy. Novartis Found Symp 241:72-81; discussion 82-76, 226-232.
Mendelson B (1986a) Development of reticulospinal neurons of the zebrafish. II. Early axonal outgrowth and cell body position. J Comp Neurol 251:172-184.
Mendelson B (1986b) Development of reticulospinal neurons of the zebrafish. I. Time of origin. J Comp Neurol 251:160-171.
Metcalfe WK, Mendelson B, Kimmel CB (1986) Segmental homologies among reticulospinal neurons in the hindbrain of the zebrafish larva. J Comp Neurol 251:147-159.
Meyer MP, Groschel-Stewart U, Robson T, Burnstock G (1999) Expression of two ATP-gated ion channels, P2X5 and P2X6, in developing chick skeletal muscle. Dev Dyn 216:442-449.
Moffatt L, Hume RI (2007) Responses of rat P2X2 receptors to ultrashort pulses of ATP provide insights into ATP binding and channel gating. J Gen Physiol 130:183-201.
Montell C (2005) The TRP superfamily of cation channels. Sci STKE 2005:re3.
Montell C, Rubin GM (1989) Molecular characterization of the Drosophila trp locus: a putative integral membrane protein required for phototransduction. Neuron 2:1313-1323.
Montell C, Birnbaumer L, Flockerzi V, Bindels RJ, Bruford EA, Caterina MJ, Clapham DE, Harteneck C, Heller S, Julius D, Kojima I, Mori Y, Penner R, Prawitt D, Scharenberg AM, Schultz G, Shimizu N, Zhu MX (2002) A unified nomenclature for the superfamily of TRP cation channels. Mol Cell 9:229-231.
Mulryan K, Gitterman DP, Lewis CJ, Vial C, Leckie BJ, Cobb AL, Brown JE, Conley EC, Buell G, Pritchard CA, Evans RJ (2000) Reduced vas deferens contraction and male infertility in mice lacking P2X1 receptors. Nature 403:86-89.
Myers PZ, Eisen JS, Westerfield M (1986) Development and axonal outgrowth of identified motoneurons in the zebrafish. J Neurosci 6:2278-2289.
Nadler MJ, Hermosura MC, Inabe K, Perraud AL, Zhu Q, Stokes AJ, Kurosaki T, Kinet JP, Penner R, Scharenberg AM, Fleig A (2001) LTRPC7 is a Mg.ATP-regulated divalent cation channel required for cell viability. Nature 411:590-595.
Nasevicius A, Ekker SC (2000) Effective targeted gene 'knockdown' in zebrafish. Nat Genet 26:216-220.
Nicke A, Baumert HG, Rettinger J, Eichele A, Lambrecht G, Mutschler E, Schmalzing G (1998) P2X1 and P2X3 receptors form stable trimers: a novel structural motif of ligand-gated ion channels. Embo J 17:3016-3028.

Nissanov J, Eaton RC, DiDomenico R (1990) The motor output of the Mauthner cell, a reticulospinal command neuron. Brain Res 517:88-98.
Noda M, Shimizu S, Tanabe T, Takai T, Kayano T, Ikeda T, Takahashi H, Nakayama H, Kanaoka Y, Minamino N, et al. (1984) Primary structure of Electrophorus electricus sodium channel deduced from cDNA sequence. Nature 312:121-127.
North RA (2002) Molecular physiology of P2X receptors. Physiol Rev 82:1013-1067.
Norton WH, Rohr KB, Burnstock G (2000) Embryonic expression of a P2X(3) receptor encoding gene in zebrafish. Mech Dev 99:149-152.
Novak AE, Jost MC, Lu Y, Taylor AD, Zakon HH, Ribera AB (2006a) Gene duplications and evolution of vertebrate voltage-gated sodium channels. J Mol Evol 63:208-221.
Novak AE, Taylor AD, Pineda RH, Lasda EL, Wright MA, Ribera AB (2006b) Embryonic and larval expression of zebrafish voltage-gated sodium channel alpha-subunit genes. Dev Dyn 235:1962-1973.
Numata T, Shimizu T, Okada Y (2007) Direct mechano-stress sensitivity of TRPM7 channel. Cell Physiol Biochem 19:1-8.
O'Malley DM, Kao YH, Fetcho JR (1996) Imaging the functional organization of zebrafish hindbrain segments during escape behaviors. Neuron 17:1145-1155.
Pineda RH, Heiser RA, Ribera AB (2005) Developmental, molecular, and genetic dissection of INa in vivo in embryonic zebrafish sensory neurons. J Neurophysiol 93:3582-3593.
Pineda RH, Svoboda KR, Wright MA, Taylor AD, Novak AE, Gamse JT, Eisen JS, Ribera AB (2006) Knockdown of Nav1.6a Na+ channels affects zebrafish motoneuron development. Development 133:3827-3836.
Postlethwait JH, Johnson SL, Midson CN, Talbot WS, Gates M, Ballinger EW, Africa D, Andrews R, Carl T, Eisen JS, et al. (1994) A genetic linkage map for the zebrafish. Science 264:699-703.
Raman IM, Sprunger LK, Meisler MH, Bean BP (1997) Altered subthreshold sodium currents and disrupted firing patterns in Purkinje neurons of Scn8a mutant mice. Neuron 19:881-891.
Rettinger J, Schmalzing G (2004) Desensitization masks nanomolar potency of ATP for the P2X1 receptor. J Biol Chem 279:6426-6433.
Ribera AB, Nusslein-Volhard C (1998) Zebrafish touch-insensitive mutants reveal an essential role for the developmental regulation of sodium current. J Neurosci 18:9181-9191.
Roberts A (2000) Early functional organization of spinal neurons in developing lower vertebrates. Brain Res Bull 53:585-593.
Roberts A, Hayes BP (1977) The anatomy and function of 'free' nerve endings in an amphibian skin sensory system. Proc R Soc Lond B Biol Sci 196:415-429.
Rohl CA, Boeckman FA, Baker C, Scheuer T, Catterall WA, Klevit RE (1999) Solution structure of the sodium channel inactivation gate. Biochemistry 38:855-861.
Runnels LW, Yue L, Clapham DE (2001) TRP-PLIK, a bifunctional protein with kinase and ion channel activities. Science 291:1043-1047.
Ruppelt A, Ma W, Borchardt K, Silberberg SD, Soto F (2001) Genomic structure, developmental distribution and functional properties of the chicken P2X(5) receptor. J Neurochem 77:1256-1265.

Ryten M, Hoebertz A, Burnstock G (2001) Sequential expression of three receptor subtypes for extracellular ATP in developing rat skeletal muscle. Dev Dyn 221:331-341.
Ryten M, Dunn PM, Neary JT, Burnstock G (2002) ATP regulates the differentiation of mammalian skeletal muscle by activation of a P2X5 receptor on satellite cells. J Cell Biol 158:345-355.
Ryten M, Yang SY, Dunn PM, Goldspink G, Burnstock G (2004) Purinoceptor expression in regenerating skeletal muscle in the mdx mouse model of muscular dystrophy and in satellite cell cultures. Faseb J 18:1404-1406.
Saint-Amant L, Drapeau P (1998) Time course of the development of motor behaviors in the zebrafish embryo. J Neurobiol 37:622-632.
Saint-Amant L, Sprague SM, Hirata H, Li Q, Cui WW, Zhou W, Poudou O, Hume RI, Kuwada JY (2008) The zebrafish ennui behavioral mutation disrupts acetylcholine receptor localization and motor axon stability. Dev Neurobiol 68:45-61.
Sandona D, Danieli-Betto D, Germinario E, Biral D, Martinello T, Lioy A, Tarricone E, Gastaldello S, Betto R (2005) The T-tubule membrane ATP-operated P2X4 receptor influences contractility of skeletal muscle. Faseb J 19:1184-1186.
Schmitz C, Perraud AL, Johnson CO, Inabe K, Smith MK, Penner R, Kurosaki T, Fleig A, Scharenberg AM (2003) Regulation of vertebrate cellular Mg2+ homeostasis by TRPM7. Cell 114:191-200.
Seiler C, Nicolson T (1999) Defective calmodulin-dependent rapid apical endocytosis in zebrafish sensory hair cell mutants. J Neurobiol 41:424-434.
Shah BS, Stevens EB, Gonzalez MI, Bramwell S, Pinnock RD, Lee K, Dixon AK (2000) beta3, a novel auxiliary subunit for the voltage-gated sodium channel, is expressed preferentially in sensory neurons and is upregulated in the chronic constriction injury model of neuropathic pain. Eur J Neurosci 12:3985-3990.
Sidi S, Friedrich RW, Nicolson T (2003) NompC TRP channel required for vertebrate sensory hair cell mechanotransduction. Science 301:96-99.
Silinsky EM, Hubbard JI (1973) Thermal synthesis of amino acids from a simulated primitive atmosphere. Nature 243:404-405.
Sim JA, Chaumont S, Jo J, Ulmann L, Young MT, Cho K, Buell G, North RA, Rassendren F (2006) Altered hippocampal synaptic potentiation in P2X4 knock-out mice. J Neurosci 26:9006-9009.
Soto F, Krause U, Borchardt K, Ruppelt A (2003) Cloning, tissue distribution and functional characterization of the chicken P2X1 receptor. FEBS Lett 533:54-58.
Souslova V, Cesare P, Ding Y, Akopian AN, Stanfa L, Suzuki R, Carpenter K, Dickenson A, Boyce S, Hill R, Nebenuis-Oosthuizen D, Smith AJ, Kidd EJ, Wood JN (2000) Warm-coding deficits and aberrant inflammatory pain in mice lacking P2X3 receptors. Nature 407:1015-1017.
Stoop R, Thomas S, Rassendren F, Kawashima E, Buell G, Surprenant A, North RA (1999) Contribution of individual subunits to the multimeric P2X(2) receptor: estimates based on methanethiosulfonate block at T336C. Mol Pharmacol 56:973-981.
Story GM, Peier AM, Reeve AJ, Eid SR, Mosbacher J, Hricik TR, Earley TJ, Hergarden AC, Andersson DA, Hwang SW, McIntyre P, Jegla T, Bevan S, Patapoutian A

(2003) ANKTM1, a TRP-like channel expressed in nociceptive neurons, is activated by cold temperatures. Cell 112:819-829.
Stowers L, Holy TE, Meister M, Dulac C, Koentges G (2002) Loss of sex discrimination and male-male aggression in mice deficient for TRP2. Science 295:1493-1500.
Streisinger G, Walker C, Dower N, Knauber D, Singer F (1981) Production of clones of homozygous diploid zebra fish (Brachydanio rerio). Nature 291:293-296.
Surprenant A, Rassendren F, Kawashima E, North RA, Buell G (1996) The cytolytic P2Z receptor for extracellular ATP identified as a P2X receptor (P2X7). Science 272:735-738.
Suzuki M, Mizuno A, Kodaira K, Imai M (2003a) Impaired pressure sensation in mice lacking TRPV4. J Biol Chem 278:22664-22668.
Suzuki M, Watanabe Y, Oyama Y, Mizuno A, Kusano E, Hirao A, Ookawara S (2003b) Localization of mechanosensitive channel TRPV4 in mouse skin. Neurosci Lett 353:189-192.
Tazerart S, Viemari JC, Darbon P, Vinay L, Brocard F (2007) Contribution of persistent sodium current to locomotor pattern generation in neonatal rats. J Neurophysiol 98:613-628.
Thomas SA, Hume RI (1990a) Irreversible desensitization of ATP responses in developing chick skeletal muscle. J Physiol 430:373-388.
Thomas SA, Hume RI (1990b) Permeation of both cations and anions through a single class of ATP-activated ion channels in developing chick skeletal muscle. J Gen Physiol 95:569-590.
Thomas SA, Hume RI (1993) Single potassium channel currents activated by extracellular ATP in developing chick skeletal muscle: a role for second messengers. J Neurophysiol 69:1556-1566.
Thomas SA, Zawisa MJ, Lin X, Hume RI (1991) A receptor that is highly specific for extracellular ATP in developing chick skeletal muscle in vitro. Br J Pharmacol 103:1963-1969.
Torres GE, Egan TM, Voigt MM (1999) Hetero-oligomeric assembly of P2X receptor subunits. Specificities exist with regard to possible partners. J Biol Chem 274:6653-6659.
Tracey WD, Jr., Wilson RI, Laurent G, Benzer S (2003) painless, a Drosophila gene essential for nociception. Cell 113:261-273.
Tsai CW, Tseng JJ, Lin SC, Chang CY, Wu JL, Horng JF, Tsay HJ (2001) Primary structure and developmental expression of zebrafish sodium channel Na(v)1.6 during neurogenesis. DNA Cell Biol 20:249-255.
Uemura O, Okada Y, Ando H, Guedj M, Higashijima S, Shimazaki T, Chino N, Okano H, Okamoto H (2005) Comparative functional genomics revealed conservation and diversification of three enhancers of the isl1 gene for motor and sensory neuron-specific expression. Dev Biol 278:587-606.
Urbani A, Belluzzi O (2000) Riluzole inhibits the persistent sodium current in mammalian CNS neurons. Eur J Neurosci 12:3567-3574.
Valera S, Hussy N, Evans RJ, Adami N, North RA, Surprenant A, Buell G (1994) A new class of ligand-gated ion channel defined by P2x receptor for extracellular ATP. Nature 371:516-519.

van Raamsdonk W, Pool CW, te Kronnie G (1978) Differentiation of muscle fiber types in the teleost Brachydanio rerio. Anat Embryol (Berl) 153:137-155.
Walker RG, Willingham AT, Zuker CS (2000) A Drosophila mechanosensory transduction channel. Science 287:2229-2234.
Weinberg ES, Allende ML, Kelly CS, Abdelhamid A, Murakami T, Andermann P, Doerre OG, Grunwald DJ, Riggleman B (1996) Developmental regulation of zebrafish MyoD in wild-type, no tail and spadetail embryos. Development 122:271-280.
Wells DG, Zawisa MJ, Hume RI (1995) Changes in responsiveness to extracellular ATP in chick skeletal muscle during development and upon denervation. Dev Biol 172:585-590.
Westerfield M, McMurray JV, Eisen JS (1986) Identified motoneurons and their innervation of axial muscles in the zebrafish. J Neurosci 6:2267-2277.
Westerfield, M. (1993) The zebrafish book. 3rd ed., Univ. of Oregon Press, Eugene.
Wilkinson WJ, Jiang LH, Surprenant A, North RA (2006) Role of ectodomain lysines in the subunits of the heteromeric P2X2/3 receptor. Mol Pharmacol 70:1159-1163.
Williams JA, Barrios A, Gatchalian C, Rubin L, Wilson SW, Holder N (2000) Programmed cell death in zebrafish rohon beard neurons is influenced by TrkC1/NT-3 signaling. Dev Biol 226:220-230.
Yang N, Horn R (1995) Evidence for voltage-dependent S4 movement in sodium channels. Neuron 15:213-218.
Yu FH, Westenbroek RE, Silos-Santiago I, McCormick KA, Lawson D, Ge P, Ferriera H, Lilly J, DiStefano PS, Catterall WA, Scheuer T, Curtis R (2003) Sodium channel beta4, a new disulfide-linked auxiliary subunit with similarity to beta2. J Neurosci 23:7577-7585.
Zhong G, Masino MA, Harris-Warrick RM (2007) Persistent sodium currents participate in fictive locomotion generation in neonatal mouse spinal cord. J Neurosci 27:4507-4518.
Zhou W, Saint-Amant L, Hirata H, Cui WW, Sprague SM, Kuwada JY (2006) Non-sense mutations in the dihydropyridine receptor beta1 gene, CACNB1, paralyze zebrafish relaxed mutants. Cell Calcium 39:227-236.